# High Resolution Seismic Surveys at U.S. Marine Corps Air Station, Cherry Point, North Carolina

Richard D. Miller
Jianghai Xia

Final Report to

U.S. Geological Survey — WRD
North Carolina District
Raleigh, North Carolina

August 1, 1996

Open-file Report No. 96-4

Kansas Geological Survey
University of Kansas
Lawrence, Kansas

# High Resolution Seismic Surveys at U.S. Marine Corps Air Station, Cherry Point, North Carolina

*by*
Richard D. Miller
Jianghai Xia

*technical support by*
Joe M. Anderson
David R. Laflen

Final Report to

U.S. Geological Survey — WRD
North Carolina District
Raleigh, North Carolina

August 1, 1996

Open-file Report No. 96-4

Kansas Geological Survey
1930 Constant Avenue
Lawrence, Kansas 66047-3726

**Abstract**

Shallow seismic reflection techniques were successful in delineating stratigraphic units and bedding geometries significant to the hydrologic modeling of sediments less than 60 m deep at the U.S. Marine Corps Air Station at Cherry Point, North Carolina. Discontinuous confining units beneath an industrialized portion of this major aircraft overhaul facility were thought to be due the erosion by a river that had cut through this area. Shallow seismic reflection techniques provided images of alternating sand and clay sequences with average thicknesses on the order of 6 to 9 m. The data have a dominant frequency of about 200 Hz, providing a minimum vertical bed resolution of about 2 m. Correlation of the CDP stacked seismic section with the drillhole-defined lithology was enhanced by incorporating electric logs and VSPs acquired in three strategically placed monitor wells. Some processed VSPs have interpretable reflections from within the upper 70 m that are consistent with the geologic section as inferred from drilling and electric logs. Subtle stratigraphic contacts, such as shell layers within sand, may be interpretable in some places on the CDP stacked sections. The land seismic reflection data provided the very high horizontal and vertical resolution necessary for determining continuity of confining units and stratigraphic variations between 10 and 60 m at this site.

**Summary**

Shallow high resolution seismic techniques were used at the U.S. Marine Corps Air Station (MCAS) at Cherry Point to delineate structures and correlate stratigraphy between the Castle Hayne Limestone (~55 m below ground surface) and Yorktown confining unit (~11 m below ground surface). The primary goal of the study was two-fold: first, to detect and delineate the subsurface trace of Miocene and younger paleochannels inferred to underlie portions of the Air Station (Mixon and Pilkey, 1976; Hine and Riggs, 1986) and second, to determine the feasibility (i.e., resolution limits and signal-to-noise ratio) of the various acoustic methods to image the upper 90 m at MCAS. Three different methods and/or techniques were used to acoustically image and correlate the subsurface geology to existing geologic, hydrogeologic, and geophysical data. The first method employed a series of thirteen distributed 73 m long CDP lines that were acquired based on the results of walkaway noise tests and velocity check shot surveys conducted at one location from within the projected trace of a

paleochannel and one from outside the extrapolated subsurface feature (trace of the paleochannel inferred from borehole logs). These carefully placed CDP lines provided essential information about the acoustic properties and the signal-to-noise ratio of the upper 75 m. These profiles also allowed the acquisition parameters and equipment to be maximized for the site and enhanced placement so areal coverage of the longer continuous profiles acquired last could be optimized. Secondly, guided by the thirteen CDP lines, three boreholes were drilled and logged both for ground truth and to allow a series of time domain walkaway vertical seismic profiles (VSPs) to be acquired in each of the three boreholes. Walkaway VSPs were instrumental in correlating geologic contacts identified on electric logs and geologists' mud logs with the time series CDP stacked seismic section. Finally, three 12-fold CDP seismic reflection profiles possessing line lengths of 2160 linear m, 1460 linear m, and 1450 linear m were proposed that targeted channel features inferred from both drilling and single-channel marine seismic data. These long continuous lines were located to optimize borehole control, previous seismic reflection lines, cultural noise, near-surface conditions, applicability to hydrologic model, and probability of encountering paleochannels of the type interpreted on marine seismic data and correlated to existing borehole interpretations. An extremely complex series of erosional and depositional features can be interpreted on the CDP seismic reflection data. Seismic reflection proved an effective tool for the horizontal extrapolation of drill-defined features from borehole to borehole.

Initial walkaway testing, check shot surveys, and the thirteen distributed CDP profiles were designed and executed to evaluate the acoustic signature, optimum acquisition equipment and parameters, near-surface velocity structure, horizontal consistency in reflector character, stationwide resolution potential, variability of the signal-to-noise ratio, and impact of cultural noise (i.e., jet aircraft, industrial facility, vehicle traffic, etc.). The walkaway noise test allowed definitive selection of equipment and parameters as well as optimum station spacing and resolution potential. The check shot survey (uphole velocity/one-way travel time) established an approximate velocity structure for the upper 25 m of sediments in wells S1W1 and S3W3. The check shot surveys were critical to correlating drill/log-defined geology with reflections interpreted on CDP stacked sections. The thirteen CDP profiles provided an excellent overview of the acoustic variability, resolution potential, and range of signal-to-noise ratios

to expect around the Air Station. Several of the spot CDP profiles suggest that practical vertical bed resolution on the order of 1.5 m is reasonable in some areas around the Air Station. It is also clear from the short CDP profiles that horizontal extrapolation from borehole to borehole would be speculative at best beneath the Pliocene Yorktown confining unit about 12 to 15 m deep. This first evaluation/feasibility stage of the seismic survey at MCAS allowed thorough analysis of several acoustic techniques and methods, which in turn permitted accurate estimations of resolution as well as optimization of acquisition equipment and parameters.

Vertical seismic profiles are an extremely effective way of correlating the two-way travel time on a seismic reflection section with depths. VSPs have become an integral part of most petroleum exploration programs but are rarely fully utilized for near-surface seismic surveys. The walkaway VSP data were acquired with both a hydrophone and a holelock geophone, each sampling on 1.5 m intervals in monitor wells VSP1, VSP2, and VSP3 for each source offset to borehole, which ranged from 3 m to as much as 42 m offset, at 3 m intervals. The locations selected for the installation of the three monitor wells were in part determined through analysis of the thirteen distributed CDP profiles from around the Air Station. The correlation of reflections with reflectors with geologic interfaces was excellent using tool depth, geologic logs, geophysical logs, and reflections recorded on VSP files. The differences in source wavelet and attenuation are responsible for the subtle differences in reflection wavelet character observed between the two data sets (i.e., VSP profiles and CDP stacked sections). As evidenced on the VSP profiles, a significant number of interpretable reflections are present in areas where the gamma log seems to suggest subtle changes in lithology but the geologist logs quite conclusively suggest material changes. This is not uncommon considering the natural gamma is a radiation sensing tool and many sedimentary materials of the type indicated to be present on the geologist log may not initiate a response on a natural gamma log. The VSPs also allow extremely accurate average velocities to be determined and approximations of interval velocities. Average velocities, of course, allow correlation of time to depth independent of the source wavelet and acoustic imaging method (i.e., they were a help in correlating to depth on the marine survey as well as the GPR survey). The two different sensing tools (i.e., holelock geophone and hydrophone) allow continuous sampling of the boreholes every 1.5 m vertically,

regardless of whether the holes were water filled or air filled, while the source was walked away from the hole as much as 42 m.

The three CDP production profiles were designed to detect and hopefully image the expression of several channel features interpreted on marine seismic, inferred in boreholes, and then extrapolated between the two. The 12-fold CDP lines possess a horizontal resolution on the order of 5 m at 15 m and a practical vertical resolution of around 1.5 m. This very high resolution data set allowed extremely detailed interpretations of Miocene scour and infill features. On all three profiles a strong reflection interpreted to be the Yorktown confining unit is relatively flat and continuous at about 12 to 15 m of depth. An apparent change in the seismic character, geometry, and depositional sequence of this shallow reflection is observed on the westernmost north lines and on the southern end of the south line. This change (acoustically extremely similar on both lines) is likely related to Quaternary erosion. It is not possible to confidently ascertain if the Yorktown has been totally replaced by a younger clay or if the top of the Yorktown is partially eroded and then infilled with younger sediments. It is also not possible to unequivocally determine how deep the younger channel might have cut. Hydrologic modeling of the Miocene portion of the sequence would be extremely difficult due to the multiple cycles of scour and infill interpreted to be present across most of the lines. From a transport and fate perspective, the apparent continuity in the 12 to 15 m clay across most of the survey area is encouraging. Once the discontinuity in the clay is fully analyzed, the degree of isolation between the various upper Tertiary aquifers can be determined and appropriate measures taken.

**Introduction**

Understanding the various factors that control transport and fate of contaminates associated with the 50-year history of aircraft refitting and manufacturing at U.S. Marine Air Station at Cherry Point, North Carolina, is critical to current groundwater management and future remediation efforts (Figure 1). Basewide horizontal extension of borehole information necessary for the generation of groundwater flow models cannot be confidently done due to the documented localized absence of both the Yorktown and Upper Castle Hayne confining units (Lloyd and Daniel, 1988). The missing confining units are interpreted to be associated with an ancient river channel (paleochannel) underlying

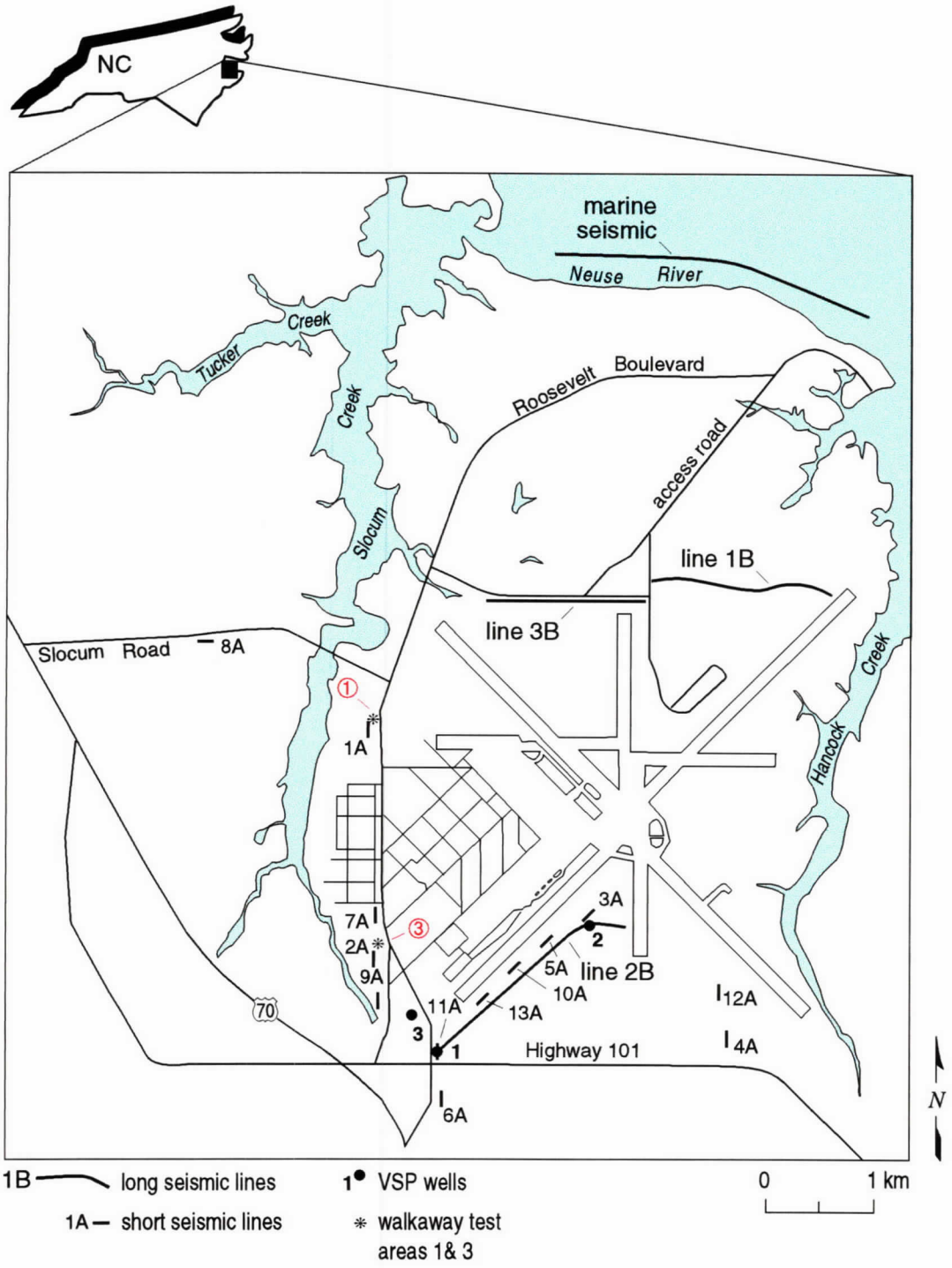


Figure 1. Site map of U.S. Marine Corps Air Station, Cherry Point, indicating the major roads, rivers, runways, seismic lines, and VSP wells.

a large portion of the industrial area of the Air Station. Contamination introduced at the ground surface during storage, disposal, and use has migrated into and resulted in the closing of several high-volume domestic and industrial water wells pumping from the 60 m deep Upper Castle Hayne aquifer. Water withdrawal from wells located near the proposed paleochannel could enhance both the velocity and direction of the contaminant transport.

Shallow high resolution seismic techniques possess the necessary resolution potential to delineate the paleochannel as inferred from drill data as well as correlate stratigraphy from well to well across the Air Station. Shallow land surveys have been successful imaging a shallow bedrock surface (< 100 m) as well as overlying unconsolidated sequences (Goforth and Hayward, 1992; Pullan and Hunter, 1990; Miller et al., 1989; Jongerius and Helbig, 1988; Birkelo et al., 1987; Miller et al., 1986). The effectiveness and importance of VSPs to accurately correlate two-way travel time reflections on CDP stacked section with borehole encountered geologic contacts for shallow surveys (i.e., <100 m) has only recently begun to become apparent (Schieck and Pullan, 1995). Incorporation of VSPs, borehole geophysical logs, and lithologic logs with marine and land seismic data will provide the most accurate and horizontally continuous representation of the unconsolidated lithology at this site.

This three-part seismic program required two site visits: September 19–26, 1994, and January 26–February 6, 1995. The site visit in September 1994 included the acquisition of thirteen short CDP lines (totaling 1971 shotpoints), walkaway noise testing (including 31 P-wave and 15 S-wave spreads), and two velocity check shot surveys (19 offset/depth records) (Figure 1). The walkaway noise tests and velocity check shot surveys were undertaken at two sites: one outside the interpreted trace of the channel (site #1) and one inside the channel (site #3). In accordance with the best information available at the time, the individual CDP lines were deployed liberally around the southern and southwestern portions of the Air Station in hopes of discriminating the reflection signature of sediments within the proposed paleochannel from those outside. Data acquired during the first visit assisted in selecting locations for the three VSP wells which, in conjunction with the marine seismic reflection survey, were instrumental in the line planning and parameter/equipment design for the three long CDP profiles (totaling 2065 shotpoints) collected during the second visit. The VSP traces (combining a total of 1445 offset/depth records) were also acquired during the

1996 trip. The intersection of the CDP survey lines with the VSP wells allowed ground truth ties that dramatically enhanced both the accuracy and confidence in correlating reflections with reflectors.

**Geology/Hydrology**

The Air Station is located on an approximately 1000 m thick sequence of Coastal Plain sediments overlying crystalline basement rock (LeGrande, 1960). The upper 60 m or so of unconsolidated material that overlays the Castle Hayne limestone (bedrock) at the Air Station represents the focus of this study (Eimers et al., 1990). The unconsolidated marine sediments above bedrock predominantly consist of alternating sands and clays with occasional shell beds and phosphatic sands. Of the nine aquifers present beneath the Air Station, only the shallowest four (surficial, Yorktown, Pungo River, and Upper Castle Hayne) are significant to this study and the hydrologic characterization as it relates to transport and fate of surface-introduced contaminant. The piezometric surface or water table at this site is generally consistent with mean sea level, which along the land survey lines ranges between 5 and 10 m below ground surface. The major clay/silt units (regionally thicker than a few meters) are generally considered and referred to as confining units while the more porous sands and limestones are the aquifers. Sand lenses and shell beds are occasionally present within confining units and clay stringers are routinely present within the aquifers. The Castle Hayne aquifer is a regionally consistent porous limestone that provides fresh water for many domestic, municipal, and industrial users in eastern North Carolina (Lloyd and Daniel, 1988).

Development of a meaningful groundwater flow model is critical to the management of groundwater resources and to the formulation of accurate contaminant isolation and extraction programs. Inadequate determination of the spatial variability and hydraulic characteristics of aquifers and confining units in this area would severely limit the usefulness of numerical groundwater flow models. The importance of compensating for localized discontinuities in the confining unit at this site is evident when considering the hydraulic conductivity (a principle input parameter for hydrologic modeling) of the four upper confining units ranges from .003 to .0003 m/d (meters/day) while the hydraulic conductivity of the aquifers ranges from 3 to 97 m/d (Eimers et al., 1990).

**Data Acquisition**

Several different types of acoustic surveying methods or techniques were employed to image geologic contacts/interfaces between 10 and 100 m deep as accurately as possible (Figure 1). A total of thirteen 24-fold, 73 m CDP lines were acquired in such a way as to utilize both the redundancy of the CDP method (Mayne, 1962) and efficiency of single point data (Glover, 1959). The three VSPs were acquired primarily to allow accurate time-to-depth conversion of reflections interpreted on the stacked sections, but the presence of key reflections also allow full-wave form correlation to the CDP stacked reflection wavelets. The three 12-fold seismic reflection profiles with surface coverage totaling over 4900 linear meters were acquired in a roll-along fashion to delineate channels inferred from other data as efficiently as possible. The integration of the various acoustic methods with the borehole derived geology greatly enhanced the continuity of the subsurface image.

The data from the September 1994 trip were recorded with a diverse set of equipment so the optimum equipment configuration, recording parameters, and technique could be selected for the long production lines. All data acquired for this portion of the study were recorded on a 48-channel Geometrics 2401X seismograph. This seismograph amplifies, filters (analog), digitizes the analog signal into a 15-bit word, and stores the digital information in a demultiplexed format. Analog filters have an 18 dB/octave roll-off from the selected -3 dB points. A 1/5 msec sampling interval resulted in a 200 msec record with a 2500 Hz Nyquist frequency. The thirteen short CDP sections were acquired with a 1000 Hz high-cut and a 200 Hz low-cut analog filter. The analog low-cut filter was necessary to properly shape the spectrum for maximum resolution of signal generated at this site (Steeples, 1990). The very site-dependent nature of acoustic source characteristics (Miller et al., 1994) prompted comparison of three types of compressional wave sources, including the 30.06 downhole rifle (projectile), the 12-gauge auger gun (downhole explosive), and both 5.5 and 9 kg sledge hammers (weight drop). Based on the signal-to-noise ratio, resolution potential (bandwidth, dominant frequency, and corner frequency), and power spectrum, the 30.06 downhole rifle was chosen as the optimum source for this study. Single 100 Hz and triple 40 Hz geophones were compared and evaluated, with the single 100 Hz geophone being selected for the study. Uphole velocity check shots were recorded to determine vertical incident travel time from the surface to reflectors. A single downhole

10 Hz hydrophone was used to record the downward traveling acoustic wave generated by a 7.3 kg sledge hammer striking a steel plate. Two 100 Hz geophones planted at the ground surface very near the well pad provided the QA/QC necessary to insure consistent time zero. The shear wave reflection technique was evaluated using the polarized miniblock seismic source (Miller et al., 1992) and single 40 Hz horizontal geophones. Guided by the results of walkaway testing and the uphole check shot survey, the initial thirteen compressional wave CDP data sets were recorded using a 120-station fixed spread and station spacing of 0.6 m, with the downhole 30.06 source moved through the spread. The results from this initial visit proved invaluable to the overall quality, economics, and consistency of data from the second visit.

The three 12-fold CDP production profiles and the VSPs were acquired during the January 1995 visit. Parameters and equipment were optimized based on the processed and analyzed results of the September trip. The seismograph used to record data from this trip was a 48-channel Geometrics StrataView. The StrataView amplifies, digitizes the analog signal into a 24-bit word, and stores the digital information in a demultiplexed format. The significant increase in dynamic range eliminated the need for a severe analog low-cut filter. Spectral analysis of data recorded with each seismograph confirmed that the effective bandwidth and upper corner frequency of the reflection data after digital filtering was not adversely affected by not recording with the analog low-cut on the StrataView. The increase in dynamic range of the StrataView in comparison to the 2401 is likely the reason for this consistency in spectral properties in spite of the absence of spectral shaping. Analysis of reflection data recorded on the first trip supported maintaining a sampling interval of 1/4 msec and a 250 msec plus record length. Field geometries were modified from the initial visit to maximize production without reducing the resolution potential of the CDP stacked sections. The 30.06 downhole source and 100 Hz geophones were deployed in an asymmetric split-spread source/receiver configuration with a nominal source-to-nearest receiver distance of 3 m and farthest receiver offset of 46 m. The greater dynamic range seismograph (StrataView) allowed for greater flexibility with respect to post-acquisition spectral shaping. The StrataView also allowed for high speed QA/QC with the nearly real-time digital filtering capabilities. Everything considered, the testing and stratigraphic analysis of the data acquired on the first trip dramatically improved the scope of the seismic project, allowing for

improved correlation to geology and both actualized signal-to-noise ratio, resolution potential, and the horizontal coverage/unit cost.

Two walkaway VSPs (one with a hydrophone and the other with a holelock geophone) were recorded at each of three VSP holes (Figure 1) (Table 1). Two profiles were recorded in each hole to allow interval velocities in both the saturated and unsaturated zones to be determined. To insure the several hundred shots recorded at each location would not suffer from appreciable deterioration in time zero or wavelet characteristics, a 5.5 kg sledge hammer was used to stack 3 to 5 shots per downhole location. Surface geophones recorded data simultaneously with each downhole receiver, allowing instantaneous inspection of shot to shot time break and wavelet consistency. Hydrophone recording stations began approximately 3 m below static water level while the holelock geophone recording was undertaken only in the air-filled portion of the hole. To increase overlap between hydrophone and geophone data, a portion of the water was removed from the borehole (this water removal process involved a packer and air lift system). Surface source stations were evenly spaced about 3 m apart extending radially away from the borehole. Downhole receiver stations were consistent for all source offsets and were separated by 1.5 m. Hydrophone surveys started approximately 2.5 m below the piezometric surface and extend the entire length of the open borehole. The holelock geophone survey began at least 6 m below the piezometric surface, moving upward to the ground surface. Resulting VSP walkaway profiles allow for interpretations of upgoing reflections and direct travel times. Interval velocity and average velocity for each station were determined for each borehole based on first arrival interpretations of the hydrophone data. Direct time to depth and waveform correlation of reflections on VSP data are possible with CDP stacked sections.

QA/QC were critical and continuous throughout acquisition and processing. Near-surface inconsistencies, traffic noise, jet aircraft noise, the extremely narrow and changing optimum recording window, and high moisture conditions made establishing QA/QC guidelines and meticulous monitoring of data an absolutely essential aspect of data acquisition. Based on subtle changes in the near-surface, minor adjustments to some parameters (e.g., source-to-near offset) were necessary to maintain the optimum recording window (Hunter et al., 1984). The seismograph CRT display, nearly real-time digital filtering, and real-time graphical display of noise levels permitted instantaneous monitoring of not only

**Table 1**

(all depth values are in meters from ground surface)

| Well ID | VSP1 | VSP2 | VSP3 |
|---|---|---|---|
| drilled hole depth (TD) | 50 | 48 | 62 |
| piezometric surface (WT) | 4.7 | 2.3 | 4.6 |
| hydrophone shallowest depth | 7.6 | 4.6 | 7.6 |
| hydrophone deepest depth | 49 | 47 | 61 |
| farthest source to well head | 30 | 46 | 58 |
| common source gathers | 3 | 4.6 | 5.8 |
| deepest hole-lock geophone depth | 18 | 18 | 12 |
| maximum air filled column | 23 | 21 | 24 |

cultural, air traffic, and vehicle traffic noise, but also cable-to-ground leakage and geophone plant quality. After each geophone was planted it was tested to insure a cable-to-ground resistance greater than 1000K ohms and an individual geophone continuity of 500 ohms (±20 ohms). As well, each geophone underwent a modified tap and twist test. No shot was recorded if background noise voltage levels on active geophones was greater than 0.05 mV. The ability of the seismograph to real-time monitor noise levels, signal quality (through digital filtering), and unacceptable geophone plants as well as the roll-switch's built-in earth leakage and continuity meters minimized the chances that any recorded shot would not be maximized for the site and equipment.

**Data Processing**

Data from this study were processed on Intel 80486 and Pentium-based microcomputers using *WinSeis*, a set of commercially available algorithms. Display parameters were determined based on scale of existing data sets, optimum exaggerations, and workable formats. During this study, the only operations or processes used were those that enhanced the signal-to-noise ratio and/or resolution potential as determined through evaluation of high confidence field file identified reflections.

The primary intent of the walkaway noise tests was to allow comparisons of various source, receiver, and instrument settings and configurations as they relate to overall improvements in the signal-to-noise ratio and frequency content. Walkaway tests are ideally suited for identification of individual events within the full wave field. Phase velocity and wave types are a couple of the most important pieces of information extractable from walkaways. This importance is due to the relationship of velocity and wave type to spread geometries and offsets (Pullan and Hunter, 1985). The level of testing is dependent on the objectives of the project and degree of difficulty obtaining the required resolution. Processing walkaway data for this study was limited to trace organizing, gain balancing, and digital filtering. Walkaway data from each source configuration or comparison parameter are displayed in a source-to-receiver order (Appendix A).

For most basic shallow high-resolution seismic reflection data, CDP processing steps are a simple scaling down of established petroleum-based processing techniques and methods (Yilmaz, 1987; Steeples and Miller, 1990). The

processing flow was similar to that used for routine petroleum exploration (Table 2). The main distinctions relate to the conservative use and application of correlation statics, precision required during velocity and spectral analysis, and the accuracy of the muting operations. A very low (by conventional standards) allowable NMO stretch (< 20%) was extremely critical in minimizing contributions from the very shallow reflected energy at offsets significantly beyond the critical angle. Limiting wavelet stretch through muting maximizes resolution potential and minimizes distortion in the stacked wavelets (Miller, 1992). Variability in depth of the first refracting horizon was as much as 10 msec across a single CDP stacked section. This depth variability was very effectively compensated for with a form of refraction statics. Processing/processes used on this data have been carefully executed with no *a priori* assumptions. Extreme care was taken to enhance through processing only what can be identified on raw data and not to create coherency on stacked sections.

Most processing steps/operations applied to shallow high-resolution seismic reflection data sets during the generation of CDP stacked sections are a simple scaled-down version of established processes developed for exploration of petroleum interests. Some processes have assumptions that are simply violated by many shallow reflection data sets and application of these processes could dramatically reduce data quality, or worse, generate artifacts. In particular, processes such as deconvolution and some forms of trim statics assume a large number of reflections with a random reflectivity sequence (Yilmaz, 1987). Migration is another process that, due to non-conventional scaling, many times appears to be necessary when in actuality geometric distortion may be a simple scale exaggeration (Black et al., 1994). The low-pass nature and coherency enhancing tendency of f-k migration improved the geometric accuracy and confidence interpreting CDP stacked sections. Consistency in arrival and apparent orientation of individual reflections after each process was critical to ensuring the authenticity of final interpretations.

The VSP data are processed to enhance correlation of drill determined geologic contacts with reflections interpreted on CDP stacked sections. The processing of VSP data is very straightforward (Appendix B, Table B1). In this case, the single-channel data are sorted into common source locations (which in appearance and for most practical purposes are equivalent to multichannel data) where the upcoming reflections can be extracted through slope filtering. After a static

**Table 2**

**Processing flow**

Primary Processing
format from SEG2 to KGSEGY
preliminary editing (automatic bad trace edit with 10 msec noise window)
trace balancing (150 msec window)
first arrival muting (direct wave and refraction)
surgical muting (removal of groundroll based on trace-by-trace arrival)
assign geometries (input source and receiver locations)
elevation correction to multiple, floating datums
sort into CDPs (re-order traces in common midpoints)
velocity analysis (whole data set analysis on 30 m/sec increments)
spectral analysis (frequency vs amplitude plots)
NMO correction (station dependent ranging from 400 to 750 m/sec)
correlation statics (2 msec max shift, 7 pilot traces, 100 msec window)
digital filtering (bandpass 25-50 250-375)
secondary editing (manual review and removal of bad or noisy traces)
CDP stack
amplitude normalization (whole trace with 40 msec delay)
correct to flat datum (15 m above sea level)
display

Secondary Processing
f-k filtering
f-k migration
deconvolution (spiking and second zero crossing)

correction is made for non-vertical travel path the data are corridor stacked. Corridor stacking is simply a summing process of all vertically incident corrected traces with a common source location. The final working display of VSP data resembles a synthetic seismogram, which allows direct overlay of the vertically incident VSP on a CDP stacked section. Incorporating the time-to-depth relationship, determined by first arrival analysis of unprocessed VSP data, with the overlay of the processed VSP data on the CDP stacked section permits high confidence correlation of reflections with reflectors.

**Results**

Shallow seismic reflection is a method that lends itself to over-processing, inappropriate processing, and minimal involvement processing. Interpretations must take into consideration not only the geologic information available but also each step of the processing flow and the presence (or absence) of reflection events on raw unprocessed data. Identification and confirmation of reflection hyperbola on walkaway noise tests is essential and is best accomplished through mathematical curve fitting, match to borehole-derived velocity structure, and comparison of file-to-file consistency. Walkaway noise tests are designed to horizontally over-sample the subsurface and record traces that place the source-to-farthest-offset at about twice the depth of interest. This allows for all aspects of the complete wave field (especially the reflections) to be thoroughly appraised.

The thirteen spot CDP sections were strategically located to determine consistency in reflection characteristics, depth to major reflectors, distribution and geometries of all reflections, signal-to-noise ratio at various places around the air station, and extremes of resolution potential across potential long CDP profiles (Figure 1). Acquisition parameters for these lines were based on the findings of the two walkaway noise tests (Appendix A). Line-to-line correlation of coherent reflections arrivals with similar wavelet characteristics and within particular time windows could be accomplished with reasonably good success and confidence. However, there is no geophysical basis for suggesting areawide continuity of reflectors as a result of apparent correlation of reflections line-to-line. In fact, in this Coastal Plain geologic setting an assumption of that nature would likely result in an incorrect geologic interpretation, and therefore a grossly inadequate hydrologic model. The short CDP stacked sections that produced the best data

quality were lines 3, 6, 8, and 13 (Figures 4, 8, 12, and 20). (Table 3 shows the geologic sequence of the confining units, an explanation of the composition of each confining unit, and the geologic and hydrologic unit designations used in interpreted figures throughout this report.) The dramatic difference in overall signal-to-noise and resolution potential of the data acquired from around the Air Station is best observed by comparing line 2 or 9 (Figures 3 and 14) with line 3 or 8 (Figures 4 and 12). Dominant frequency of the best stacked reflections is around 180 to 200 Hz. Considering the reflection characteristics of the four higher quality lines and the velocity information from both hyperbolic curve fitting and uphole surveys, the practical vertical resolution on long CDP profiles should be around 1.5 to 2.5 m and the horizontal resolution should be about 6 m at 25 m of depth based on the square root of the radius of the first Fresnel zone.

Line 8 possesses some of the most interesting reflection geometries (Figure 12). The 12 m deep reflector is interpreted to have a cut or scour feature that could represent the edge of a paleochannel extending beyond the imageable area of this line. It is reasonable to suggest that the 12 m reflector on the east is of different age than the one on the west side of the section. This age difference implies that the west side might be the eastern edge of an infill channel sequence. Correlating from short CDP line to short CDP line is clearly not possible after considering the channel fill feature interpreted on line 8.

Features that are significant to the shallow geologic setting clearly have the potential to dramatically change over very short distances. This is clearly demonstrated by the 40 msec reflection on line 8 (Figure 12). Even though the time tie between the 40 msec reflections at CDPs 2030 and 2190 are within a few msec, the cut-and-fill feature interpreted between those CDPs clearly indicates that any reflector can change age and lithology across distances as short as this 75 m line. A similar feature can be interpreted on line 6, but the lower signal-to-noise ratio makes detailed analysis speculative. Three VSP boreholes and three long seismic lines were proposed after considering line locations, near-surface characteristics, resolution potential, maximization of information for a hydrologic model, and the complement to existing boring information of all thirteen seismic lines collected as part of this initial test.

Interpretation of the seven highest signal-to-noise ratio short stacked sections provide informative comparisons and interpretations of wavelet characteristics and associated geology. The interpretation of line 3 (which was the basis

## Table 3
## Designation of Geologic and Hydrologic Units

QUATERNARY — Includes the surficial aquifer and the Yorktown confining unit.

Surficial aquifer. The surficial aquifer is the uppermost aquifer of the study area and is exposed at land surface in streambeds throughout the Air Station. This aquifer consists of unconsolidated and interfingering beds of fine sand, silt, clay, shell and peat beds, and scattered deposits of coarser-grained material as part of relic beach ridges and alluvium.

**Basal contact of channel cuts.**

**Channel infill.**

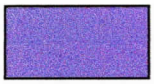

**Yorktown confining unit.** The Yorktown confining unit is composed of clay and sandy clay with locally discontinuous, thin beds of fine sand, silty sand, or shells. The Yorktown confining unit is not exposed at land surface on the Air Station, but the Neuse River channel may be incised into it in this vicinity (Winner and Coble, 1989). The Yorktown confining unit is missing in at least one area beneath the southern part of the Air Station.

TERTIARY — Includes the Yorktown aquifer, Pungo River confining unit and aquifer, Upper and Lower Castle Hayne confining units and aquifers, and the Beaufort confining unit and aquifer.

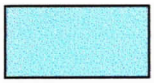

**Pungo River confining unit.** The Pungo River confining unit is composed of contiguous sandy clays of the lowermost Yorktown Formation and the upper clay and sandy silt beds of the Pungo River Formation (Kimrey, 1964; 1965). The Pungo River confining unit is inferred missing in at least one place at the south end of the Air Station, possibly because of erosion, nondeposition of clay, or the presence of a paleochannel.

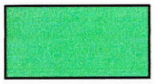

**Upper Castle Hayne confining unit.** Regionally the upper Castle Hayne confining unit consists of interbedded clays, sandy clays, silts, sands, and phosphatic and nonphosphatic limestones that occur in the basal unit of the Pungo River Formation. Beneath the Air Station, however, this confining unit consists of sand, silty sand, and abundant shells and shell fragments. Thin beds of sand are also present. The upper Castle Hayne confining unit overlies the upper Castle Hayne aquifer, which is present everywhere beneath the Air Station.

**Lower Castle Hayne confining unit.** The lower Castle Hayne confining unit is composed of clay, sandy clay, and sand. This unit is slightly thicker in the northern part of the Air Station (Eimers et al., 1994).

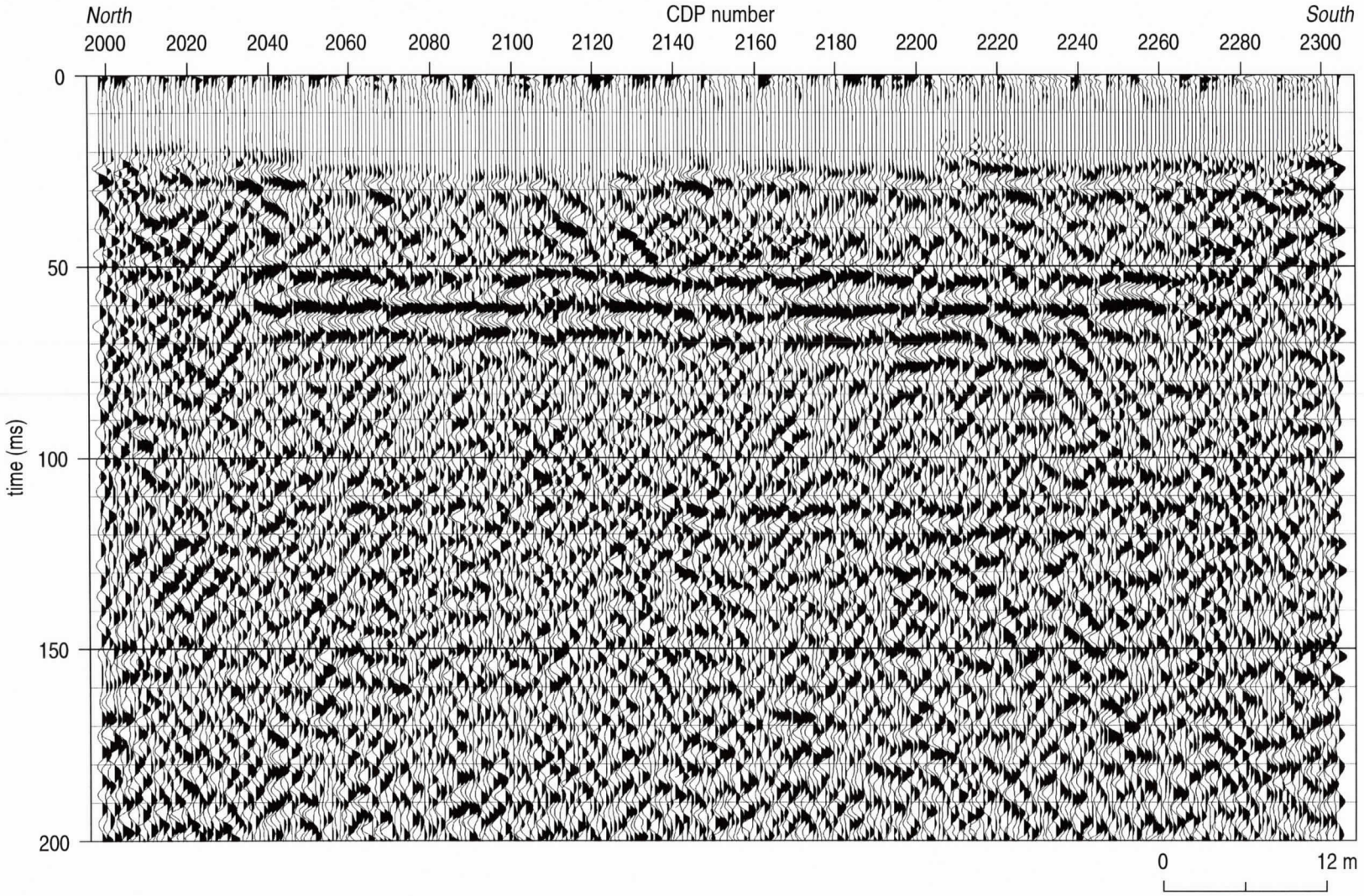


Figure 2. Nominal 24-fold spot CDP stacked section of line 1 from site #1.

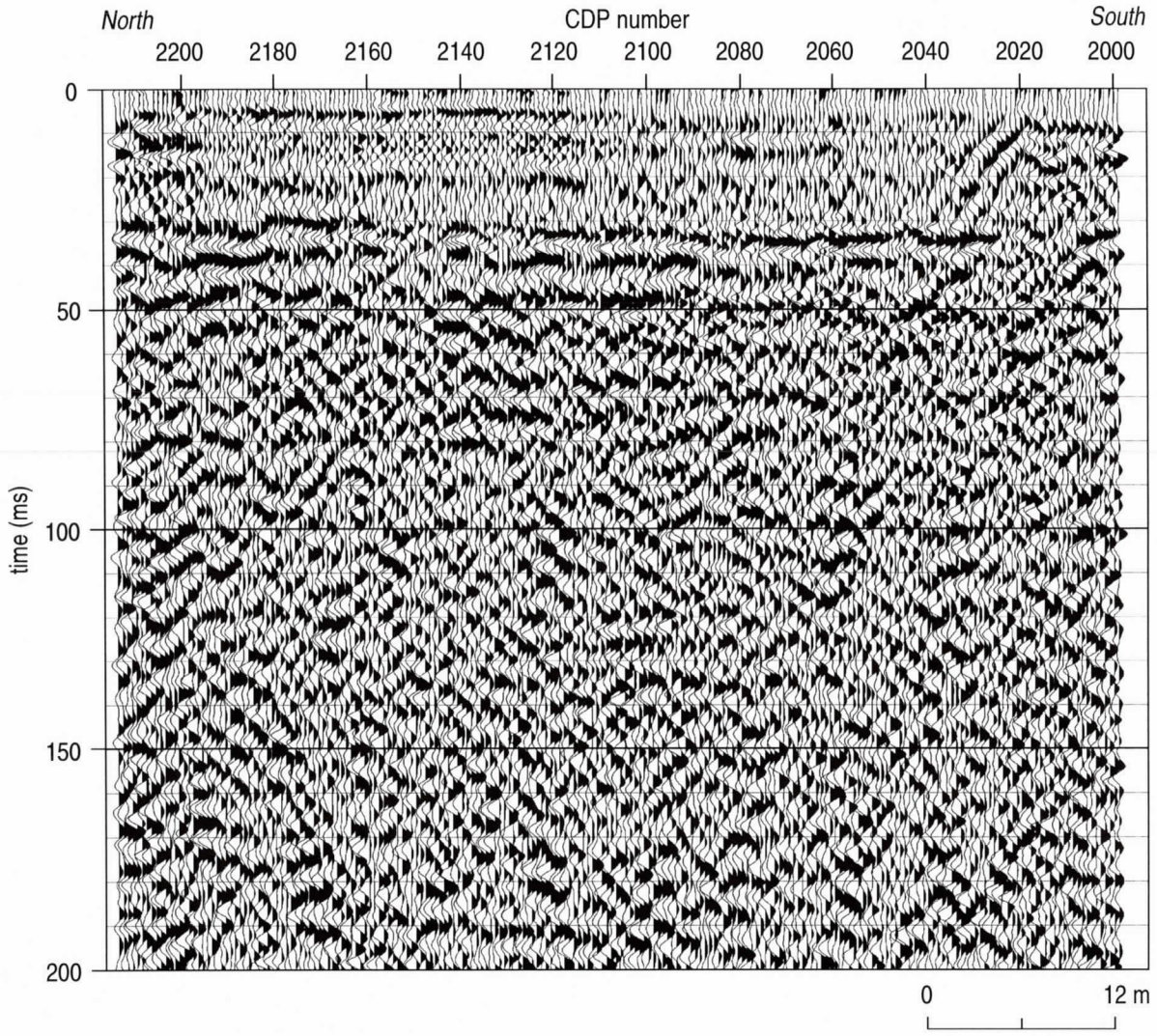


Figure 3. Nominal 24-fold spot CDP stacked section of line 2 from site #3.

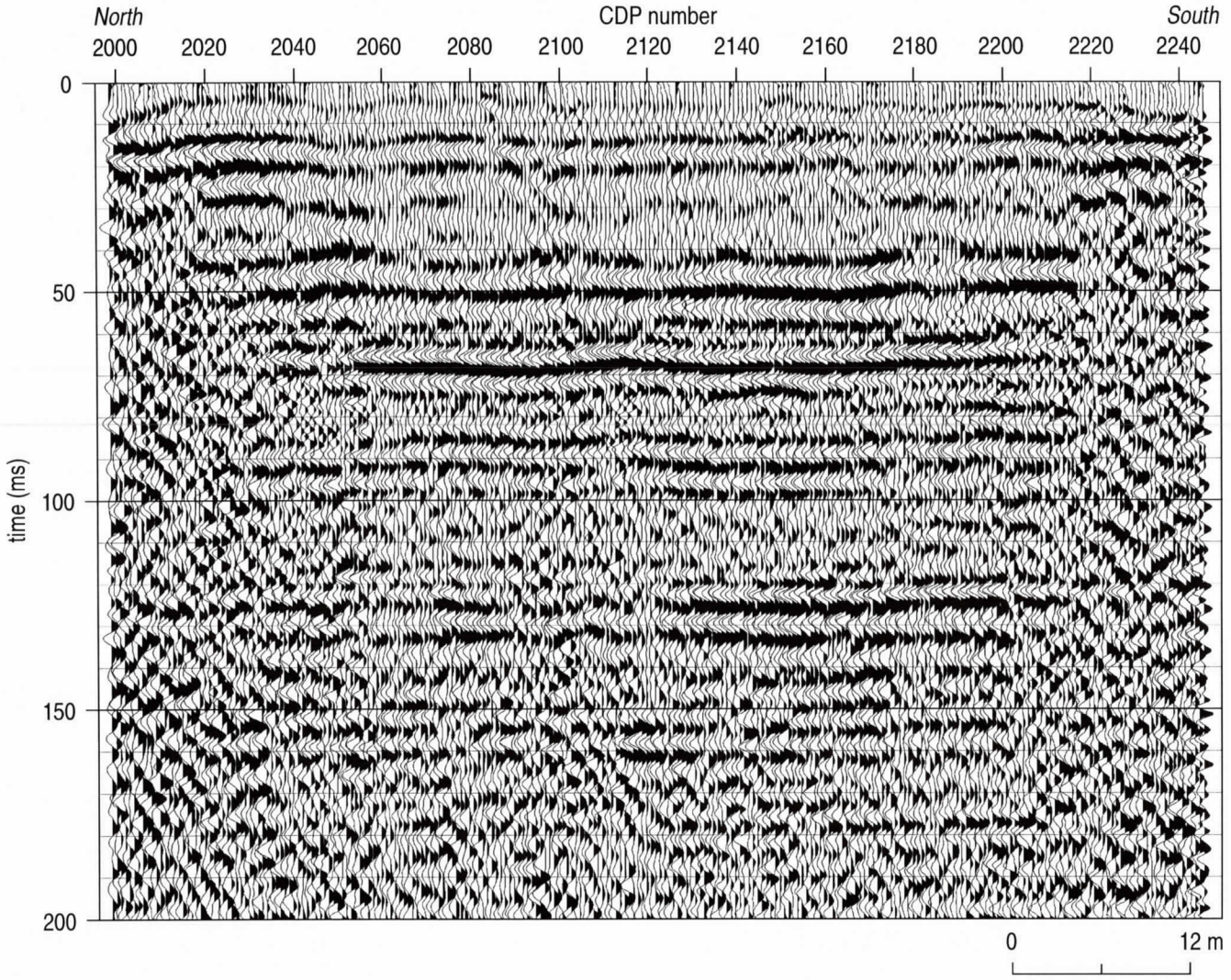


Figure 4. 24-fold spot CDP stacked section of line 3. Section instrumental in location of VSP #2 well.

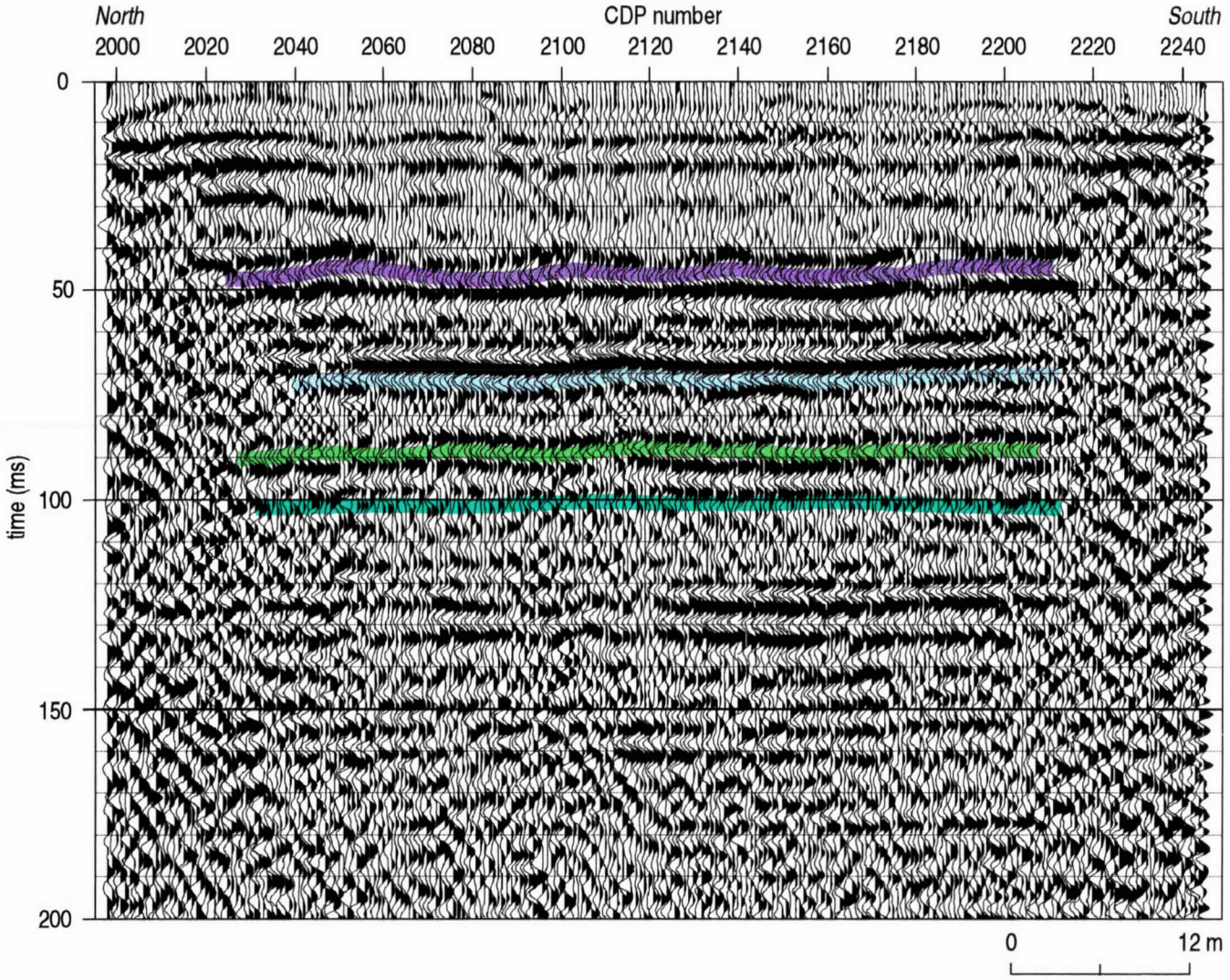


Figure 5. Interpreted nominal 24-fold spot CDP stacked section of line 3. Section instrumental in location of VSP #2 well.

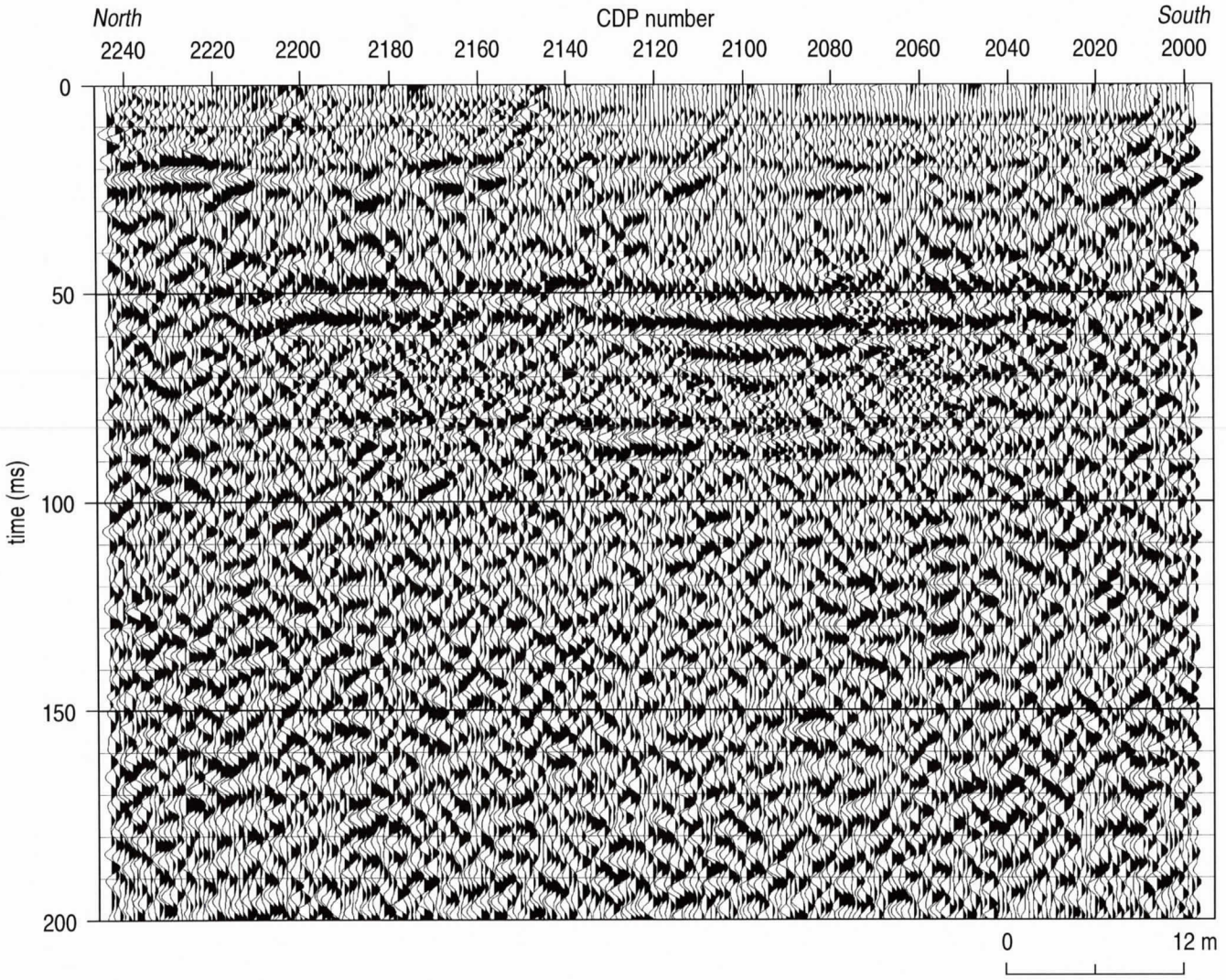


Figure 6. Nominal 24-fold spot CDP stacked section of line 4.

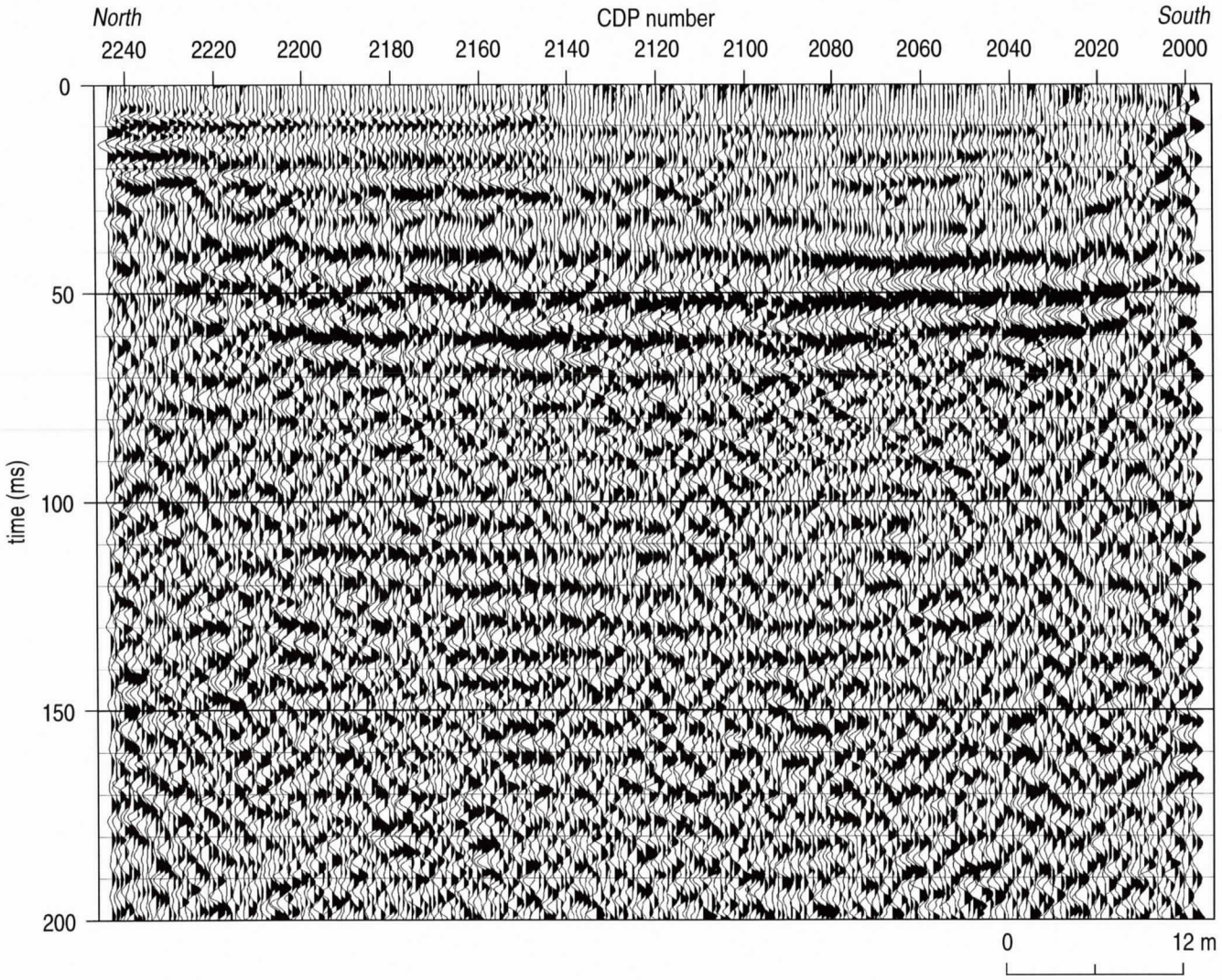


Figure 7. Nominal 24-fold spot CDP stacked section of line 5.

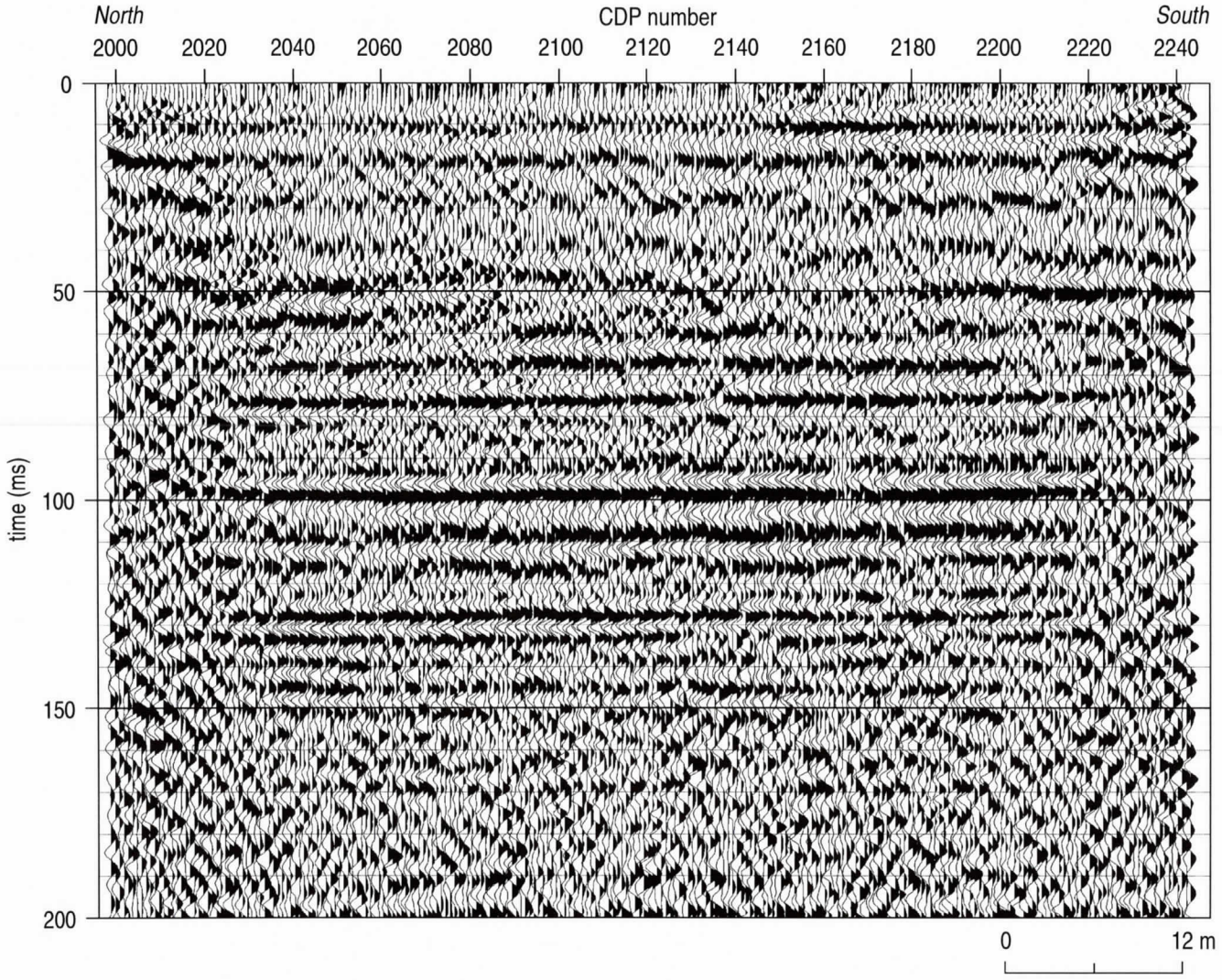


Figure 8. Nominal 24-fold spot CDP stacked section of line 6.

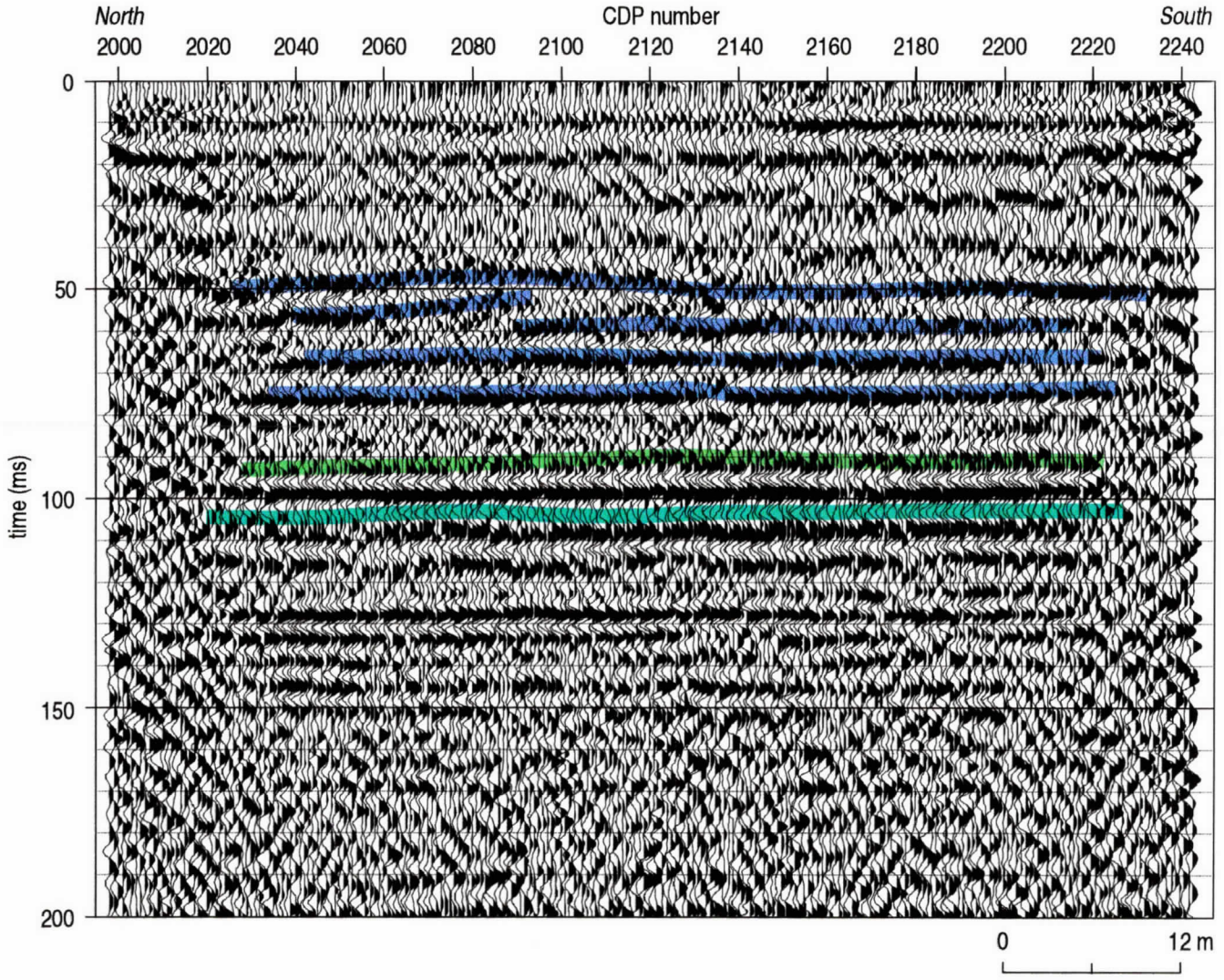


Figure 9. Interpreted nominal 24-fold spot CDP stacked section of line 6.

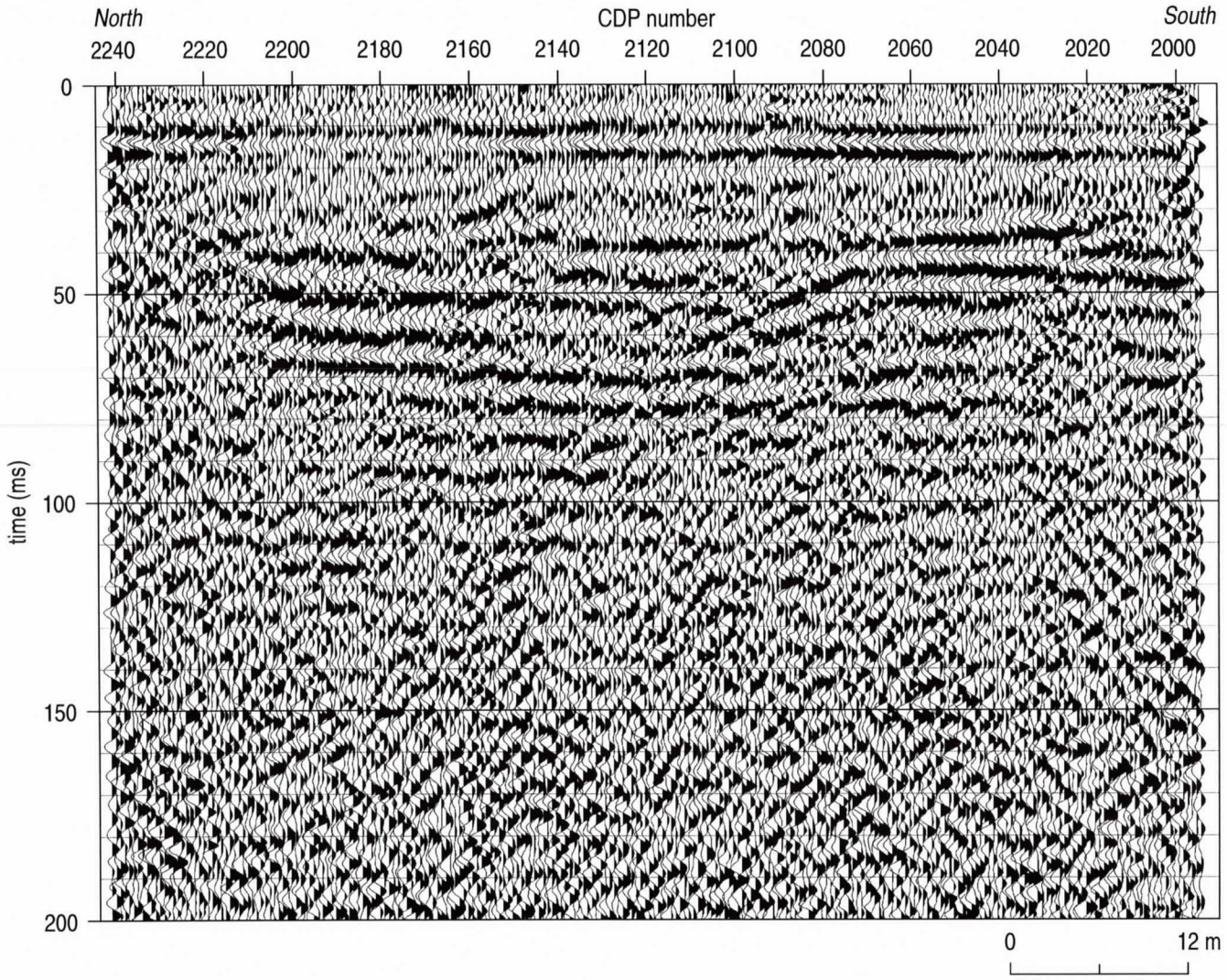


Figure 10. Nominal 24-fold spot CDP stacked section of line 7.

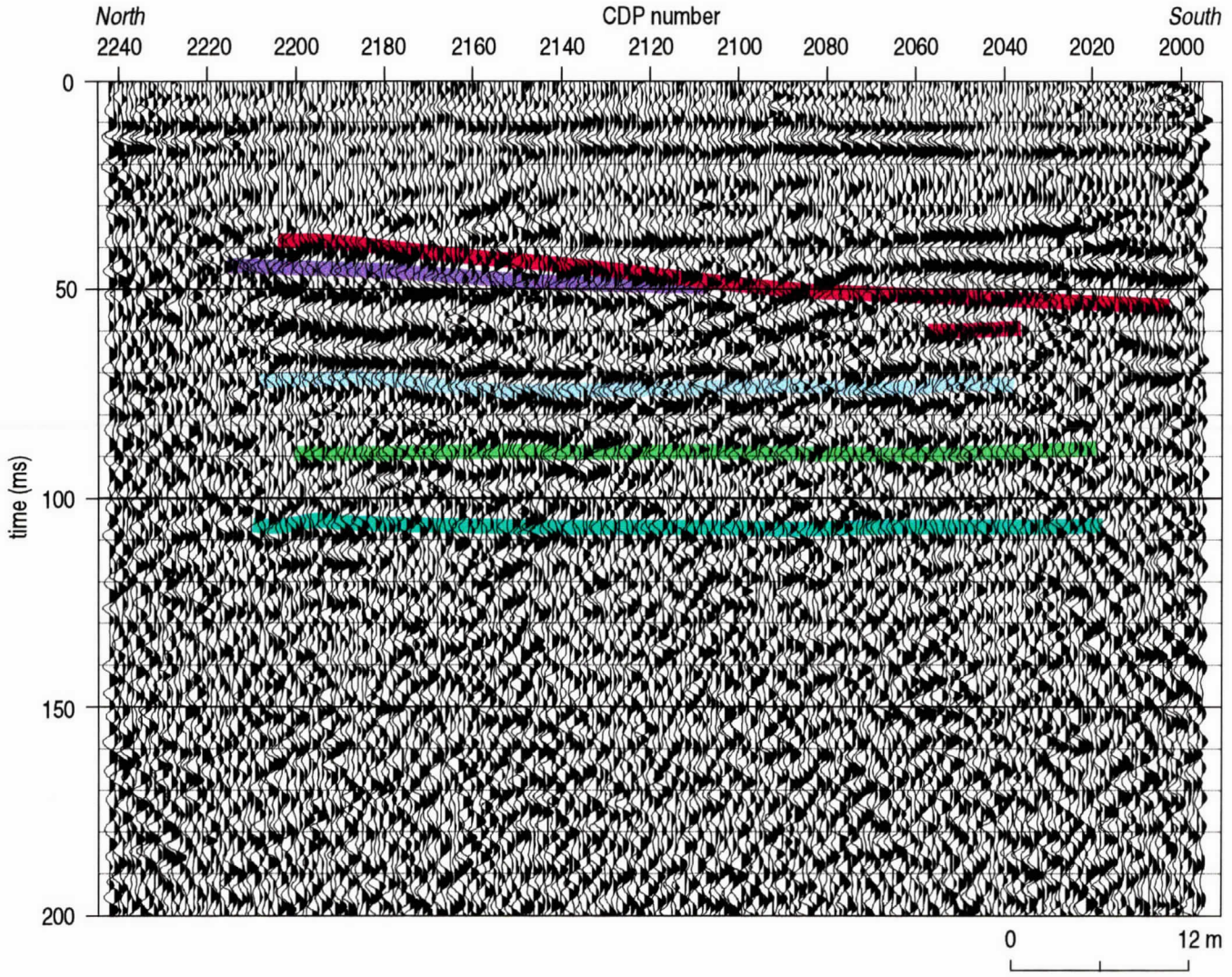


Figure 11. Interpreted nominal 24-fold spot CDP stacked section of line 7.

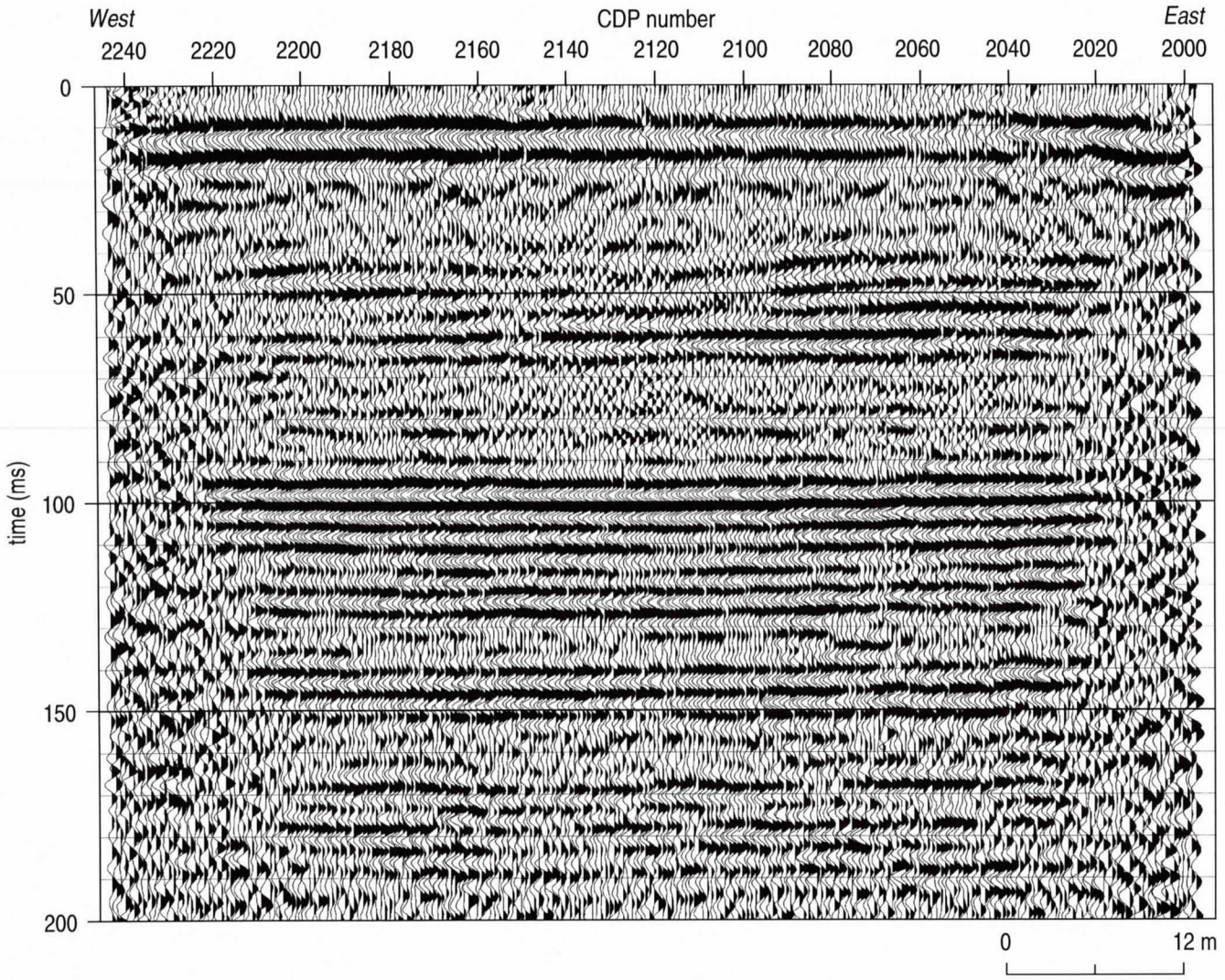


Figure 12. Nominal 24-fold spot CDP stacked section of line 8.

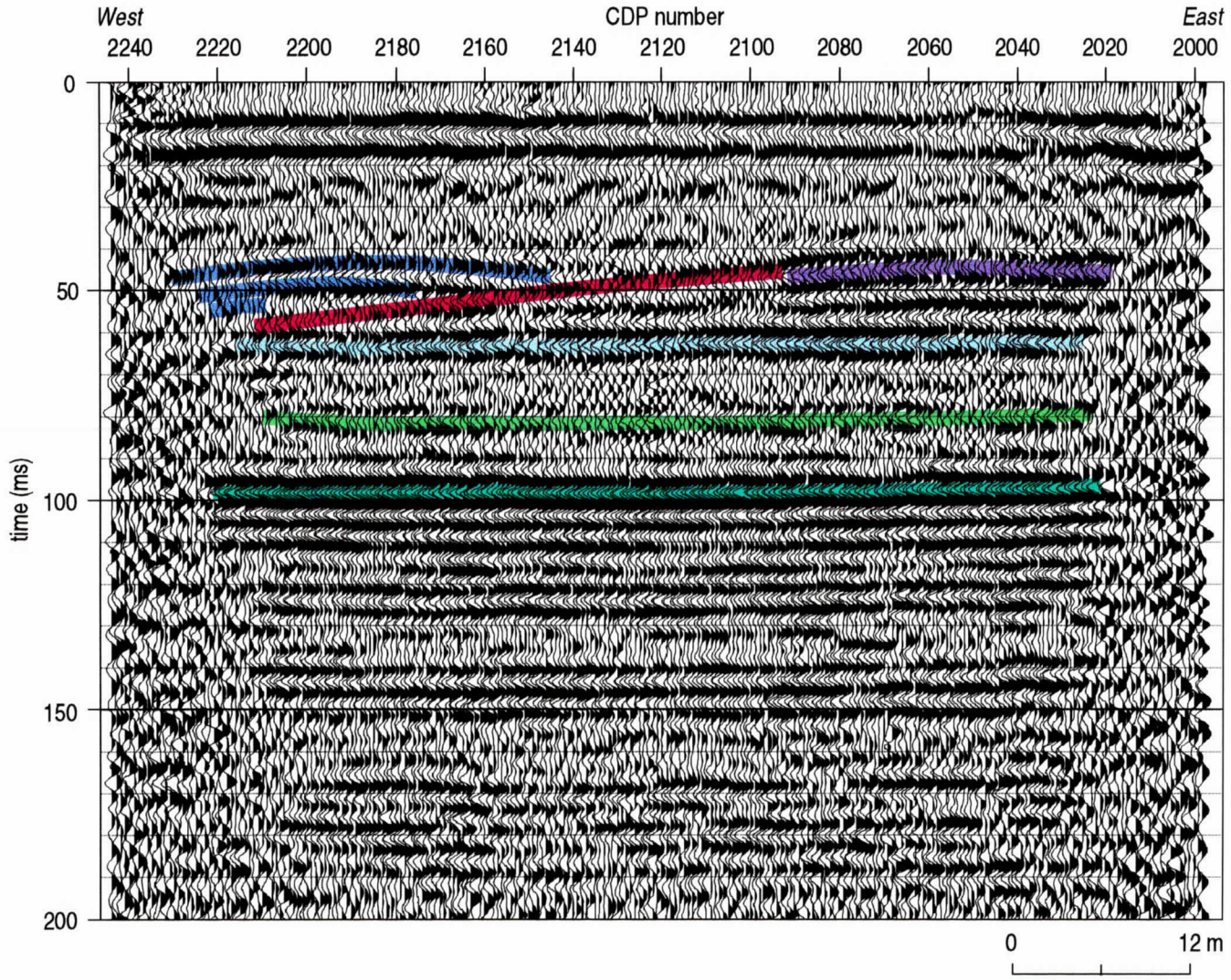


Figure 13. Interpreted nominal 24-fold spot CDP stacked section of line 8.

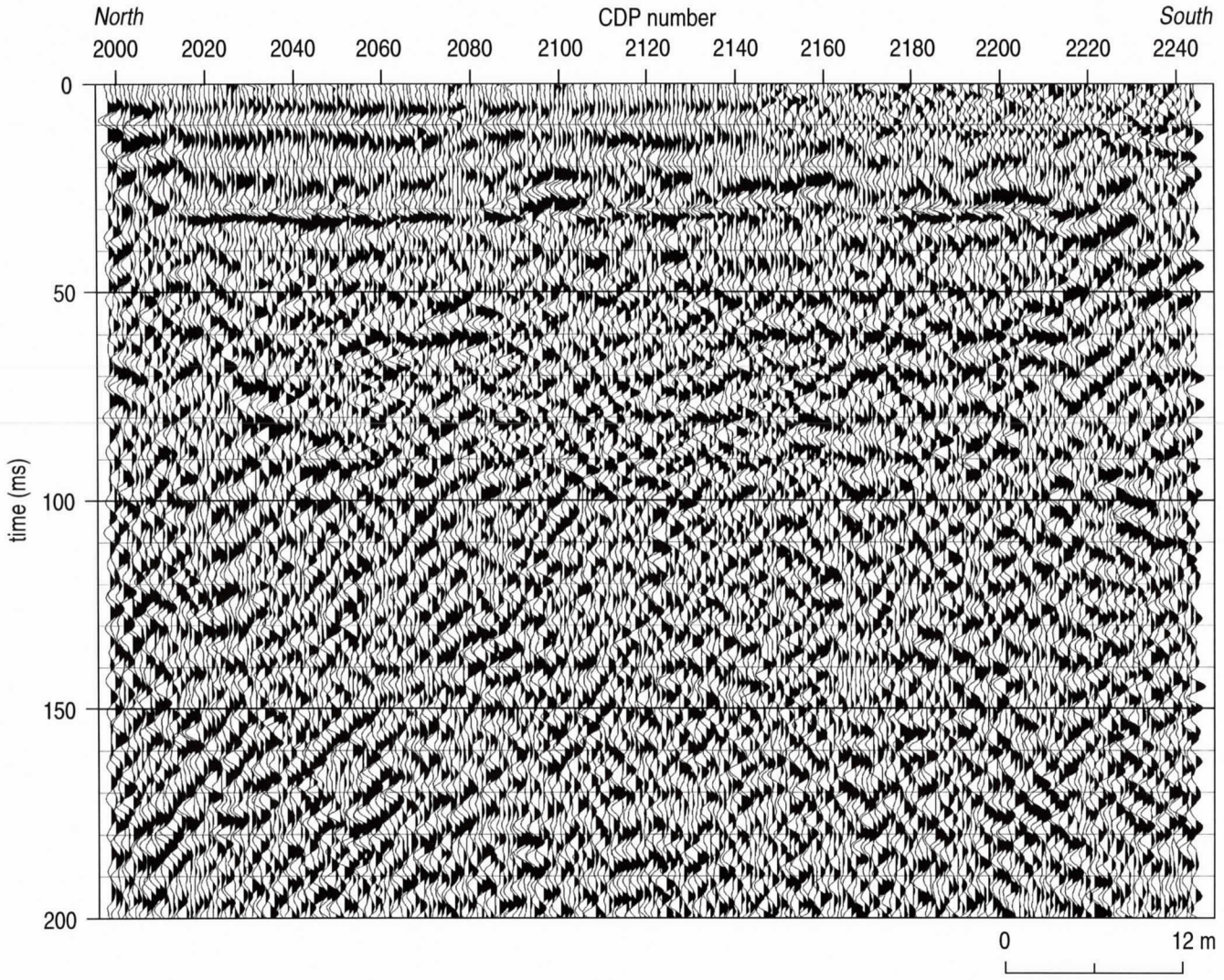


Figure 14. Nominal 24-fold spot CDP stacked section of line 9.

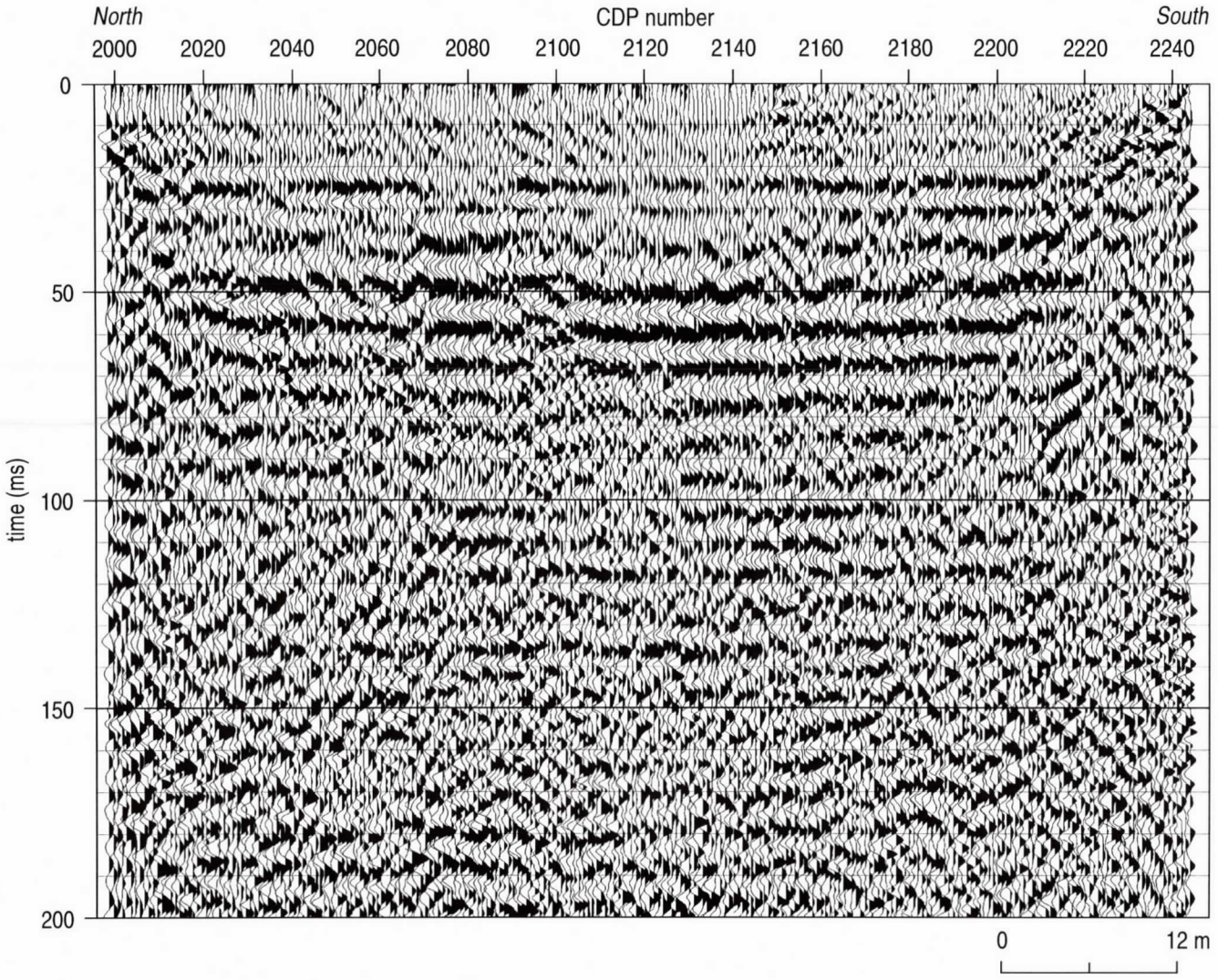


Figure 15. Nominal 24-fold spot CDP stacked section of line 10.

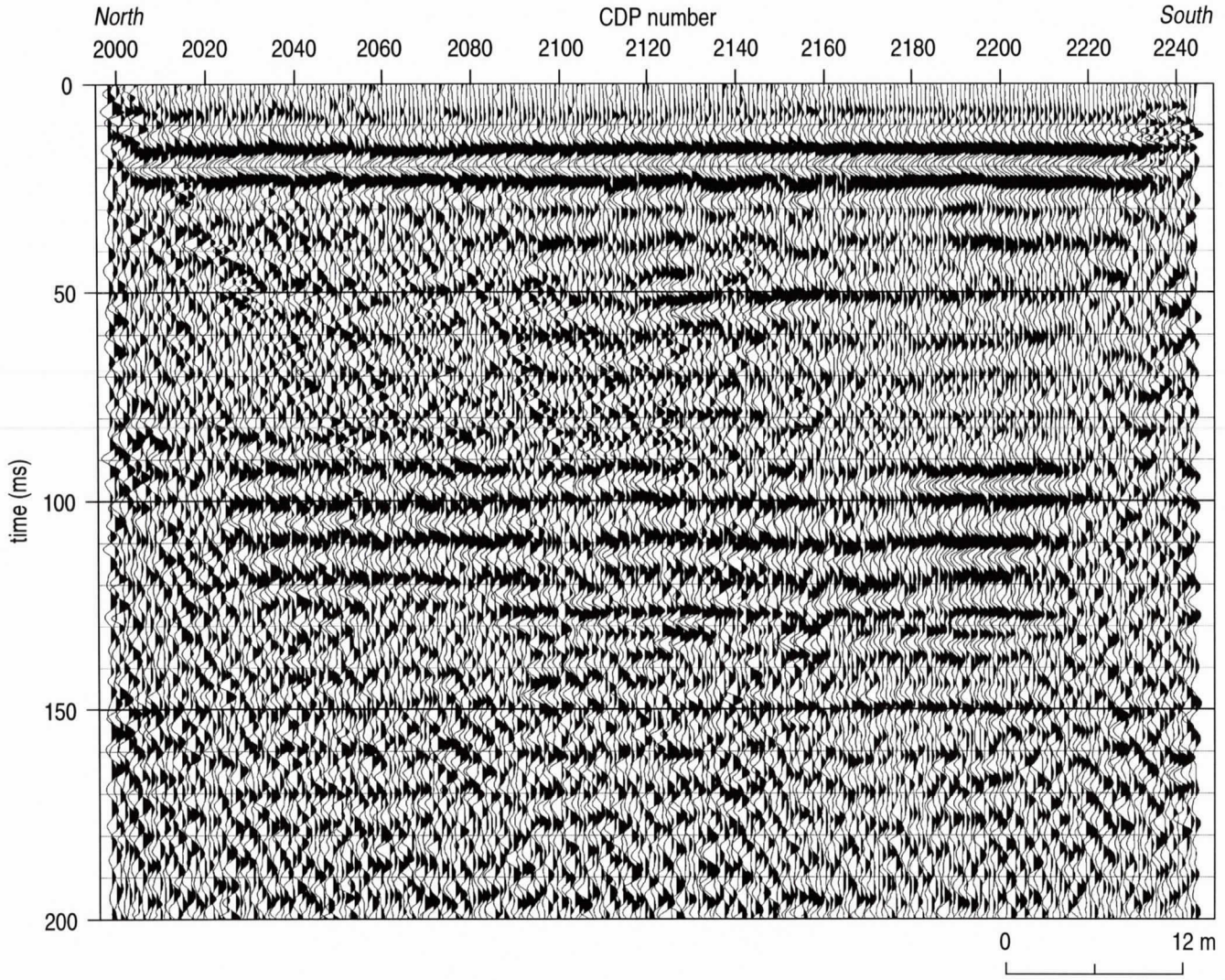


Figure 16. Nominal 24-fold spot CDP stacked section of line 11. In part responsible for placement of VSP #1 well.

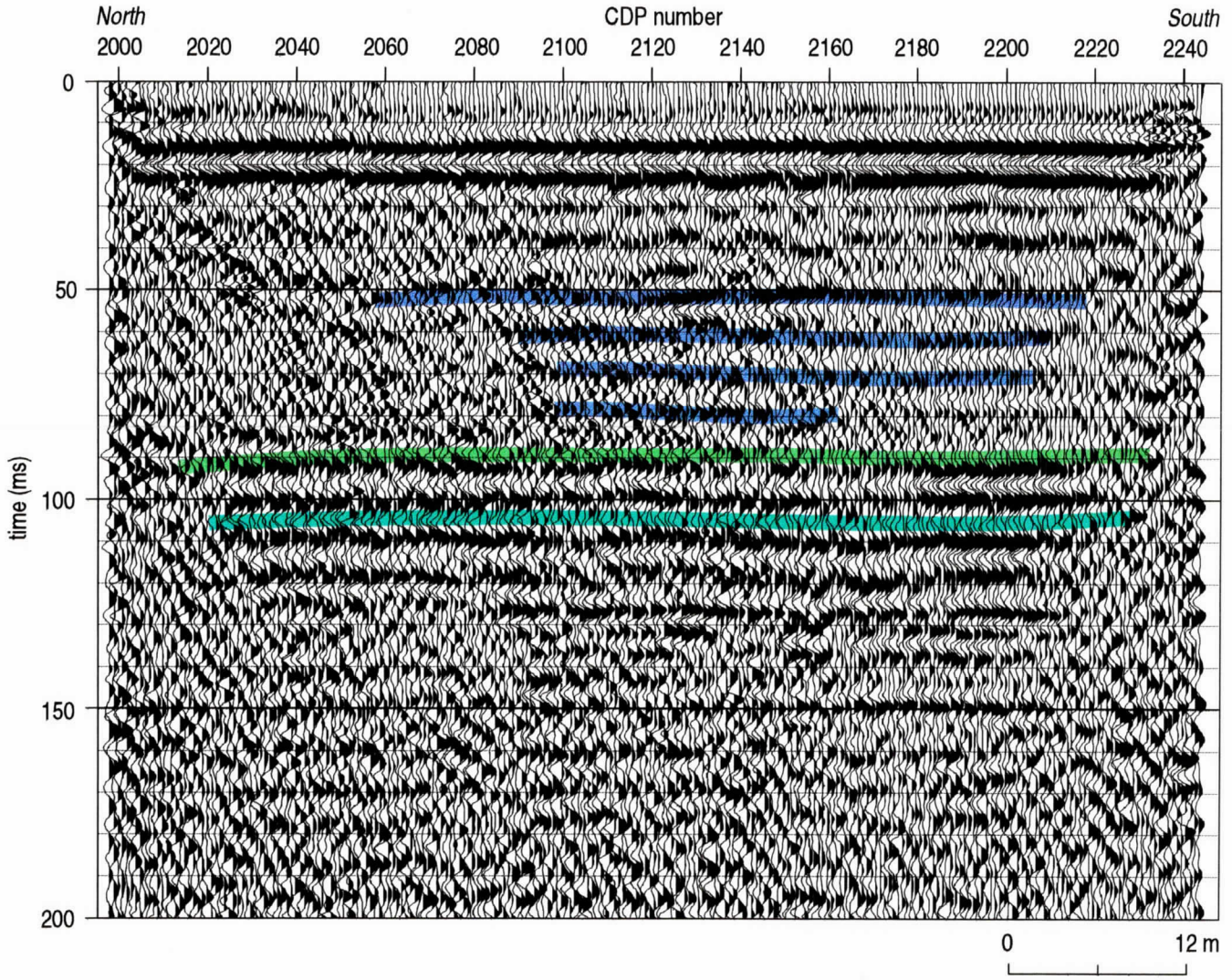


Figure 17. Interpreted nominal 24-fold spot CDP stacked section of line 11.

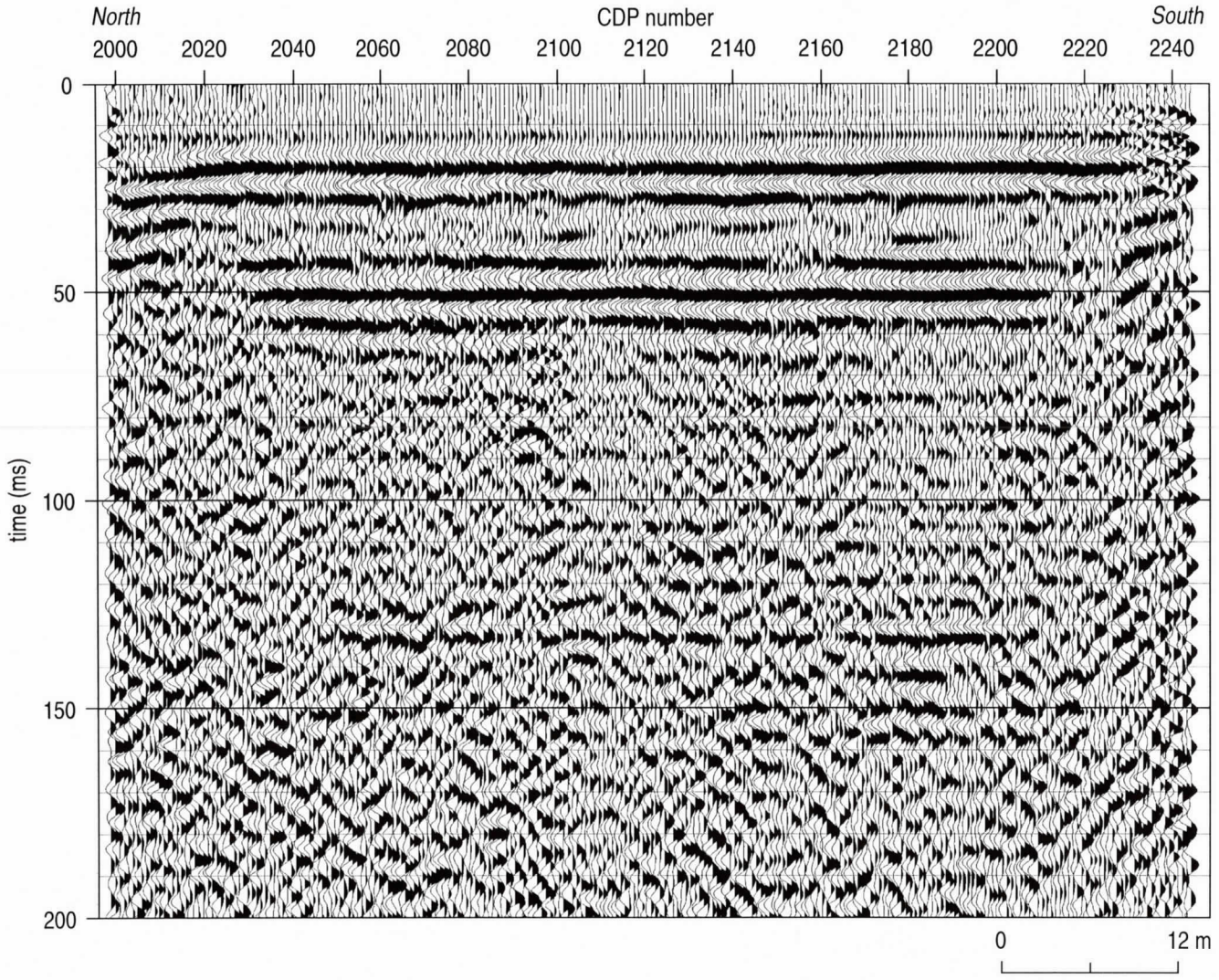


Figure 18. Nominal 24-fold spot CDP stacked section of line 12.

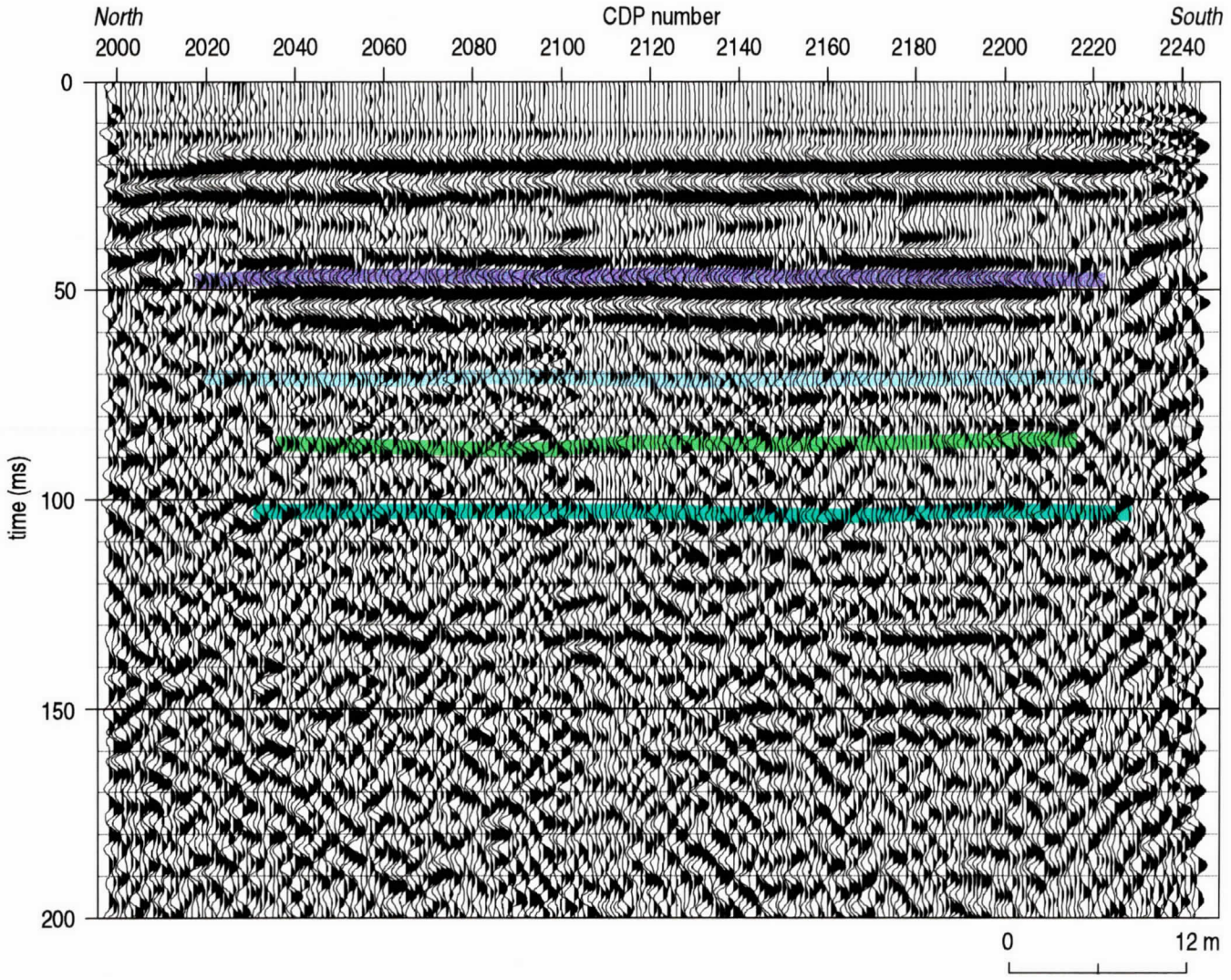


Figure 19. Interpreted nominal 24-fold spot CDP stacked section of line 12.

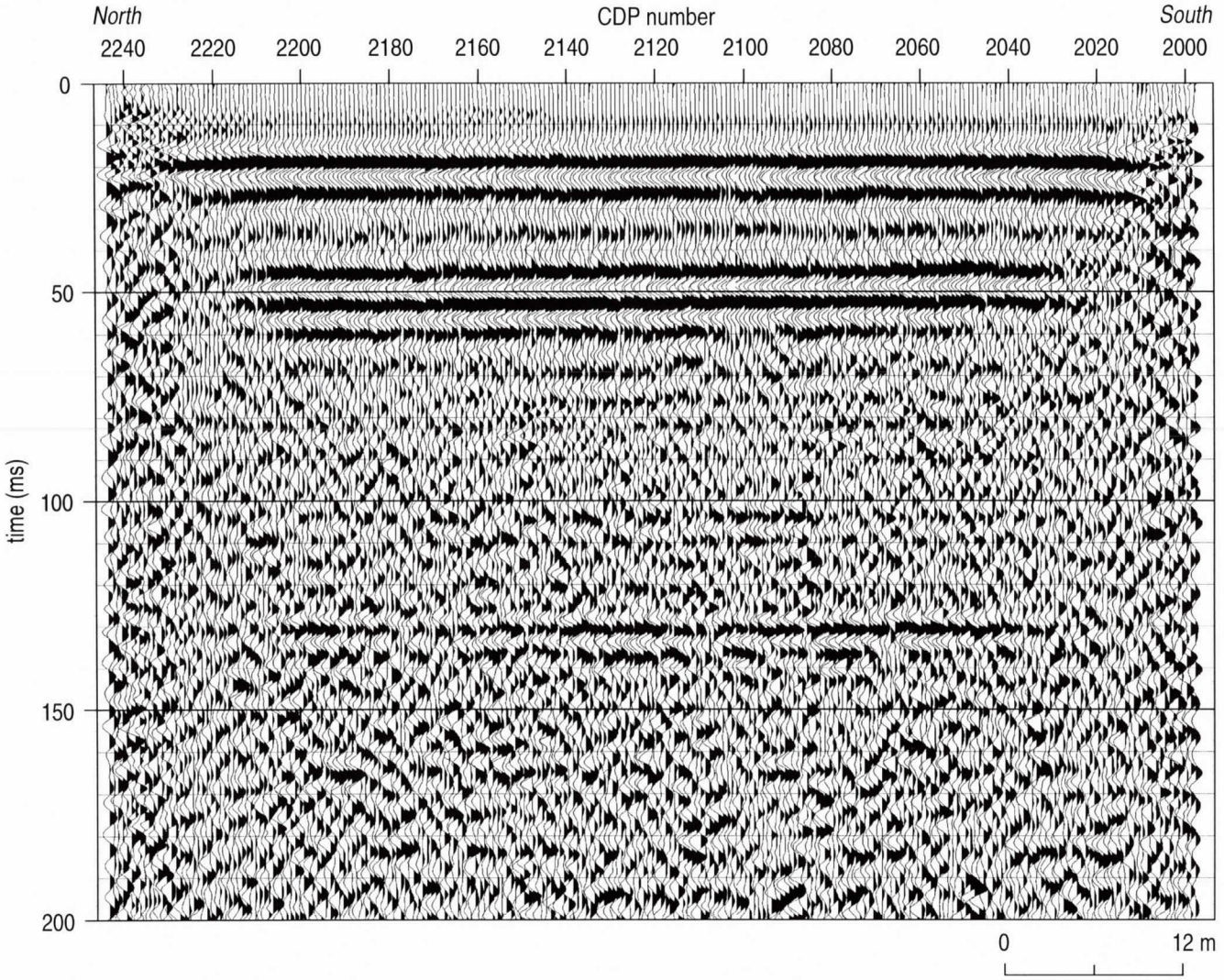


Figure 20. Nominal 24-fold spot CDP stacked section of line 13.

for the location of VSP #2 well) possesses several very high frequency reflection events that seem to correlate very well with the known geology (Figure 5). The resolution potential of line 3 is on the order of a few feet based on a dominant frequency of about 180 Hz. The color interpretations are coded according to inferred geologic units as determined from borehole velocities, electric logs, and geologists logs (Table 3). The complete geologic section appears to be present along lines 3 and 12 (Figures 5 and 19). Reflections interpreted along lines 6, 11, and 13 (Figures 9, 17, and 21) are significantly different, appearing to possess much lower resolution potential and narrower bandwidth than those on lines 3 and 12. It is likely, based on the difference in wavelet properties and borehole information, that reflections above about 70 msec (55 m) on lines 6, 11, and 13 are from within the paleochannel and are, of course, much younger than the reflections at equivalent times on lines 3 and 12. Interpretations of lines 7 and 8 (Figures 11 and 13) both suggest transition between channel materials and a complete, relatively undisturbed section. Line 7 appears to have imaged the eastern/northeastern edge of the proposed paleochannel that may pass beneath the industrial area of the Air Station (Daniel, 1996). Line 8 data is extremely high quality and has likely imaged a part of a completely separate channel east of the paleochannel, or this channel could be a tributary to the major channel present farther southwest. By incorporating the 13 stacked section interpretations with borehole information (including the VSPs) and the three long CDP lines (to be discussed later), a very reasonable geologic framework can be developed for the unconsolidated material in the upper 55 m at each line location.

The walkaway VSPs were designed to allow accurate designation of two-way travel time from the ground surface to reflectors of interest and to provide a wiggle trace representation of the reflectivity sequencing of the wells (Appendix B). The wiggle trace display allows correlation of reflection wavelets with specific acoustic boundaries (Figures 22, 23, and 24). The two-tool sampling method (hydrophone and holelock geophone) was necessary to provide a continuous velocity profile from the ground surface to the bottom of each borehole. Sufficient overlap (redundancy in measurements at or near the water table surface) between the two tools was provided to insure accurate values in the transition zone. Due to a lack of saturation, and therefore poor casing-to-borehole coupling—and since the interval sampled with the geophone was the vadose zone while the hydrophone data were all collected at least 1.5 m below the water

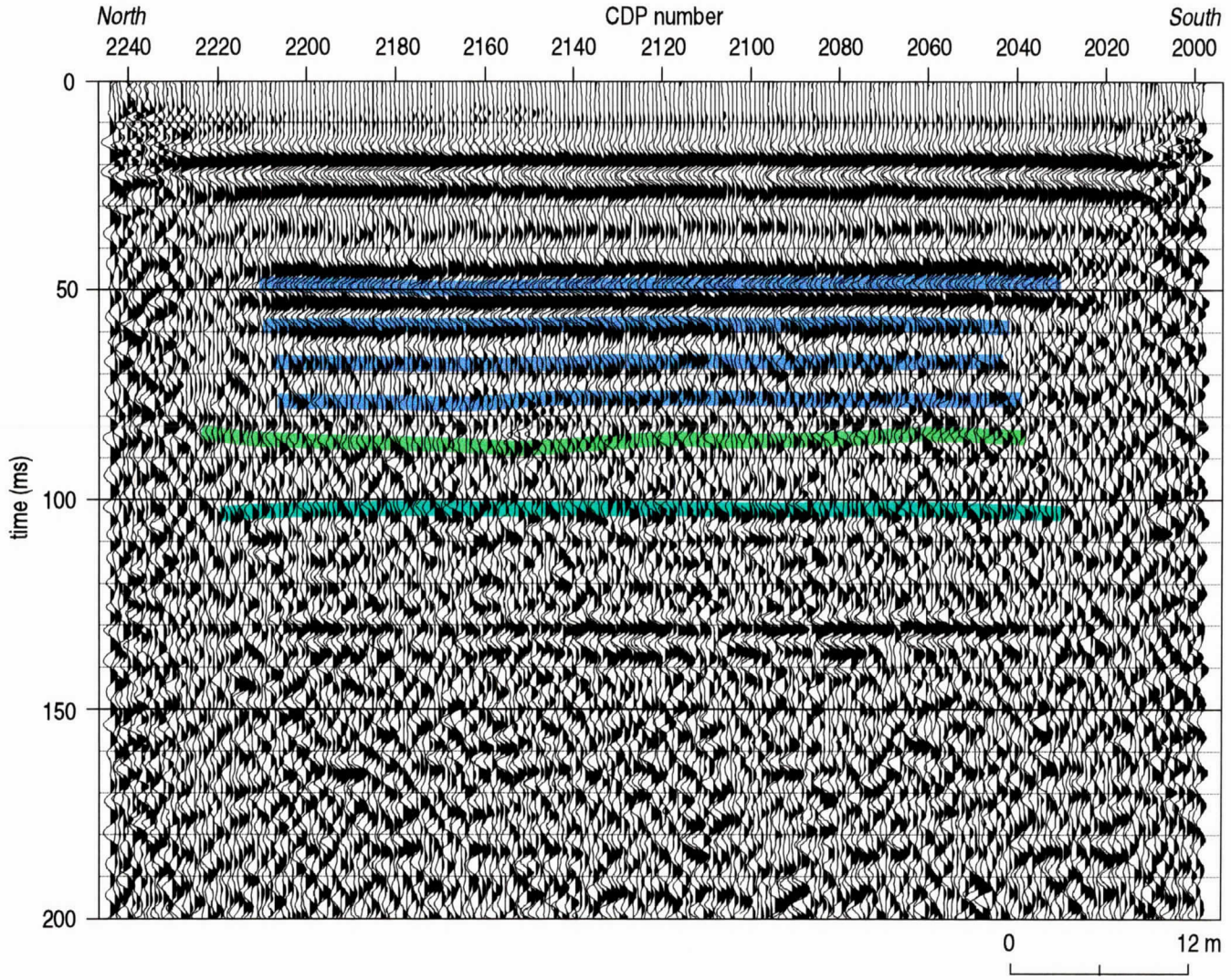


Figure 21. Interpreted nominal 24-fold spot CDP stacked section of line 13.

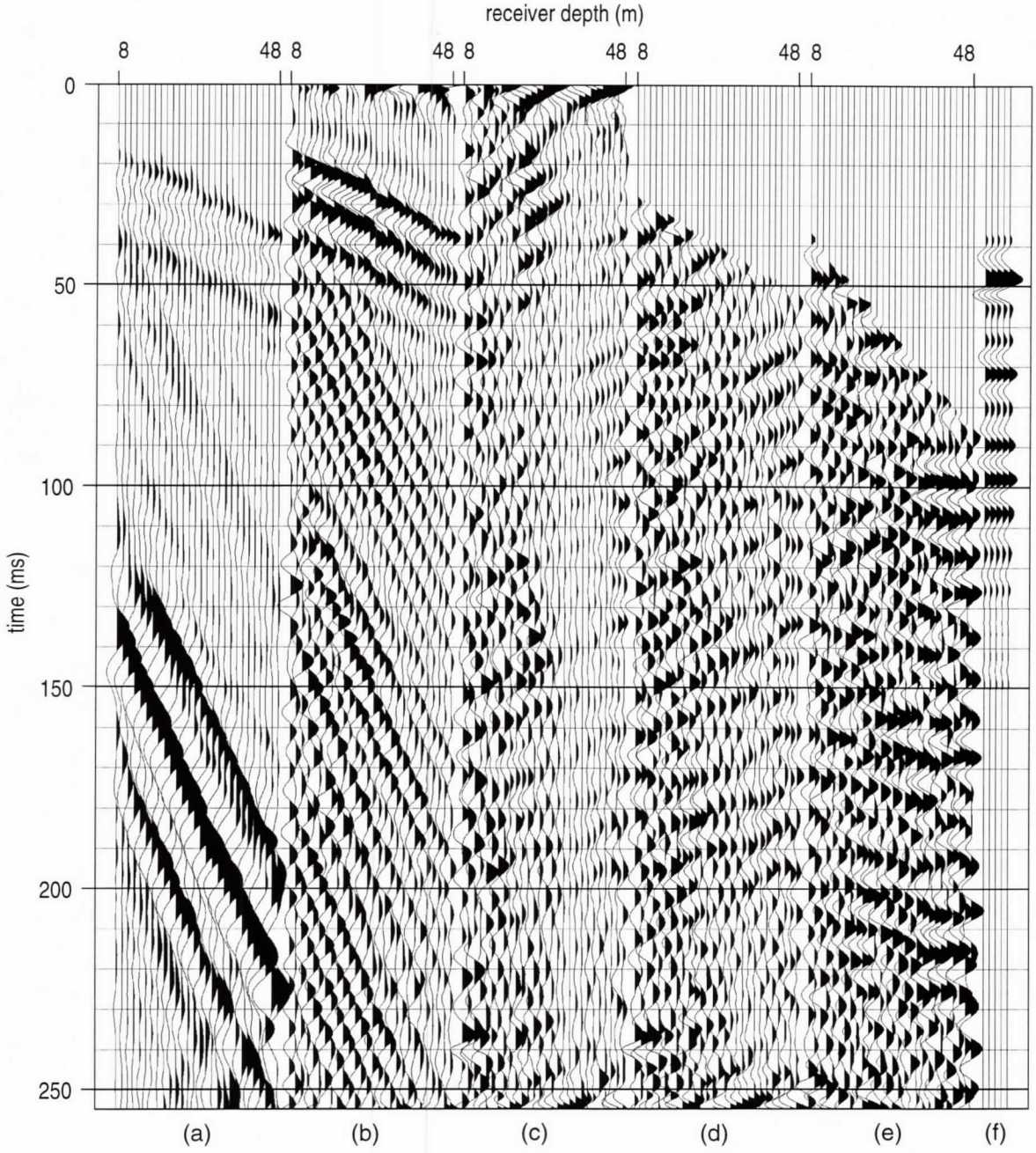


Figure 22. VSP files with 18 m source offset showing (a) raw data, (b) filtered and scaled, (c) fk filtering, (d) filtering and muting, (e) static correction, and (f) corridor stack from well VSP #1.

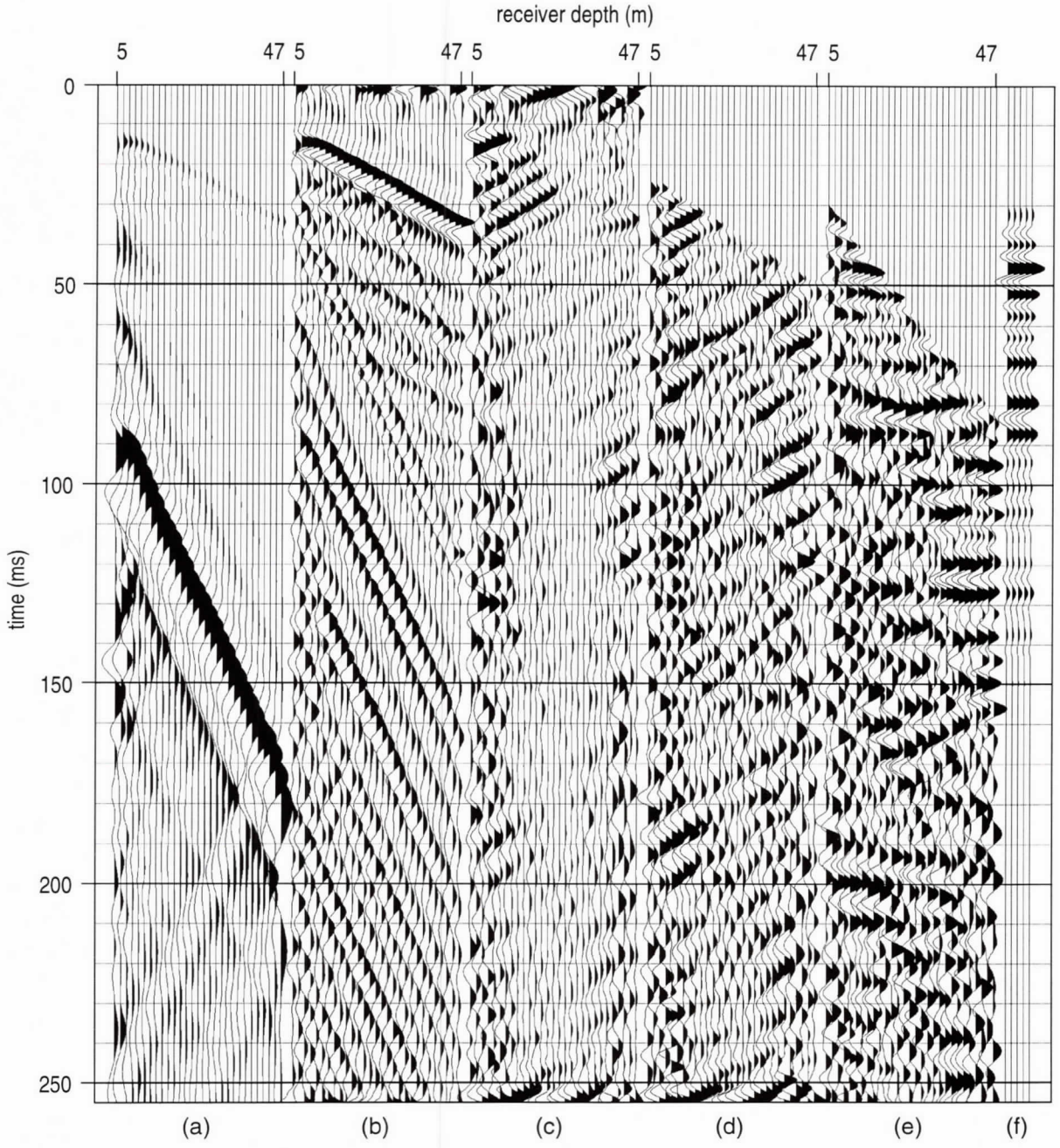


Figure 23. VSP files with 18 m source offset showing (a) raw data, (b) filtered and scaled, (c) fk filtering, (d) filtering and muting, (e) static correction, and (f) corridor stack from well VSP #2.

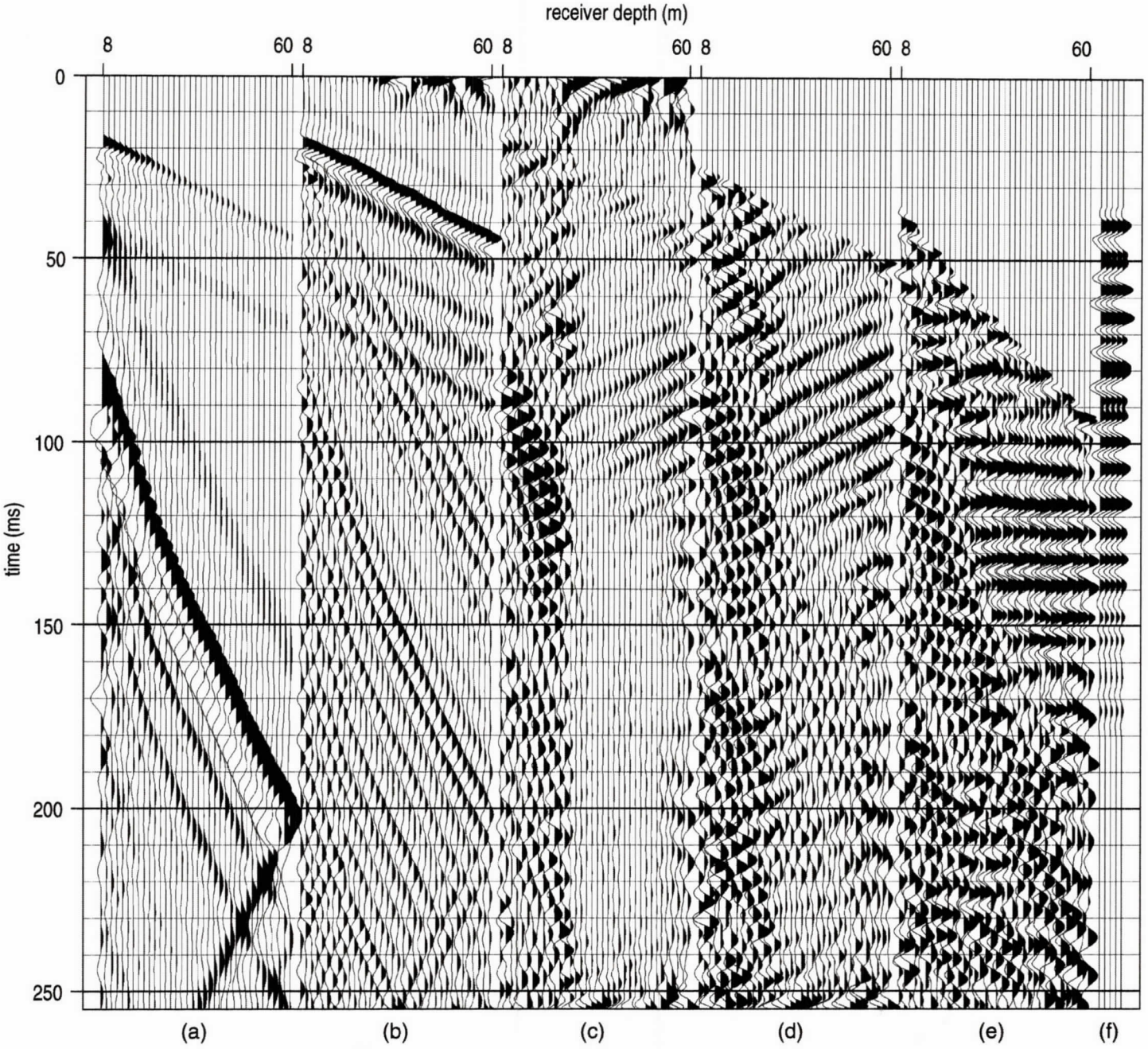


Figure 24. VSP files with 18 m source offset showing (a) raw data, (b) filtered and scaled, (c) fk filtering, (d) filtering and muting, (e) static correction, and (f) corridor stack from well VSP #3.

table—the holelock geophone data were not of as high a quality as data from hydrophones. Interval and average velocity curves (Appendix B, Figures B1 through B12) are determined from the same data set for each well (Table B2). Since the primary focus of the uphole survey was to acquire average velocity and a VSP for each borehole, the data set is not optimum for interval velocity. With the 1/4 msec sampling interval used to acquire this data the interval velocity between any two stations possesses a potential error range of about 25%. Only interpretations of gross lithology would be prudent from interval velocity values alone.

Monitor well VSP #2 is located within a high-fold portion of CDP profile line 2B and therefore should have a high correlation/similarity with that CDP line. The seven-step process used to obtain the corridor stacked traces is designed to enhance reflections at the expense of all other arrivals (Table B1). Corridor stacked traces are most effective when used in association with not only geophysical logs but also synthetic seismograms derived from acoustic logs. In this case, the natural gamma logs and the VSP corridor stack matches extremely well. The stack from well VSP #2 is an excellent match to the natural gamma ray log, geologist drilling log, and the CDP stacked section, allowing high confidence in event identification.

Correlating coherent events on CDP stacked sections with any borehole defined geologic feature or unit can be confidently made only with an irrefutable tie between reflection hyperbola interpreted on field files and coherent events on CDP stacked sections. AGC scaled field files from this site possess several high quality reflection hyperbola (Figure 25). The shallowest event (zero offset time of about 26 msec) clearly diverges from the refraction arrival at close offsets. At longer offsets the 26 msec event becomes asymptotic to and interferes with the refraction wavetrain. The bedrock is easily identified at about 75 msec and correlates extremely well with both the VSP derived time/depth conversions and the electric logs. The variability of the sediments within each formation is evident when comparing reflected energy between 50 and 75 msec on these two selected field files, which are separated by several hundred feet (Figure 25). At least six unique reflection events as well as direct wave, refractions, air-coupled wave, and ground roll can be confidently identified on the majority of field files from this survey.

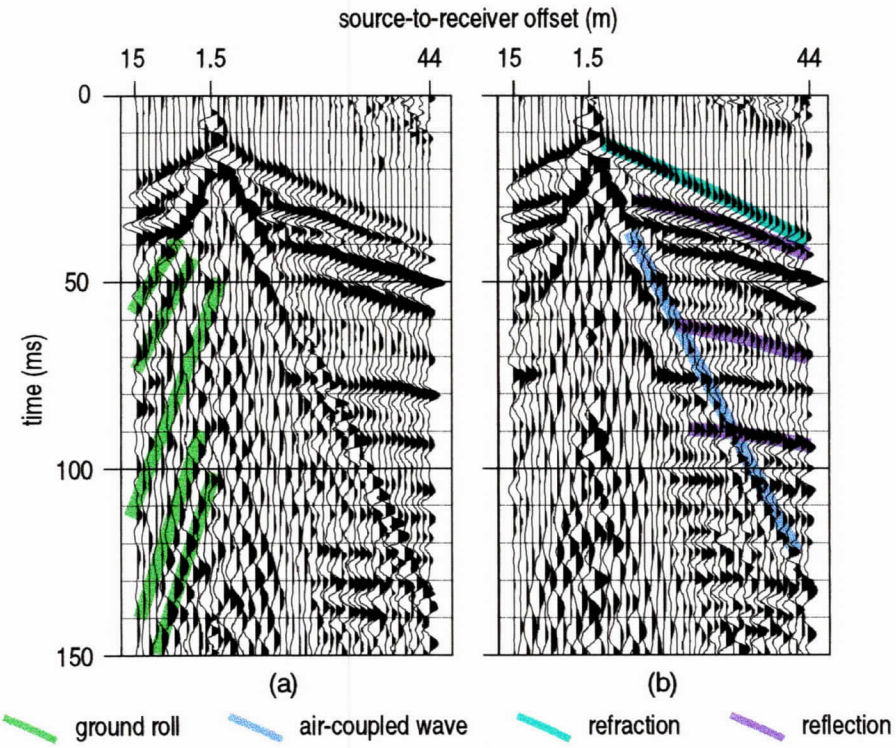


Figure 25. AGC scaled field files from two different places on line 1A. The reflection arrivals are evident on both records. Evident from comparison of (a) and (b) are the changes in subtle reflections between 50 and 70 msec.

The three long CDP profiles represent the focus of the shallow seismic reflection effort to image the paleochannel proposed based on extrapolation and correlation of widely-spaced boreholes and outcrop studies. Two of the lines are north of the aircraft flight lines (i.e., runways, hangers, parking areas, etc.) (Figure 26). The nominal 12-fold subsurface coverage extends from near the Environmental Affairs Department (EAD) office complex to the northern end of runway 23R. The longest of these lines is located on the southern end of the Air Station and extends from the edge of the asphalt plant near the end of delta taxiway to just beyond the dog kennel near gate #6 (Figure 27). The lines were deployed to intersect the trace of the proposed paleochannel at as oblique an angle as possible, while maintaining minimal chances of human disturbance, maximum near-surface saturation, minimum cultural noise, and maximum information potential (Figure 1). Analysis of factors that contributed to the excellent data obtained on spot CDP lines 3, 6, 8, and 13 were incorporated in determining the line locations.

Analysis of interference phenomena, reflection geometries, and wavelet characteristics of the CDP stack of line 1B (easternmost of the two northern lines) (Figure 28) provides no evidence indicating the presence of a major paleochannel between the Castle Hayne and about 9 m from the ground surface. The CDP stacked section possesses excellent coherence on three reflections interpretable above the upper Castle Hayne confining unit.

Using a generalized velocity function derived from the three VSPs conducted along the southern end of the Air Station, the shallowest mappable reflection (purple) is from about 12 to 15 m (Figure 29). The second coherent reflection (light blue) is interpreted to be about 25 to 35 m deep and is probably part of the Pungo River confining unit. The boundary between the Yorktown and Pungo River separates the Pliocene from the Miocene. There seems to be only a few small cut-and-fill channel features present at the top of the Miocene portion of the section. On the southern end of the Air Station the top of the Miocene is characterized by dramatic channel features that in places cut completely through the Pungo River confining unit. Identification of this portion of the time section as Miocene assumes the entire section between the Pungo River and the unconfined aquifer is present. This portion of the section appears to lack wavelet consistency across the section, suggesting little or no consistency in bedding plains. On the western half of the line the westward dipping sequence

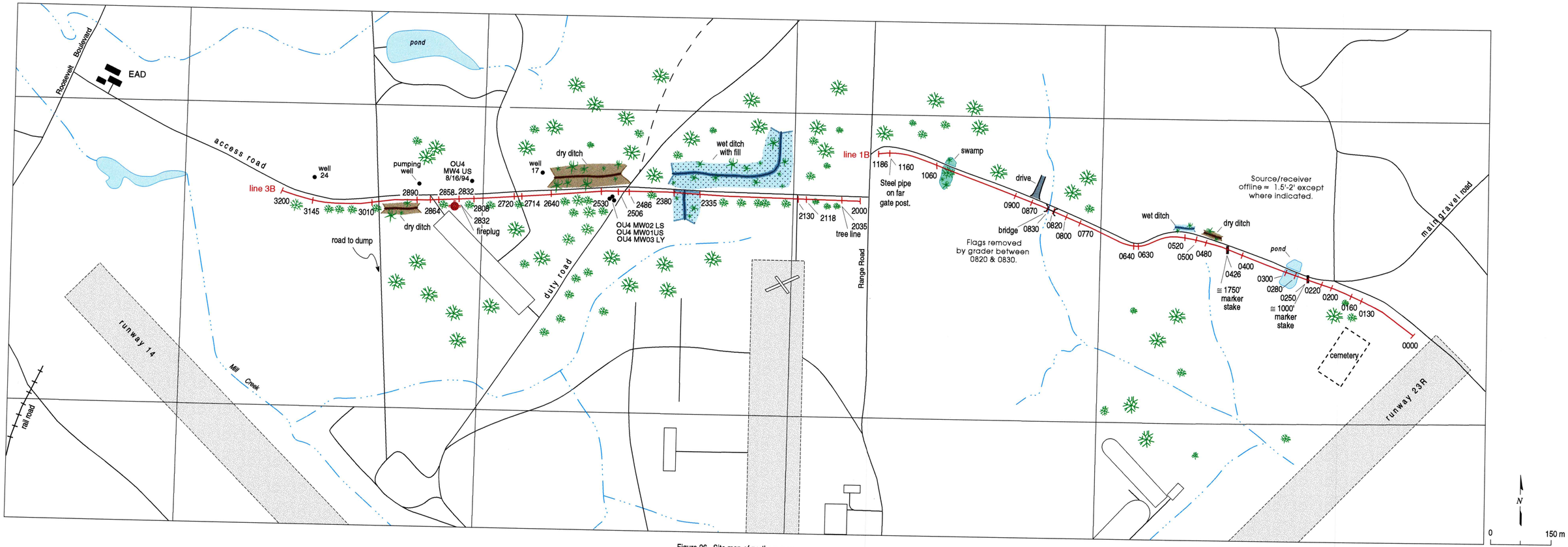


Figure 26. Site map of northern area.

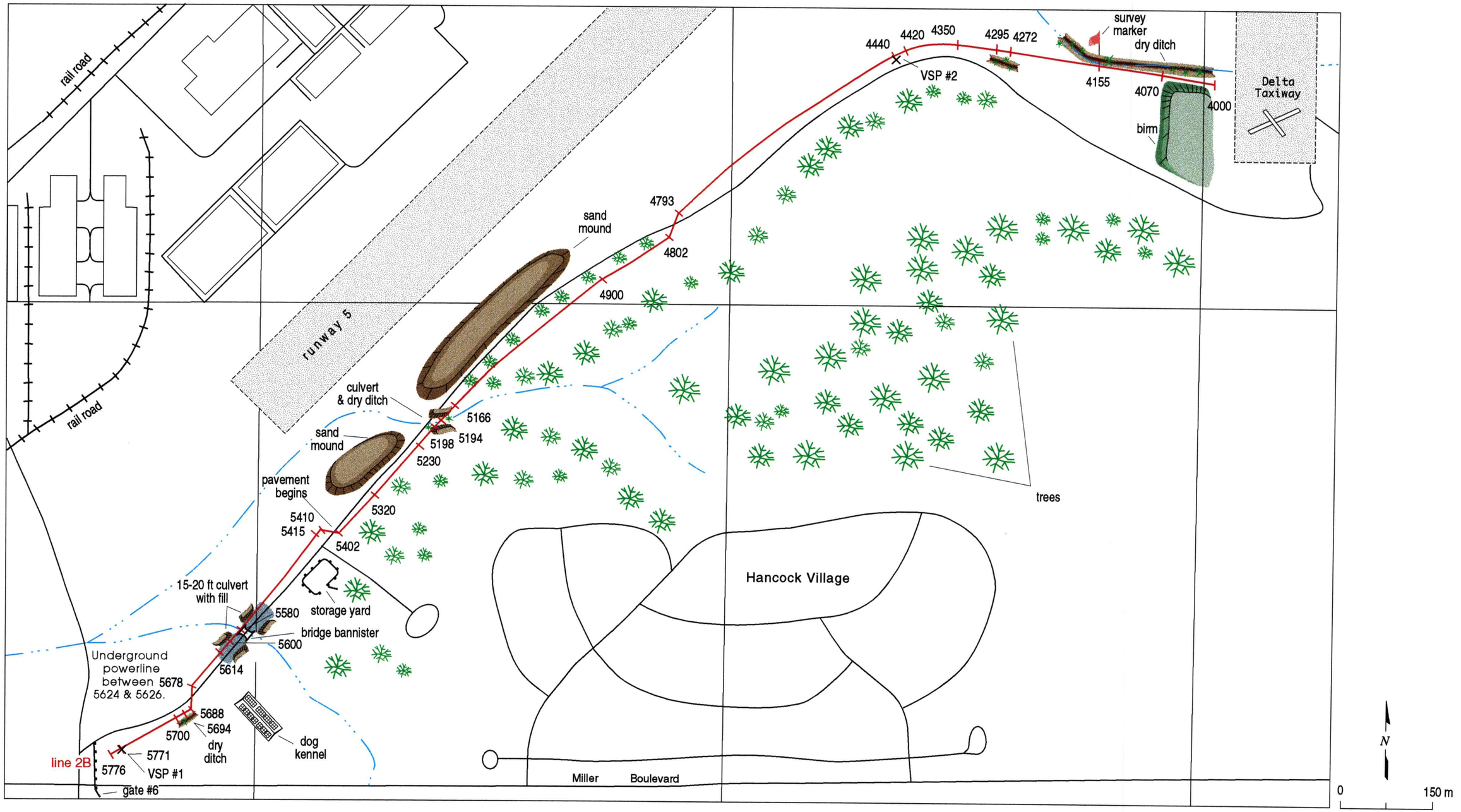


Figure 27. Site map of southern area.

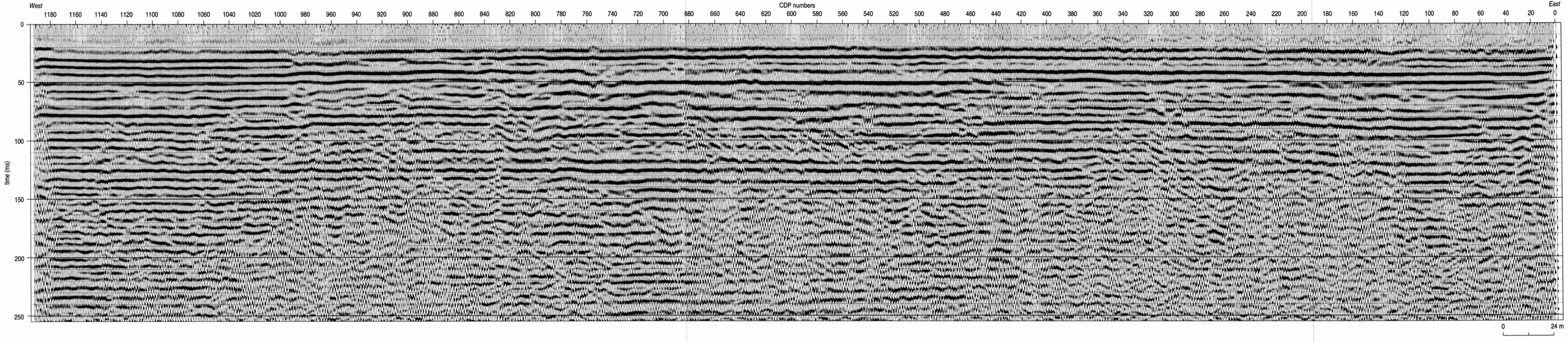


Figure 28. Uninterpreted 12-fold CDP stacked section of line 1B, the easternmost of the northern lines.

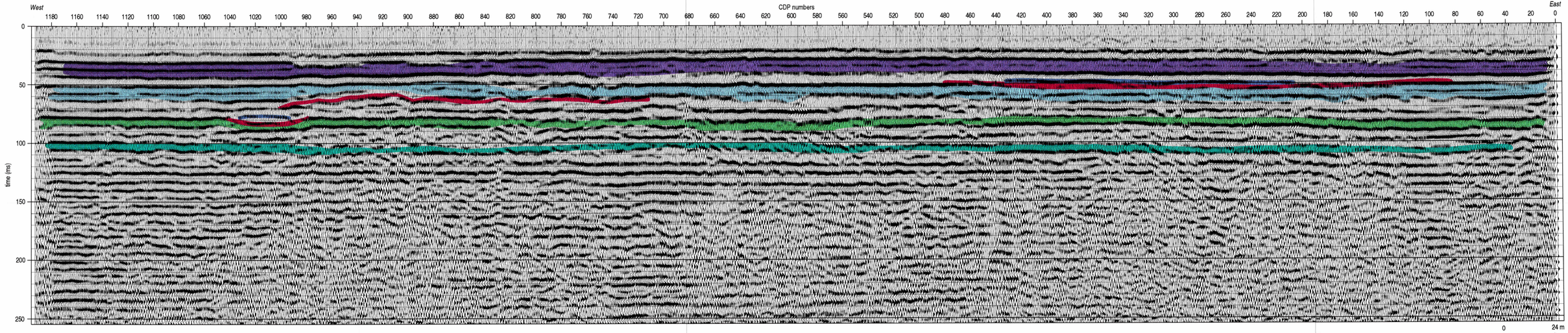


Figure 29. Interpreted 12-fold CDP stacked section of line 1B, the easternmost of the northern lines.

between about 25 and 55 m are likely indicative of changes in stream channels, shorelines, and/or local drainage. The most significant channel is completely within the Pungo River between CDPs 700 and 1000. The type and size feature is very common with that portion of the section. The upper Castle Hayne confining unit (green), at a depth of about 50 to 55 m, appears continuous with only subtle topographic features. The reflection at about 95 msec equates to a reflector at about 75 m and is likely the top of the lower Castle Hayne confining unit. With the exception of the cut and fill features present between about 25 and 55 m of depth, the seismic reflection section suggests only subtle thickness and possibly a few stratigraphic changes across the entire 0.6 mile section.

The approximately 0.6 mile line (line 3B) acquired in the road ditch along the road connecting Roosevelt Boulevard and Range Road possesses a great deal of data variability as a result of changes in near-surface conditions and reflector geometry changes (Figure 30). The most dramatic discontinuity on this line occurs around CDP 730. This abrupt change in reflection geometries and characteristics is interpreted to be suggestive of a major lithologic or structural change. In this case, this abrupt change is most likely related to a major channel feature. The eastern portion of the section is acoustically extremely similar and time ties very well with the line 1B. A VSP in strat well #4, which is located at about CDP 20 on this section, would provide a valuable tie to the lithology as determined from samples and geophysical logs. The general character of the reflection data from line 3B is slightly different from line 1B in terms of dominant frequency and horizontal consistency in interpreted reflections.

The four prominent reflections interpreted in purple, light blue, green, and blue green on the eastern portion of the line 3B section correlate very well with the VSP section from well VSP #2 (Figure 31). Several dramatic cut-and-fill features can be interpreted within the Miocene portion of the section. With the image of the subsurface provided by lines 1B and 3B it is possible to propose the trace of the channel which has an eastern boundary marked by the discontinuity at CDP 740 on line 3B. The vertical discontinuity at CDP 740 is not a processing artifact and does represent the true acoustic image of the subsurface in this area.

There are three features on line 3B that seem significant to the hydrologic setting in this area. The first and most significant is the paleochannel interpreted between CDP 730 and the west end of the line. Based on the present seismic interpretation, there seems to be two channels divided at CDP 1020 by an

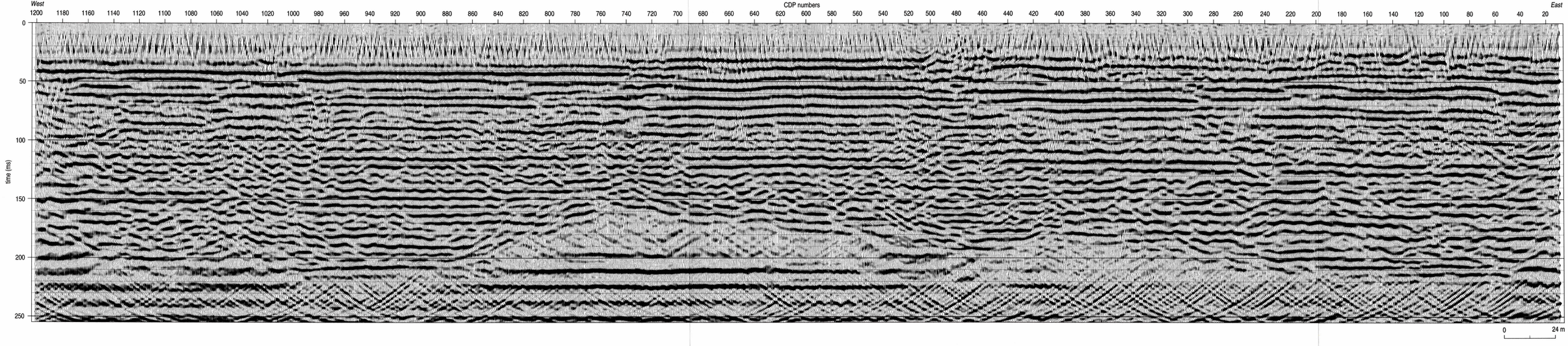


Figure 30. Uninterpreted 12-fold CDP stacked section of line 3B, the westernmost of the northern lines.

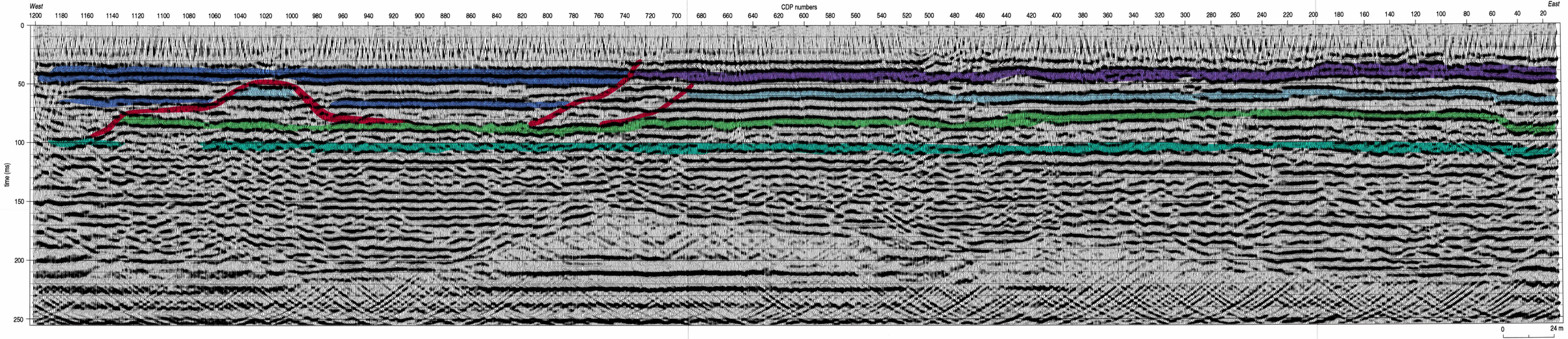


Figure 31. Interpreted 12-fold CDP stacked section of line 3B, the westernmost of the northern lines.

embayment or old stream bank. The east channel is not as deep and, based on the two traces of the eastern channel boundary, two unique cut-and-fill sequences might be responsible for its configuration. Clearly the top of the upper Castle Hayne has been eroded but, based on the reflection characteristics, the unit is still present. The second feature of interest is the deeper channel west of CDP 1020. Some caution must be exercised when interpreting change this close to the end of a seismic section due to low fold effects, however the interpretation present is not unreasonable. The second deeper channel appears to cut through and completely remove the upper Castle Hayne confining unit. If this is truly an accurate interpretation, it has major significance to hydrologic models and pumping in this area. The third feature of interest is again in a low-fold area and must be considered with caution. There appears to be a significant channel cut into, but not through, the upper Castle Hayne confining unit around CDP 40 and west. This channel must be localized since there is no indication of a depressed arrival time on the upper Castle Hayne reflection on the western end of line 1B. The channels interpreted on line 3B range in size from the channel centered under CDP 860, which is 250 m wide and 60 m deep, to the small erosional feature on the east end that is 7 m deep and at least 30 m wide. The major channel appears to be west of CDP 1040 with a maximum depth of at least 70 m and a width that cannot be determined with this data.

Interpretations of line 3B required inclusion of drill data, marine seismic, VSP from the south end of the Air Station, and the other two long seismic lines (Figure 31). Based on reflection characteristics alone, the west side of the line seems a stronger candidate for native with the channel present east of CDP 730. However, once all the data were incorporated, the most reasonable interpretation put the channel extending westward from CDP 730.

Line 2B intersects both wells VSP #2 and VSP #1, allowing both geophysical log and VSP correlations to coherent reflections (Figure 32). Borehole interpretations of VSP #2 (located at CDP 350) suggest the Yorktown confining unit is present at a depth of about 15 m, and correlates to the 40 msec reflection (purple) (Figure 33). The next significant unit (at least in terms of the natural gamma logs) is a 33 m deep clay, possibly the Pungo River confining unit (light blue), which is represented by a reflection at about 65 msec on the reflection section and 68 msec on the VSP. Based on the assumption that this borehole is within a complete part of the geologic section, the portion of the time section

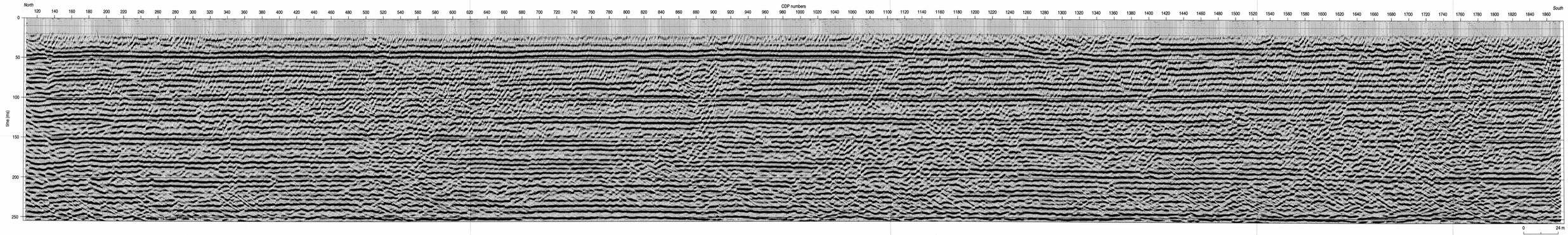


Figure 32. Uninterpreted 12-fold CDP stacked section of line 2B, the southernmost line.

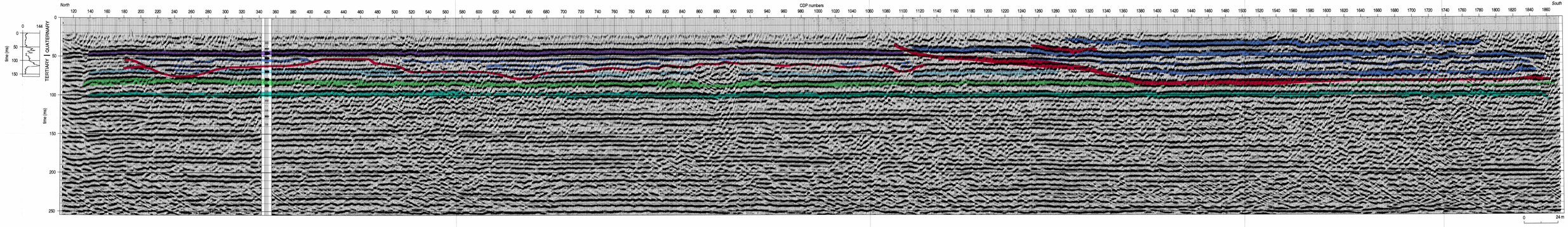


Figure 33. Interpreted 12-fold CDP stacked section of line 2B, the southernmost line.

between the Yorktown confining unit (~40 msec) and the Castle Hayne (~75 msec) is all Miocene. Within that time section are a complex set of horizontally varying small channel sequences. The very consistent and relatively flat upper Castle Hayne (green) is interpreted at about 75 msec (55 m), and equally flat and uniform is the 90 msec (blue green) confining unit that separates the upper Castle Hayne from the lower Castle Hayne. On this section, as on line 3B, an abrupt discontinuity is evident at about CDP 1120. It is interesting to also note the similarities between the discontinuities shown on lines 3B, 2B, and 8A. It is not unreasonable to suggest these discontinuities in the shallow clay layer (~40 msec) could be either related or at least represent a similar geologic process or sequence.

The higher signal-to-noise ratio data recorded on line 3B provided for a more complete and definitive interpretation (Figure 33). Of course, the dramatic change in reflection characteristics and general geometries apparent across the discontinuity previously noted could represent hydrologically the most significant single feature. Within the Miocene part of the section the geometry of the cut-and-fill features and overall channel fill sequences are extremely consistent with features and geometries within equivalent-age marine sediments as interpreted on seismic data collected just off-shore (Hine and Riggs, 1986). The similarities of events interpretable on this section compared to nearby shallow marine studies included not only the age of the cut-and-fill channel sequences, but also the general shape and cyclic nature of the deposits.

Several features on the interpreted line 2B section are of particular interest and could have bearing on the hydrologic properties of the section above the Castle Hayne confining unit. Regardless of the interpretation provided above the upper Castle Hayne confining unit, the critical point is that there seems to be continuity in the basal contact of the Castle Hayne confining unit across the entire line. It is possible, however, to suggest the confining unit might be missing or at least extremely thin on the south end of the line. It appears that the Castle Hayne has not been the victim of sufficient scouring to have breached the isolation between the Pungo River aquifer and the upper Castle Hayne as provided by the upper Castle Hayne confining unit (green).

The apparent erosional truncation of the 33 m deep (~60 msec) clay layer identified in well VSP #2 at CDPs 300 and 510 is overwhelming evidence of the dangers of well-to-well correlations in this setting. If VSP #2 were to have been drilled at CDP 250 or CDP 550 as opposed to CDP 350, a completely different

picture of the trace of the paleochannel might well have been interpreted from drill data only. The channel feature interpreted to be present between CDPs 470 and 630 possesses no obvious internal layering and is therefore likely uniformly infilled with a single type of material. If encountered during drilling, this interval could easily be classified as a sand pile.

A more speculative interpreted geometry is the apparent channel boundary just south of the major discontinuity in the 40 msec reflection interpreted at about CDP 1090. This structure is likely a division between the two clearly unique depositional settings. Structures interpreted north of this boundary appear to represent multiple repetitive sequences of cut and fill during late Tertiary, followed by the deposition of a single consistent reflector, likely in a very low energy setting during the Quaternary. Structures interpreted south of this mesa possess very little geometry, are represented by lower frequency reflections, and are likely the result of relatively uniform deposition, possibly the result of several episodes of sea level change. Based on the interpretation that the boundary indicated in red south of CDP 110 is a channel edge, the material interpreted in dark blue is Quaternary channel deposits.

Interpretations of reflections on CDP stacked sections suggests that horizontal correlation of units shallower than the Castle Hayne is not possible with well data only in this part of the Coastal Plain. The variability previously noted on marine seismic data nearby is consistent with the apparent structures noted within the Miocene portion of the section (Hine and Riggs, 1986). The Yorktown confining unit and Pungo River confining unit identified on many geologist and electric logs from boreholes around the Air Station may not always be the same confining units. The variability in log characteristics and geologist descriptions of these units is consistent with the suggestion here that most apparent layering within the upper 55 m possesses limited horizontal extent.

The discontinuities noted on lines 1B, 3B, and 8A are similar not only in approximate depth but also in the general character of the features. Extra care was taken to ensure that these features were not the result of processing artifacts or interpretive cycle skipping. The horizontal continuity and lack of any time offset on the Castle Hayne reflections (green and blue green) along line 2B and no similarities in appearance between the Castle Hayne and Yorktown (purple) event are the most convincing pieces of evidence refuting any suggestion that these discontinuous features are artifacts.

With the exception of an interpreted minor scour at about CDP 880, the upper and lower Castle Hayne show little or no apparent structure across this more than 1 mile of seismic line. The complex series of cut-and-fill features interpreted in the sediments above the Castle Hayne are consistent with most borehole log identifications of multiple shell layers, stringers, and lenses. The reflections as interpreted on the CDP stacked sections provide an image of the subsurface consistent with borehole-defined lithology while at the same time suggesting the multiple unique aquifer/confining unit sequences present across the Air Station may be a significantly over-simplified geologic representation and may actually better be described as the surficial, unconfined aquifer extending to the top of the upper Castle Hayne confining unit.

## Conclusions

Shallow seismic reflection was extremely successful in delineating hydrologically significant changes in the near-surface geologic units at the U.S. Marine Corps Air Station at Cherry Point. The incorporation of land CDP seismic reflection data with VSP data, geophysical logs, and geologist stratigraphic borehole logs greatly enhances both the confidence and the overall understanding of the geology and hydrogeology of any area. This data set allows for a reasonable inference as to the possible location of some subsurface expression of the paleochannel speculated from sporadic drill data.

## Acknowledgments

This work was supported by the U.S. Geological Survey under Contracts 1434HQ-94-PO-0066 and 1434HQ-95-SA-0664. We appreciate the support of Charles C. Daniel III and Beth Wrege of the U.S. Geological Survey during acquisition. Alex Cardinell of the U.S. Geological Survey and Renee Henderson with the Department of Defense provided valuable logistical assistance. We also thank p.acker for graphics and Mary Brohammer for manuscript preparation and editorial suggestions.

## References


Birkelo, B.A., D.W. Steeples, R.D. Miller, and M.A. Sophocleous, 1987, Seismic reflection study of a shallow aquifer during a pumping test: *Ground Water*, v. 25, p. 703-709, Nov.-Dec.

Cardinell, A.P., D.A. Harned, and S.A. Berg, 1990, Continuous seismic reflection profiling of hydrogeologic features beneath New River, Camp Lejuene, North Carolina: U.S. Geological Survey Water-Resources Investigations Report 89-4195, 33p.

Daniel III, Charles C., 1996, personal communication, July 26.

Eimers, J.L., C.C. Daniel III, and R.W. Coble, 1994, Hydrogeology and simulation of ground-water flow at U.S. Marine Corps Air Station, Cherry Point, North Carolina, 1987-90: U.S. Geological Survey Water-Resources Investigations Report 94-4186, 75p.

Eimers, J.L., W.L. Lyke, and A.R. Brockman, 1990, Simulations of ground-water flow in aquifers in Cretaceous rocks in the central Coastal Plain, North Carolina: U.S. Geological Survey Water-Resources Investigations Report 89-4153, 101p.

Goforth, T., and C. Hayward, 1992, Seismic reflection investigations of a bedrock surface buried under alluvium: *Geophysics*, v. 57, p. 1217-1227.

Glover, R.H., 1959, Techniques used in interpreting seismic data in Kansas: Kansas Geological Survey Bulletin 137, W.W. Hambleton, ed., p. 225-240.

Haeni, F.P., 1986, Use of continuous seismic reflection methods in a hydrologic study in Massachusetts, a case study, in National Water Well Association Conference on Surface and Borehole Geophysical Methods and Ground Water Instrumentation, Denver, Colorado, October 15-17, 1986, Proceedings: Worthington, Ohio, National Water Well Association, p. 381-395.

Haeni, F.P., 1988, Evaluation of the continuous seismic refraction method for determining the thickness and lithology of stratified drift in the glaciated northeast, in A.D. Randall and A.I. Johnson, eds., Regional aquifer systems of the United States–The northeast glacial aquifers: American Water Resources Association Monograph 11, p. 63-82.

Hine, A.C., and Riggs, S.R., 1986, eds., Geologic framework, Cenozoic history, and modern processes of sedimentation on the North Carolina continental margin, *in* Textoris, D.A., ed., SEPM Field Guidebooks, southeastern U.S. third annual midyear meeting, 1985: Raleigh, North Carolina, p. 129-194.

Jongerius, P., and K. Helbig, 1988, Onshore high-resolution seismic profiling applied to sedimentology: *Geophysics*, v. 53, p. 1276-1283.

Kimrey, J.O., 1964, The Pungo River Formation, a new name for middle Miocene phosphorites in Beaufort County, North Carolina: *Southeastern Geology*, v. 5, no. 4, p. 195-205.

Kimrey, J.O., 1965, Description of the Pungo River Formation in Beaufort County, North Carolina: North Carolina Department of Conservation and Development, Division of Mineral Resources, Bulletin No. 79, 131p.

Knapp, R.W., and D.W. Steeples, 1986, High-resolution common depth point seismic reflection profiling: field acquisition parameter design: *Geophysics*, v. 51, p. 283-294.

LeGrande, H.E., 1960, Geology and ground-water resources of the Wilmington-New Bern area: Raleigh, North Carolina Department of Water Resources, Division of Ground Water, Ground-Water Bulletin 1, 80p.

Lloyd, O.B., Jr., and C.C. Daniel, 1988, Hydrogeologic setting, water levels, and quality of water from supply wells at the U.S. Marine Corps Air Station, Cherry Point, North Carolina: U.S. Geological Survey Water-Resources Investigations Report 88-4034, 76p.

Mayne, W.H., 1962, Horizontal data stacking techniques: *Supplement to Geophysics*, v. 27, p. 927-938.

Miller, R.D., 1992, Normal moveout stretch mute on shallow-reflection data: *Geophysics*, v. 57, p. 1502-1507.

Miller, R.D., S.E. Pullan, D.A. Keiswetter, D.W. Steeples, and J.A. Hunter, 1992, Field comparison of shallow S-wave seismic sources near Houston, Texas: Kansas Geological Survey Open-file Report 92-33.

Miller, R.D. S.E. Pullan, D.W. Steeples, and, J.A. Hunter, 1994, Field comparison of shallow P-wave seismic sources near Houston, Texas: *Geophysics*, v. 59, p. 1713-1728.

Miller, R.D., S.E. Pullan, J.S. Waldner, and F.P. Haeni, 1986, Field comparison of shallow seismic sources: *Geophysics*, v. 51, p. 2067-2092.

Miller, R.D., D.W. Steeples, and M. Brannan, 1989, Mapping a bedrock surface under dry alluvium with shallow seismic reflections: *Geophysics*, v. 54, p. 1528-1534.

Mixon, R.B., and Pilkey, O.H., 1976, Reconnaissance geology of the submerged and emerged Coastal Plain province, Cape Lookout area, North Carolina: U.S. Geological Survey Professional Paper 859, 45 p.

Pullan, S.E., and J.A. Hunter, 1990, Delineation of buried bedrock valleys using the optimum offset shallow seismic reflection technique: Soc. Explor. Geophys. Investigations in Geophysics, Investigations in Geophysics no. 5, Stan H. Ward, ed., Volume 3: Geotechnical, p. 75-87.

Schieck D.G., and S.E. Pullan, 1995, Processing a shallow seismic CDP survey: An example from the Oak Ridges Moraine, Ontario, Canada: in SAGEEP 95 Proceedings (Symposium on the Application of Geophysics to Engineering and Environmental Problems), Orlando, Florida, April 23-26.

Steeples, D.W., 1990, Early spectral shaping boosts data quality: *Oil and Gas Journal*, v. 88, no. 38, Sept. 17, p. 49-55.

Steeples, D.W., and R.D. Miller, 1990, Seismic-reflection methods applied to engineering, environmental, and groundwater problems: Soc. Explor. Geophys. Investigations in Geophysics, Investigations in Geophysics no. 5, Stan H. Ward, ed., *Volume 1: Review and Tutorial*, p. 1-30.

Sylwester, R.E., 1983, Single-channel, high-resolution seismic reflection profiling, a review of the fundamentals and instrumentation: in R.A. Geyer, ed., Handbook of Geophysical Exploration at Sea: Boca Raton, Florida, CRC Press, p. 77-122.

Winner, M.D., Jr., and R.W. Coble, 1989, Hydrogeologic framework of the North Carolina Coastal Plain Aquifer system: U.S. Geological Survey Open-file Report 87-690, 155p.

Yilmaz, O., 1987, Seismic data processing: Soc. Explor. Geophys. Investigations in Geophysics, Investigations in Geophysics no. 2, S.M. Doherty, ed., p. 1-30.

## Appendix A: VSP Data and Interpretations

Walkaway tests were performed at site #1 (line 1A, which was interpreted from modeling to be outside the paleochannel), and site #3 (line 2A) where a paleochannel is suggested (Figure 1). The walkaway test spreads were deployed near the well cluster at site #1. The 96 receivers for the P-wave experiment were laid parallel to Roosevelt, each separated by 0.6 m. The highest signal-to-noise reflection interpretable within the depth range of interest possesses a vertically incident time of about 45 to 50 msec (Figure A1). Comparisons of the geometric shape and arrival time of this proposed reflection with theoretical hyperbolic curves suggest excellent correlation to a reflector at a depth of about 27 to 33 m and an NMO velocity of around 640 m/sec. From velocity check shots (uphole survey) at site #1 the average velocity to 30 m was just over 640 m/sec. It is therefore justified to be cautiously optimistic that this curved arrival is a primary reflection from about 30 m.

The downhole 30.06 possesses the highest signal-to-noise ratio and resolution potential of the three sources tested at site #1 (Figure A1). The 200 Hz analog low-cut filter applied to all the sources dramatically reduces the ground roll and the 100 Hz refraction "ring." The sledge hammer produced a seismogram with nearly equivalent reflection signature and frequency content as the downhole 30.06 when the 200 Hz analog low-cut filter was applied (Figure A2). The dominant negative characteristics of the sledge hammer were the ratio of air-coupled wave to reflection energy, the potential for inconsistent source energy, surface coupling, and the slight degradation of resolution potential due to stacking. The auger gun was much too energetic and possessed a lower reflection frequency bandwidth, likely as a direct result of the higher level of energy release (Knapp and Steeples, 1986) (Figure A3). Reflections from beneath the Castle Hayne are very evident on auger gun data regardless of acquisition filters. An increase in upper corner frequency of the reflection bandwidth, higher dominant frequency, and a more minimum phase source wavelet was more evident on shot gathers from the downhole 30.06 than either the sledge hammer or auger gun after the application of a digital filter (Figures A4, A5, and A6). This is especially true of the records that were recorded with a 200 Hz analog filter. Analog filtering seems to provide slightly higher resolution potential than nearly equivalent digital filtering. This pre-A/D spectral shaping allows the full dynamic range of the 15-bit seismograph to exploited. Analysis of compressional wave tests at site #1 lead to the recommendation that production data be acquired with the downhole 30.06 fired into shallow holes and recorded with 200 Hz analog low-cut filters, 100 Hz geophones, a source and receiver spacing of 0.6 m, and 24-fold redundancy.

Testing at site #3 (line 2A) was not as extensive as at site #1 due mainly to the results and recommendations developed from testing at site #1 (the auger gun was not tested at this site). The increased time and source-to-receiver offset of the direct and refracted wave cross-over at site #3 in comparison to site #1 is evidence of either a thicker low velocity near-surface layer or a dramatic decrease

in compressional wave velocity. Consistent with site #1, the ratio of air-coupled wave to reflections is lower with the downhole 30.06 (Figure A7) than the sledge hammer (Figure A8). A well-developed reflection with a zero offset time of about 50 msec is evident on seismograms from all three sources. Examination of reflections on digitally filtered 200 Hz analog low-cut filter data leaves little doubt that the downhole 30.06 possesses the highest resolution and signal-to-noise ratio potential of the sources tested at this site (Figures A9 and A10). The ratio of air-coupled wave to reflection energy is a very important criteria at this site when considering that a large portion of the near-vertically incident reflection energy returning from reflectors within the depth range of interest will arrive after the air-coupled wave. Based on the optimum reflection recording window, the ineffectiveness of digital filtering to enhance reflections arriving after ground roll or air-coupled waves on sledge hammer data, the need for maximum coherency of the shallowest reflections, a low signal-to-noise ratio on sledge hammer data, and the extremely small optimum reflection window for reflection returning from depths less than 25 m, the downhole 30.06, 0.6 m receiver shot and receiver spacing, and 200 Hz analog low-cut filter were selected as optimum for this site and target.

Shear waves were tested at site #1 in hopes of improving the resolution potential. This potential for improved resolution of shear wave data over compressional wave data is directly related to the slower phase velocity of shear (S) waves in comparison to compressional (P) waves in the same sediments. Few sources with truly high quality broadband horizontally polarized shear wave production have been identified (Miller et al., 1992). For this test a modified wood block (steel plates on the ends to avoid deformation and spikes for ground coupling) was aligned perpendicular to the survey line and struck on the ends with a 7.3 kg sledge hammer. Source impacts from both directions were collected onto each shot gather according to source-to-receiver offset. Shear wave receivers were deployed with orientations sensitive to motion perpendicular to the survey line. The data were gathered together according to common shot location with the polarity of the right-to-left shot reversed. This display format allows visual separation of the polarized nature of S-waves and permits easy separation of the shear waves from compressional waves. Little in the way of confidently interpretable reflected energy is present on S-wave gathers regardless of analog filter settings (Figures A11, A12, A13, and A14). Some suggestion of curved arrivals is visible within very narrow time/offset windows. An abundance of Love wave and mode converted energy is evident. The very limited apparent bandwidth and low signal-to-noise ratio is likely responsible for the inability of S-wave energy to produce high-confidence interpreted reflections on seismograms. The lack of any confident reflection arrival forced discontinuation of S-wave testing and eliminated S-waves as a viable approach to image the proposed bedrock channel.

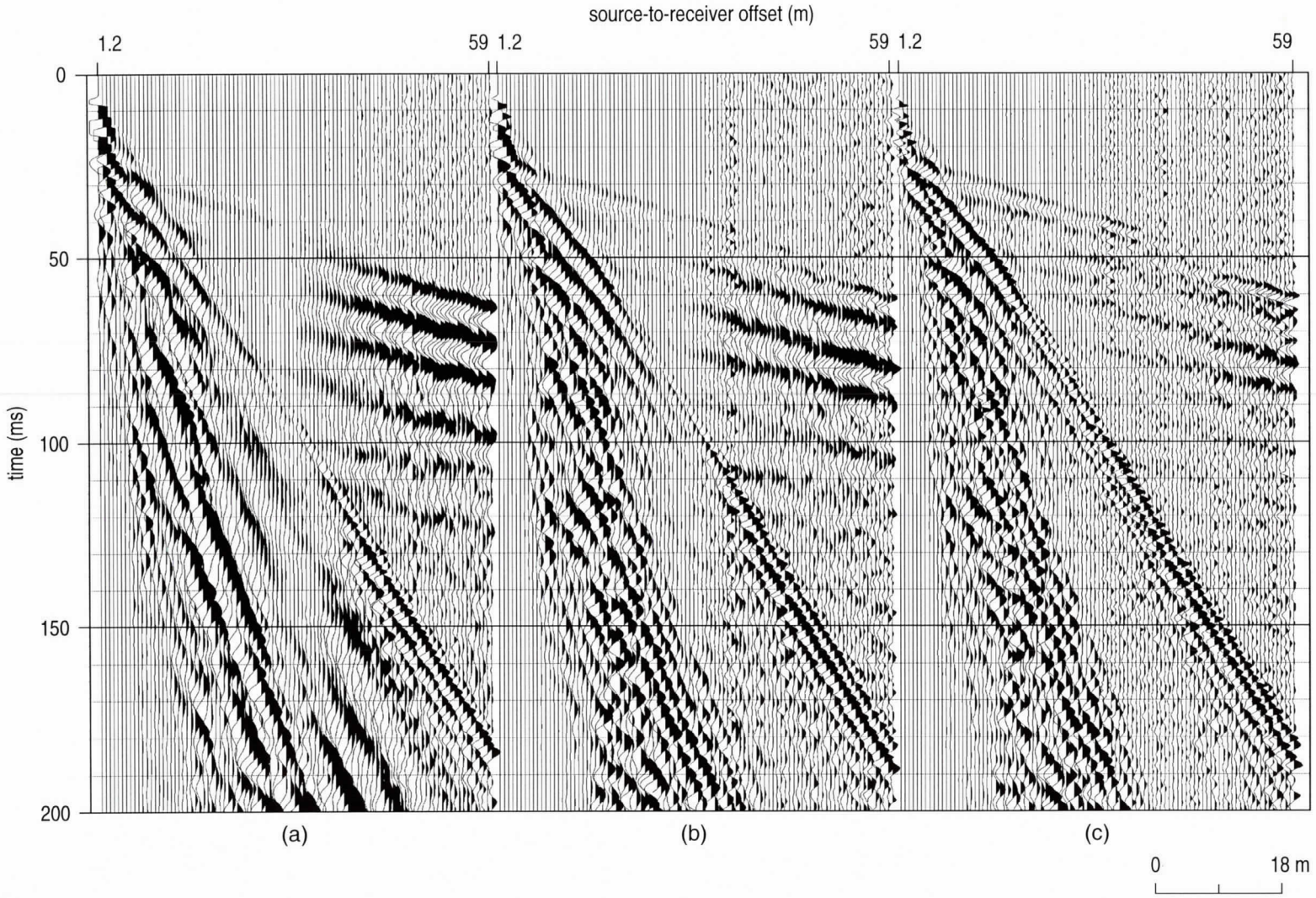


Figure A1. Walkaway field files from site #1 using downhole 30.06 recorded with (a) no analog low-cut filter, (b) 100 Hz, and (c) 200 Hz.

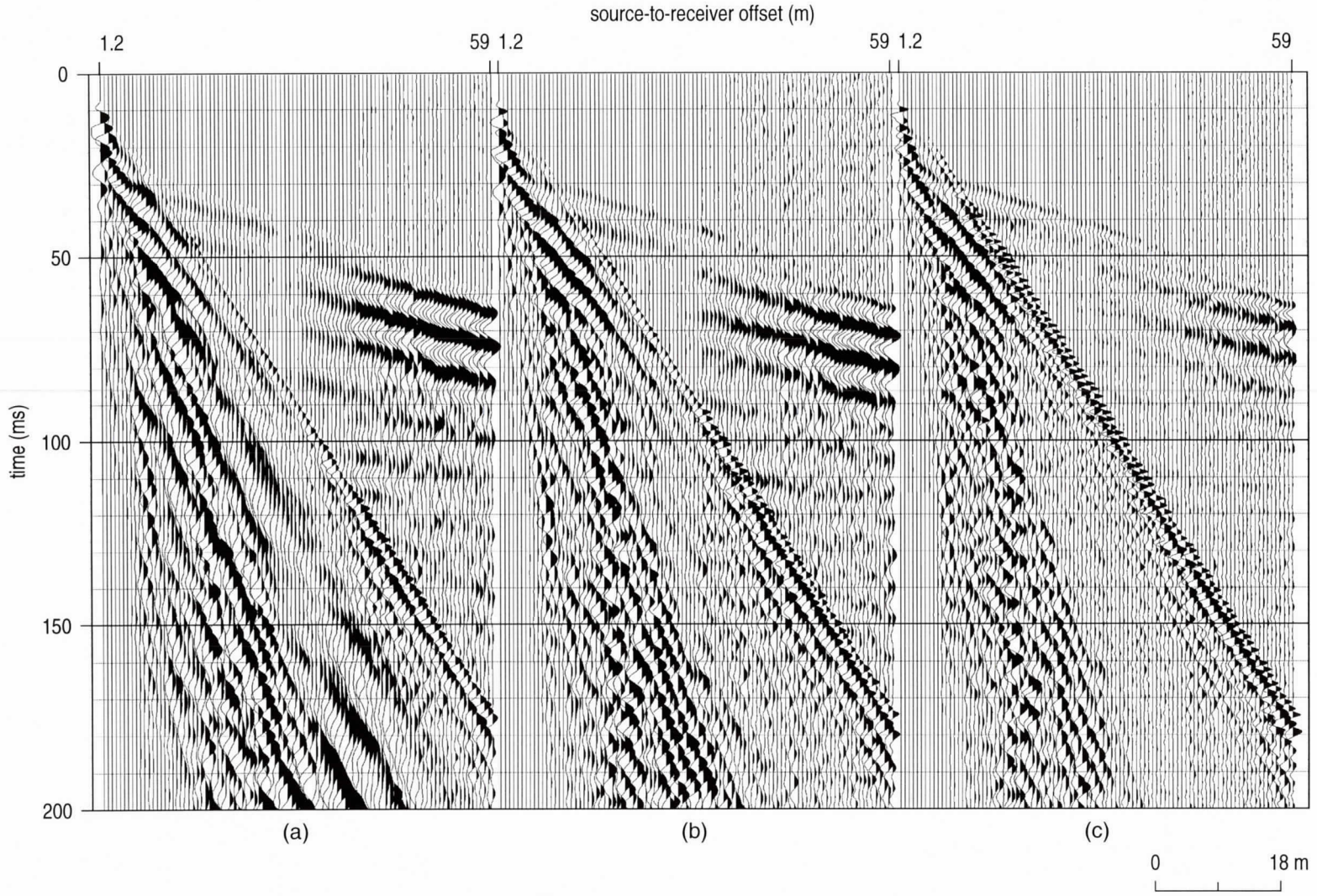


Figure A2. Walkaway field files from site #1 using sledgehammer recorded with low-cut filter (a) out, (b) 100 Hz, and (c) 200 Hz.

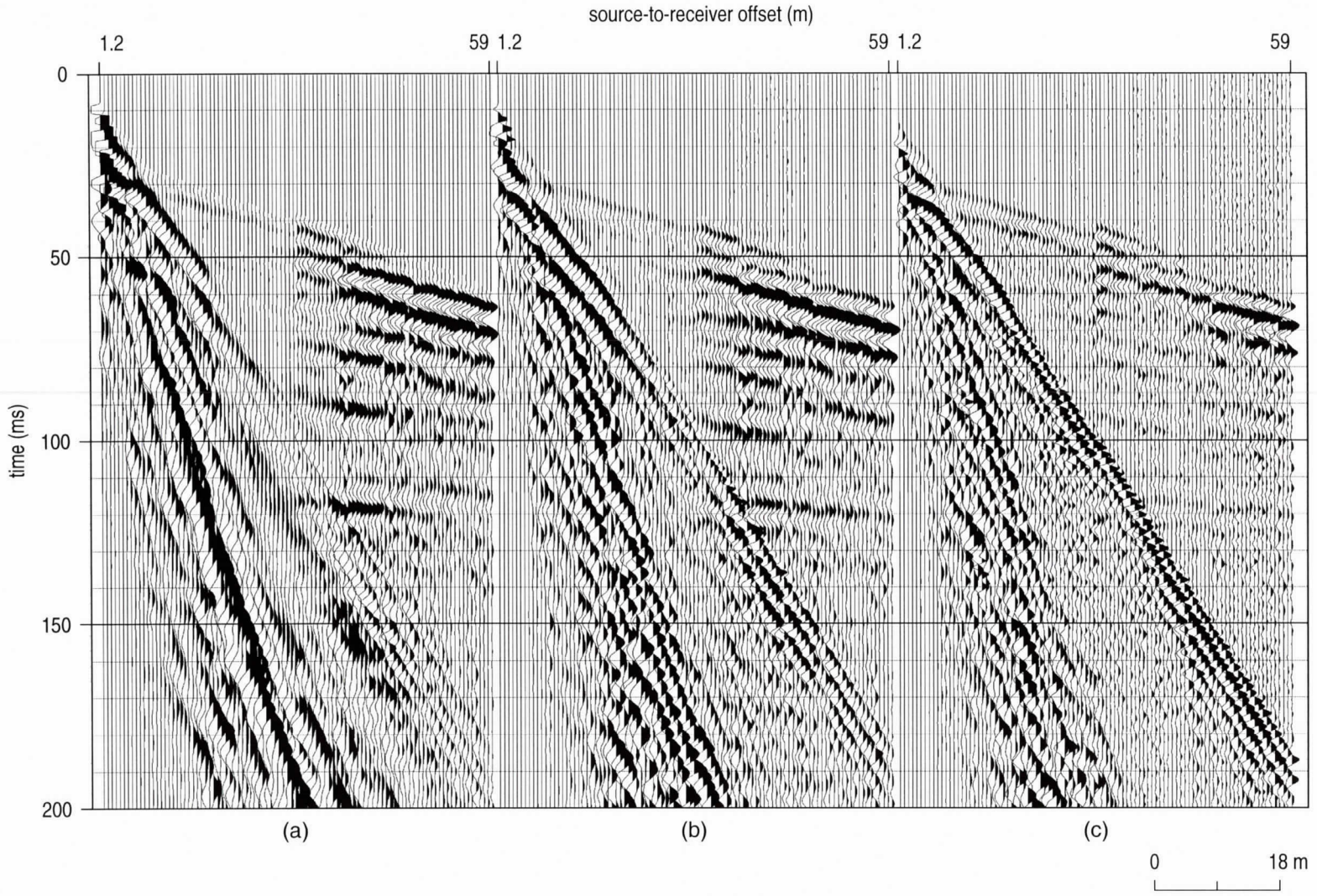


Figure A3. Walkaway field files from site #1 using 12-gauge auger gun recorded with low-cut filter (a) out, (b) 100 Hz, and (c) 200 Hz.

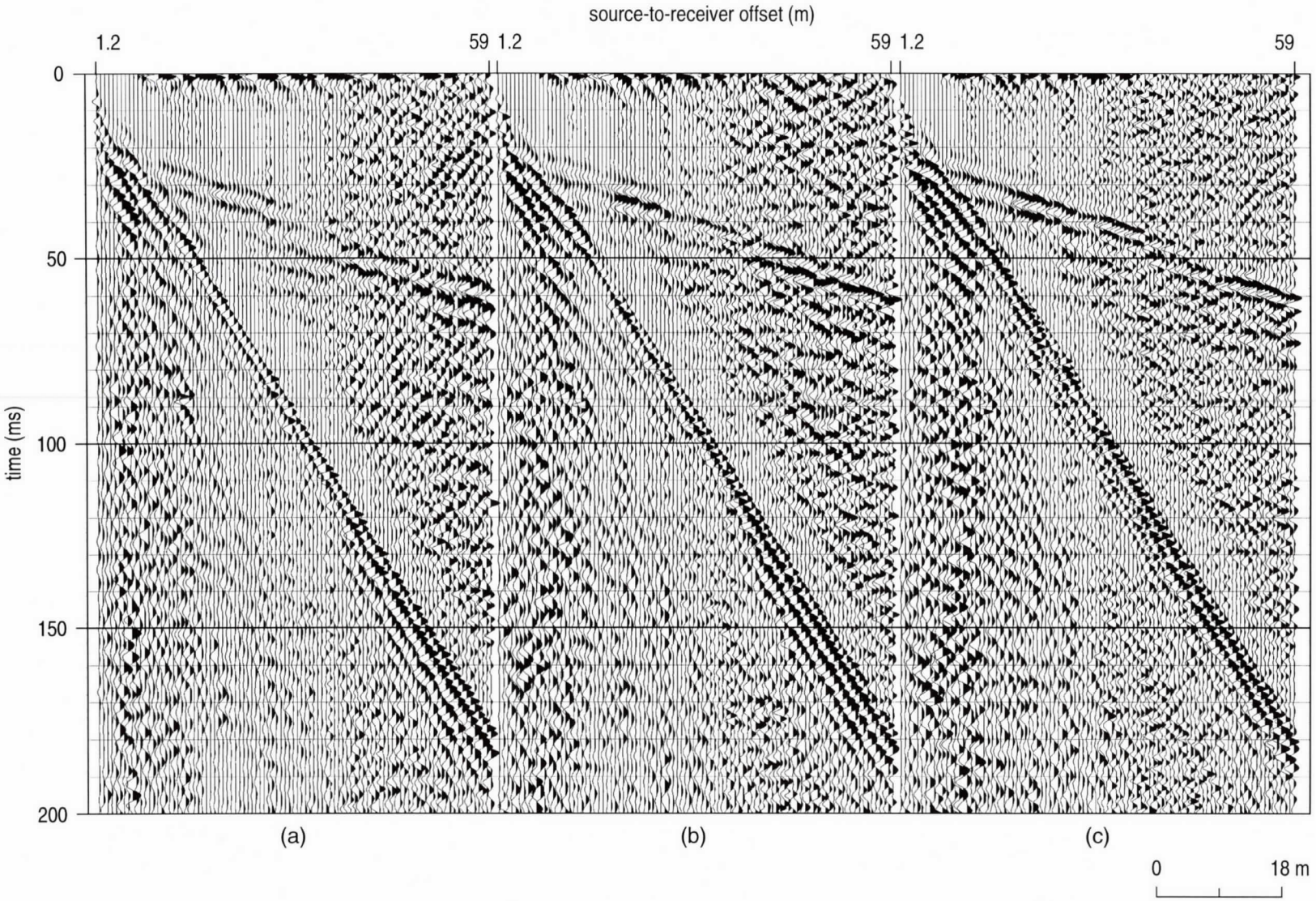


Figure A4. A 100-200-400-600 digital filter applied to files from Figure A1.

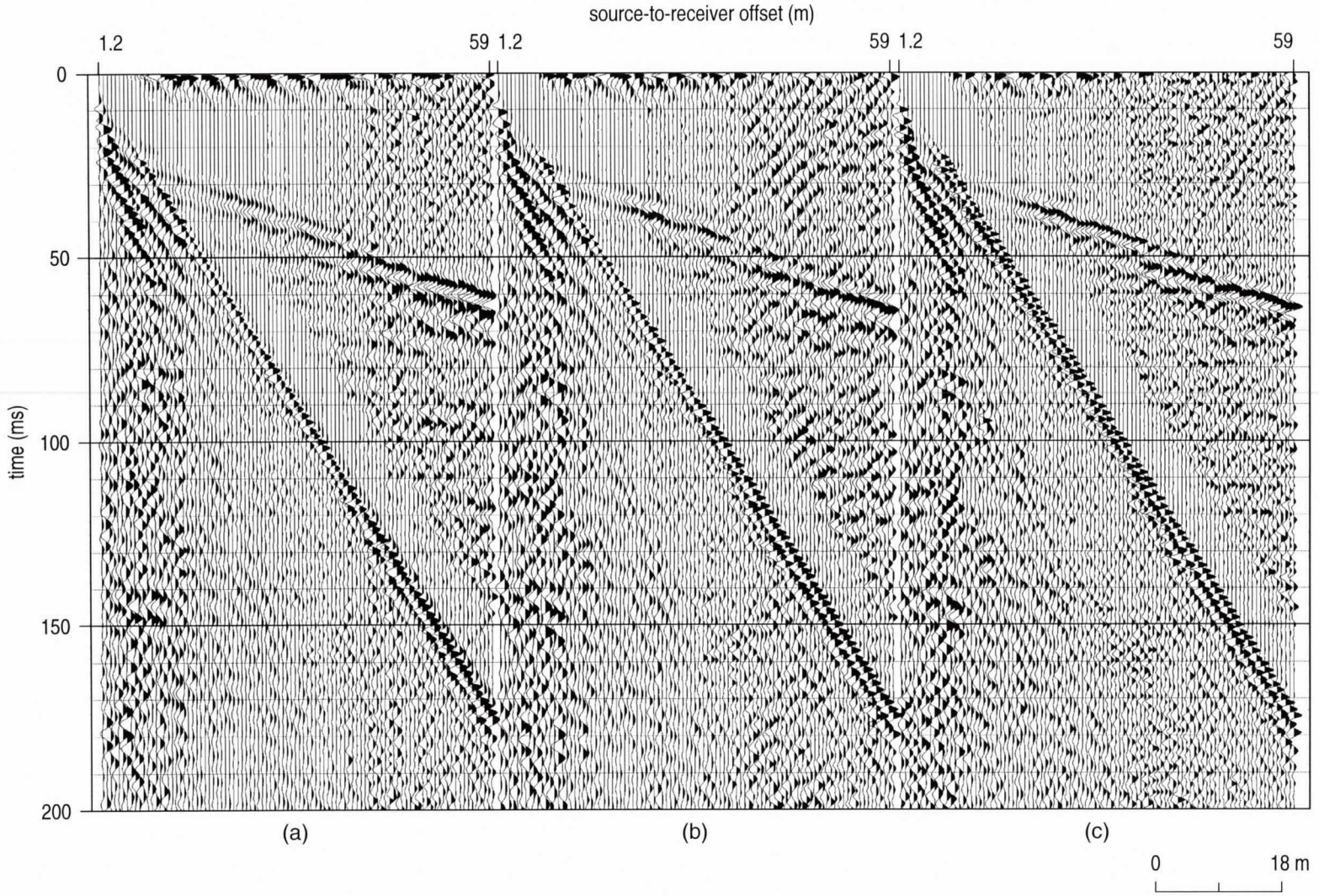


Figure A5. A 100-200-400-600 digital filter applied to files from Figure A2.

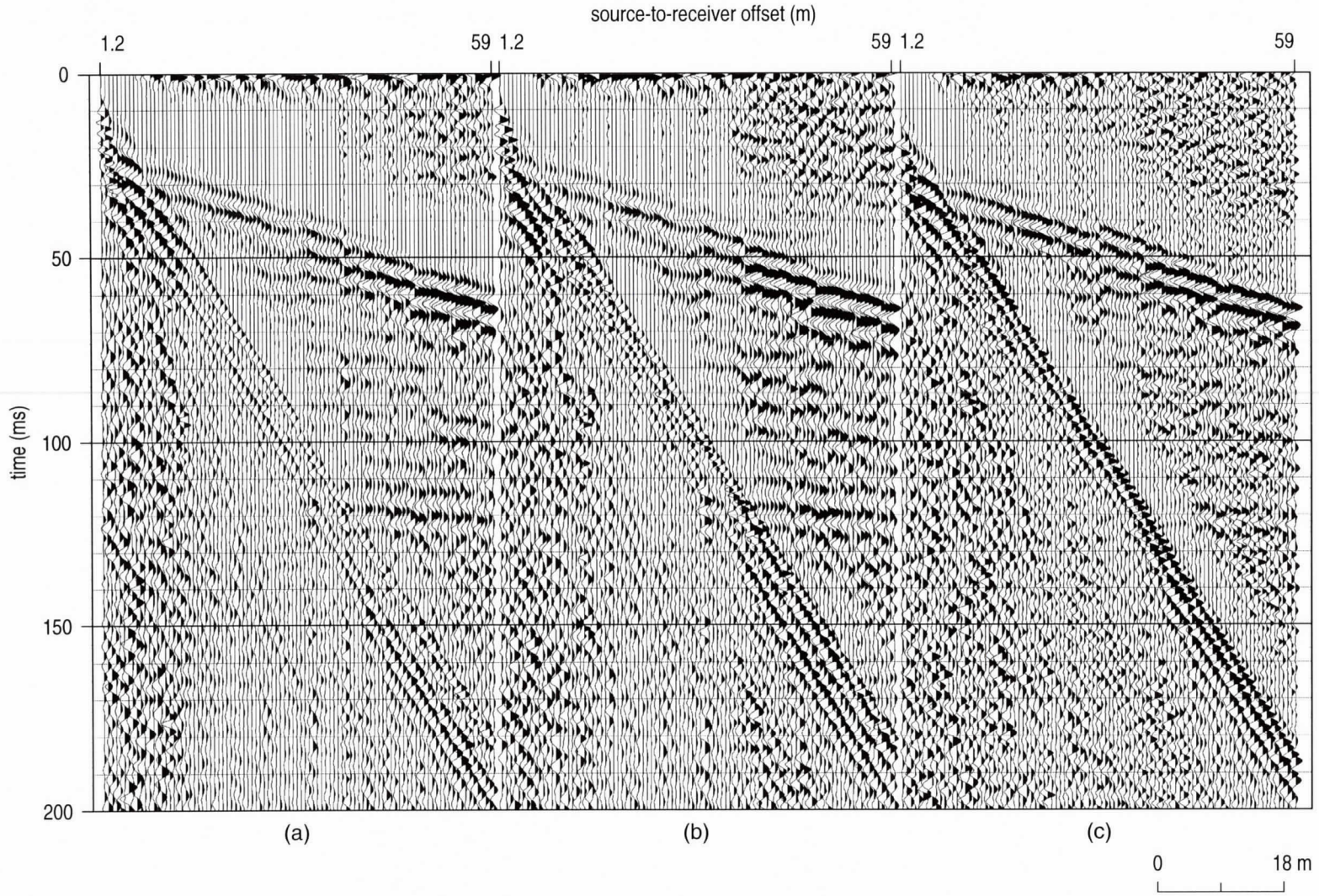


Figure A6. A 100-200-400-600 digital filter applied to files from Figure A3.

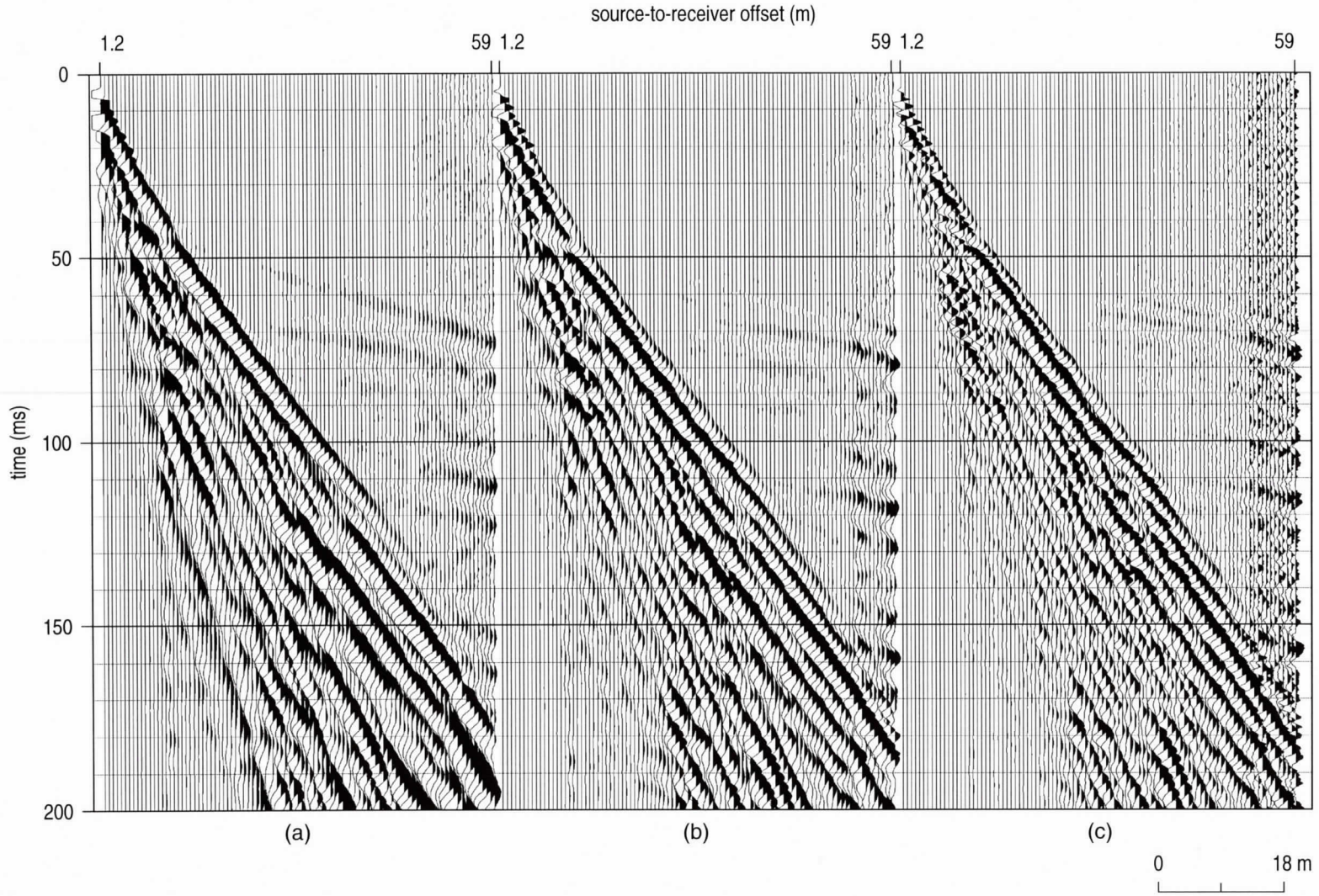


Figure A7. Walkaway field files from site #3 using downhole 30.06 recorded with (a) no analog low-cut filter, (b) 100 Hz, and (c) 200 Hz.

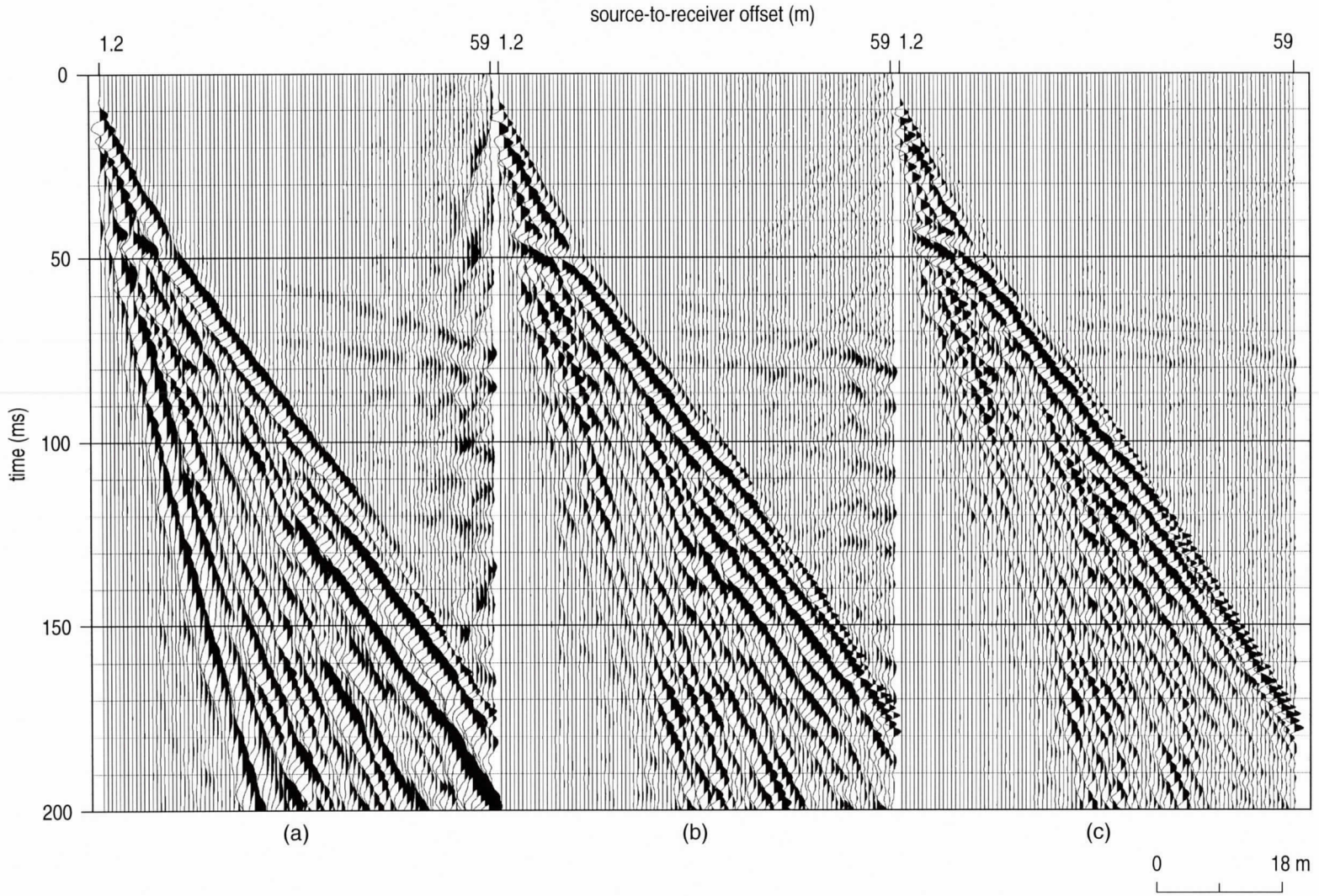


Figure A8. Walkaway field files from site #3 using sledgehammer recorded with low-cut filter (a) out, (b) 100 Hz, and (c) 200 Hz.

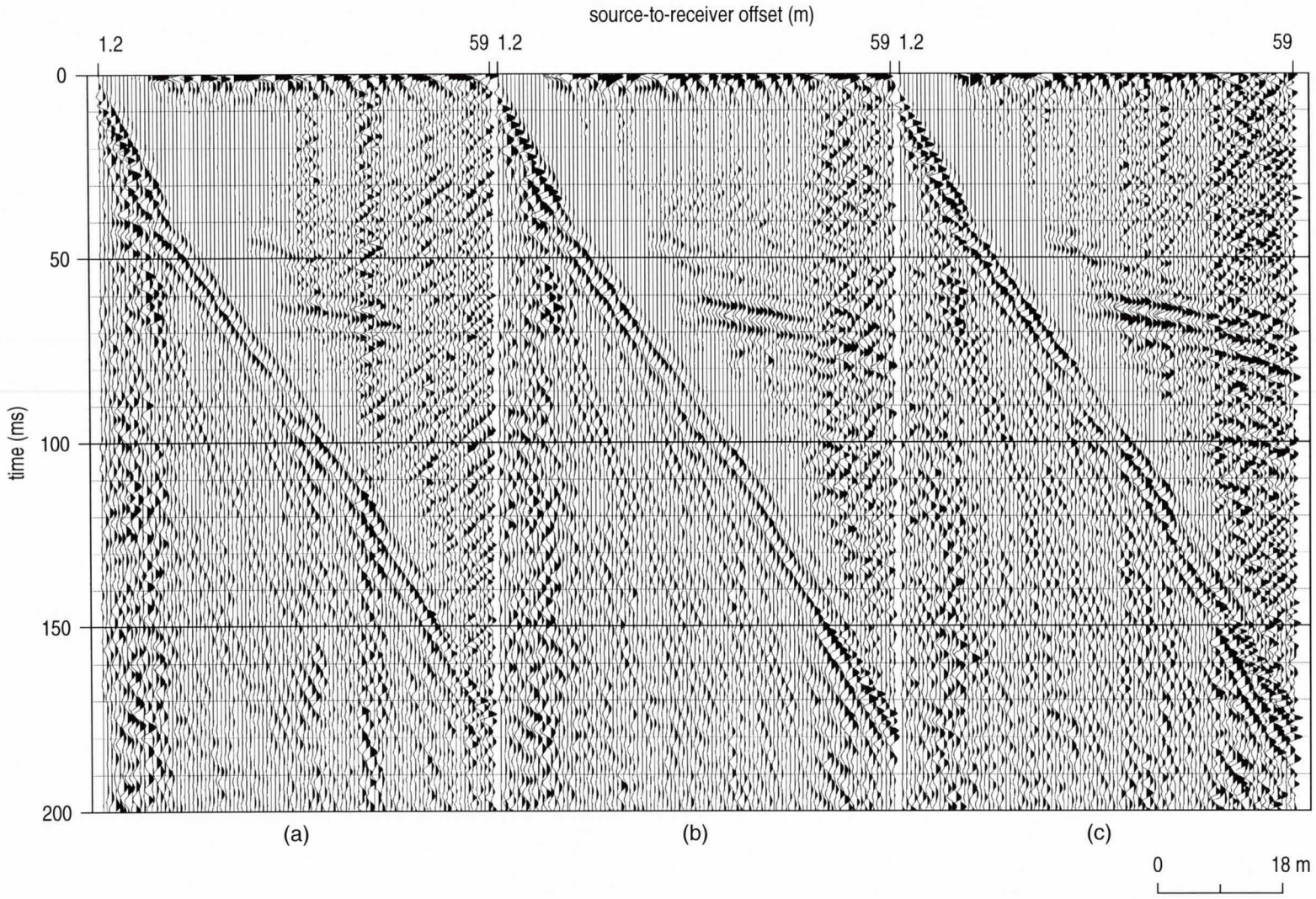


Figure A9. A 100-200-400-600 digital filter applied to files from Figure A7.

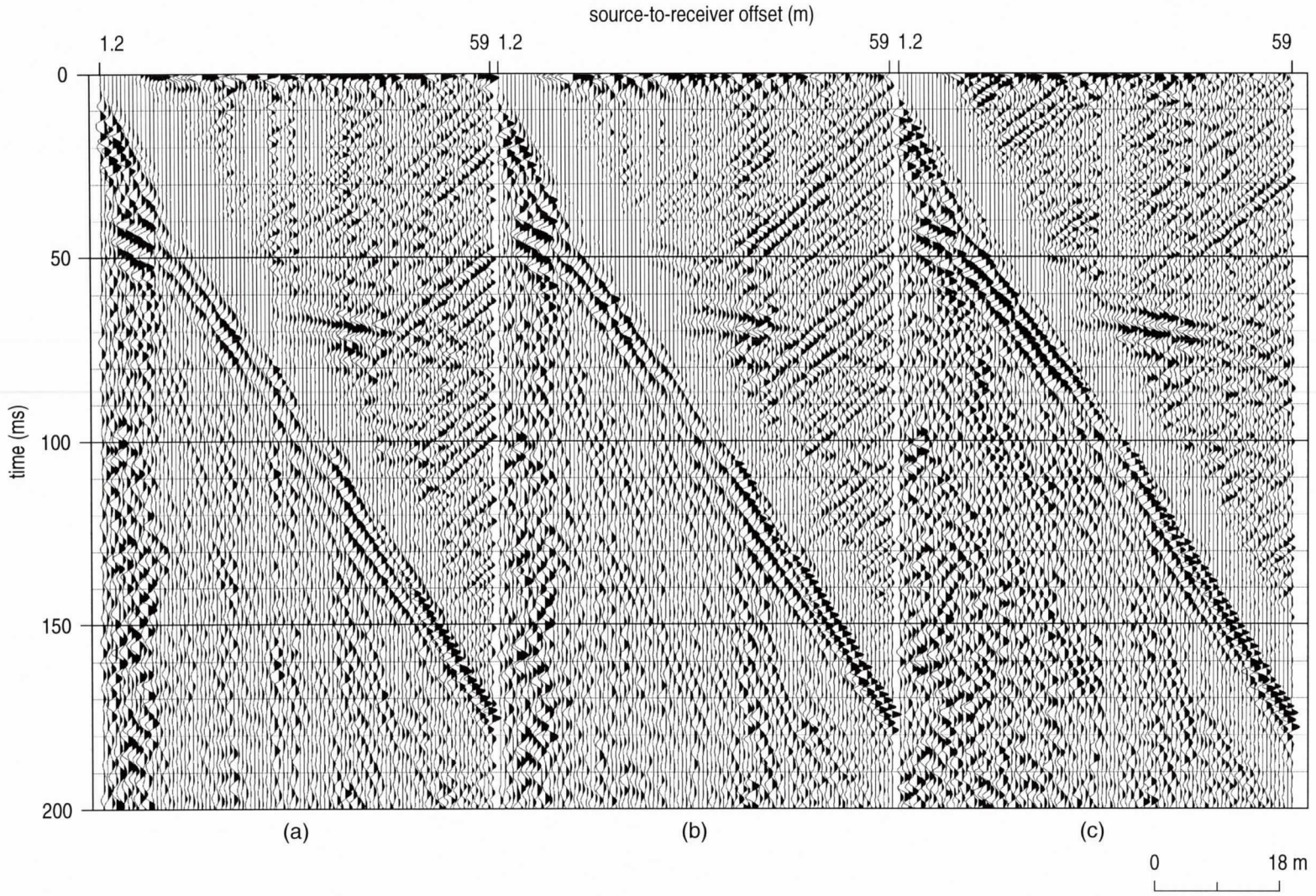


Figure A10. A 100-200-400-600 digital filter applied to files from Figure A8.

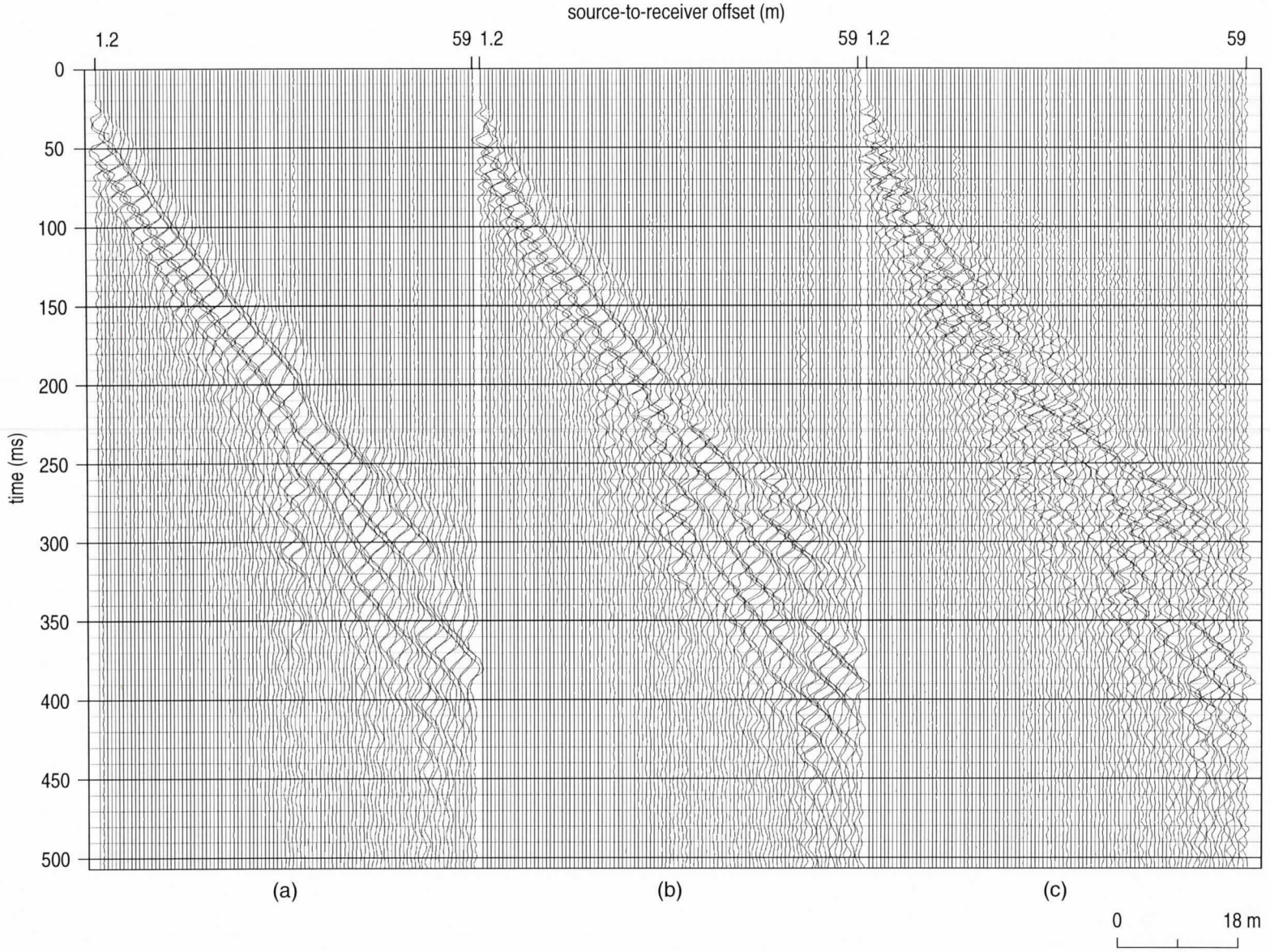


Figure A11. Combined forward and reverse polarity S-wave field files with every other wiggle trace reversed to allow visual inspection of polarization and coherence of potential reflection events. The S-wave mini block source was recorded with analog low-cut filters (a) out, (b) 50 Hz, and (c) 100 Hz.

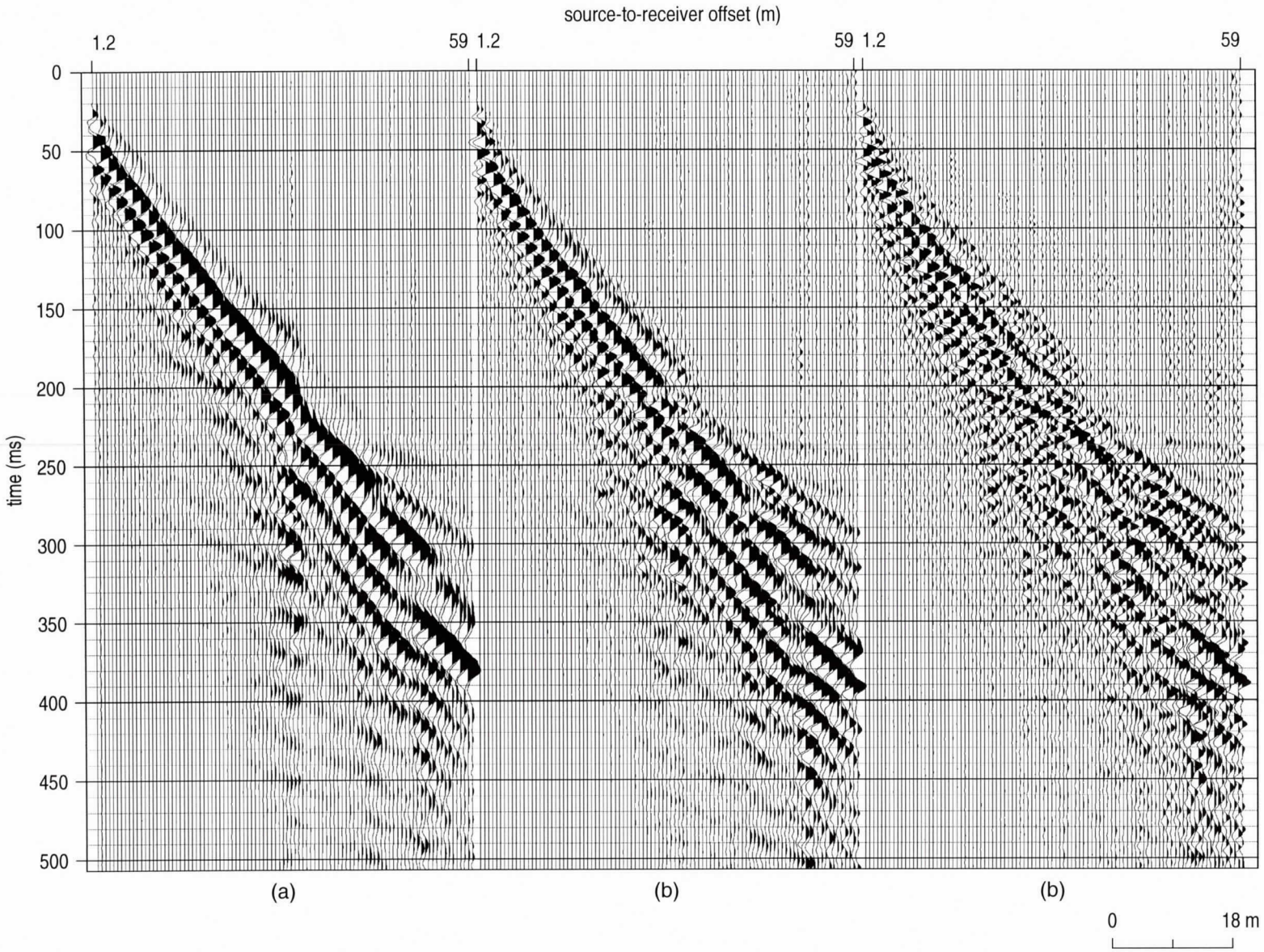


Figure A12. Combined forward and reverse polarity S-wave field files with every other variable wiggle trace reversed to allow visual inspection of polarization and coherence of potential reflection events. The only potential reflection that can be identified with any degree of confidence has a zero offset time of about 180 msec. The S-wave mini block source was recorded with analog low-cut filters (a) out, (b) 50 Hz, and (c) 100 Hz.

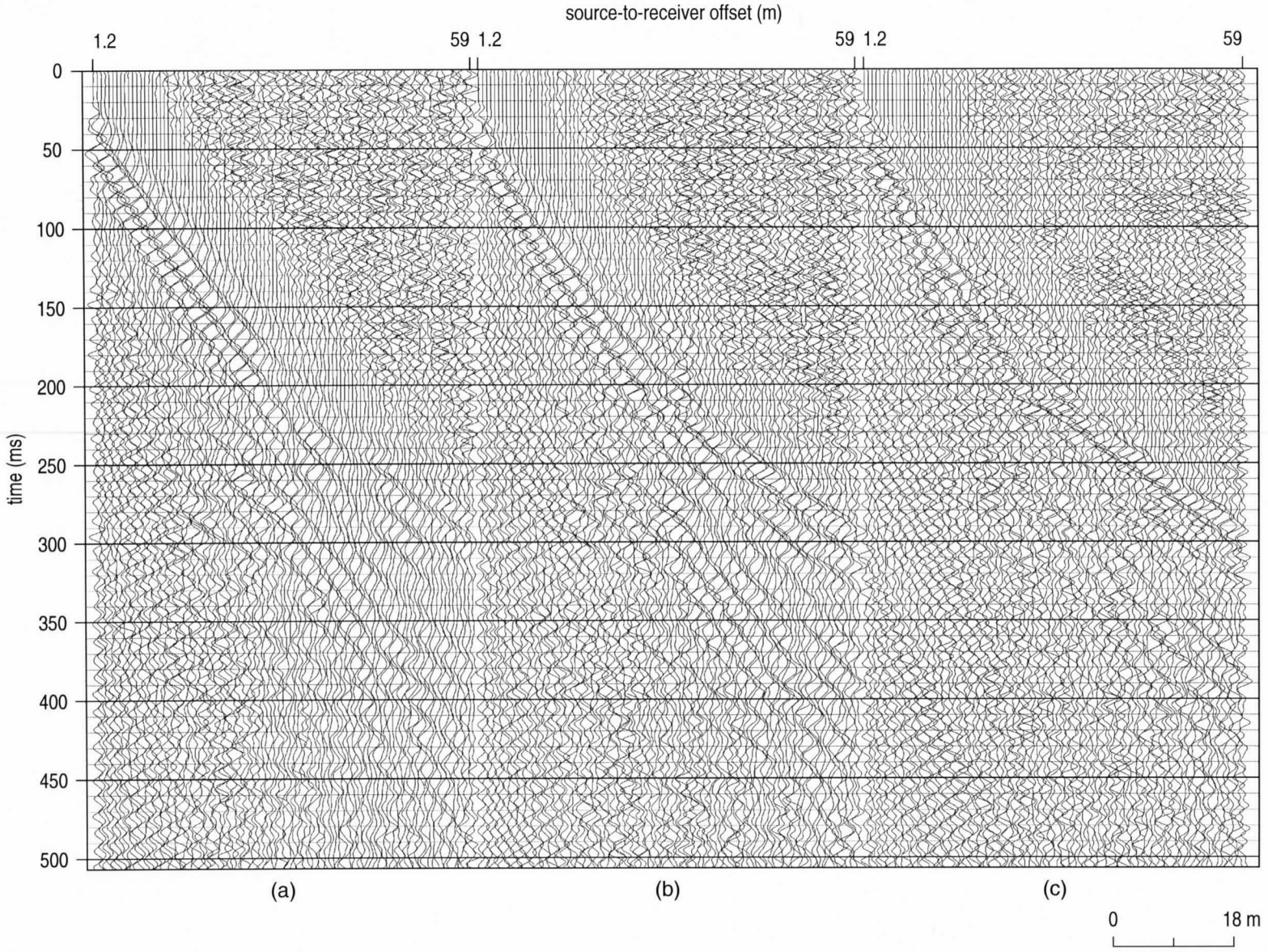


Figure A13. S-wave shot gather of Figure A11 with a 25-50, 125-250 Hz digital filter and 100 msec AGC scale applied. Digital filtering did little to enhance potential reflection events evident with this display format.

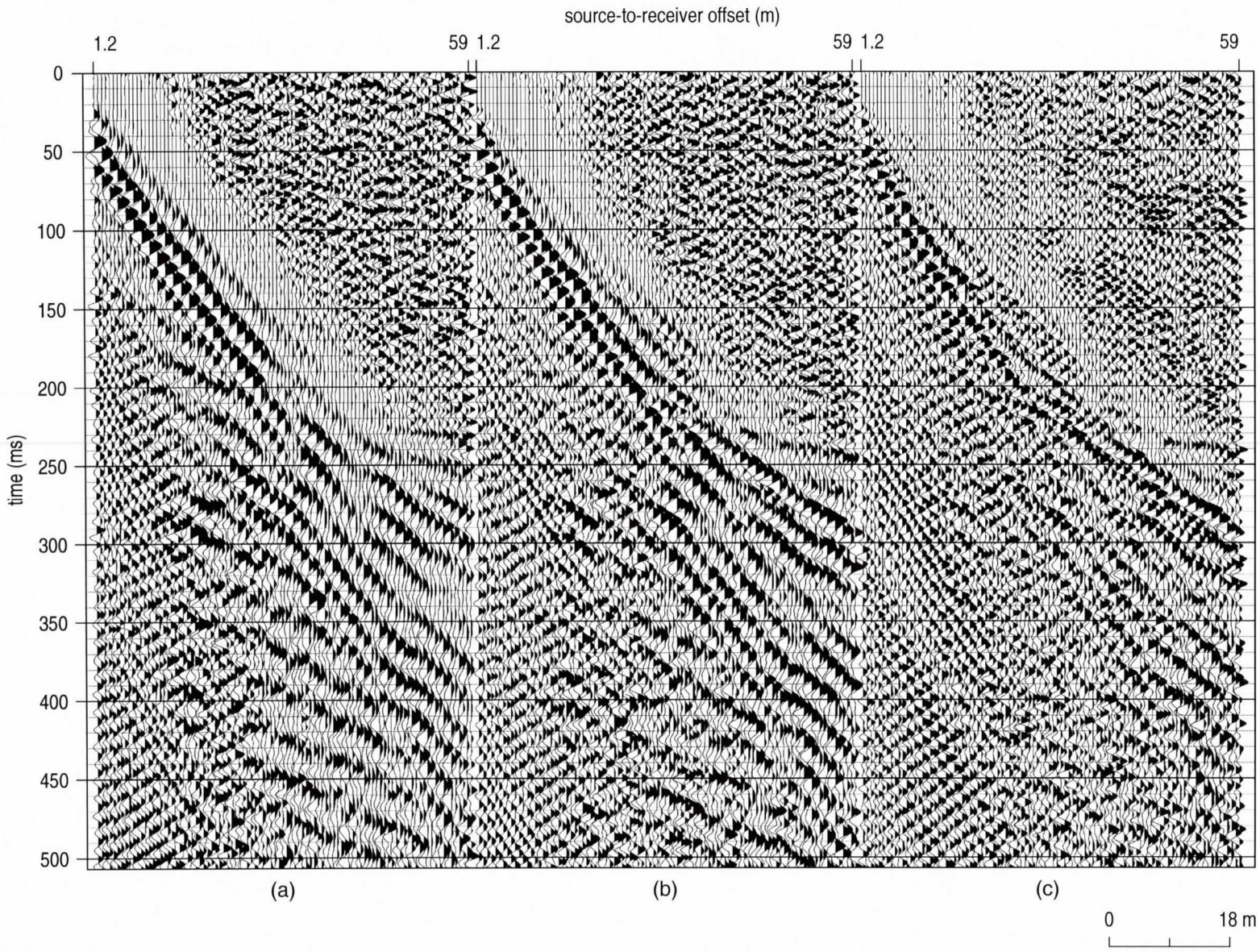


Figure A14. S-wave shot gather of Figure A12 with a 25-50, 125-250 Hz digital filter and 100 msec AGC scale applied. Digital filtering did little to enhance potential reflection events evident on raw data. Some suggestion of reflections on data acquired with no analog low-cut are interpretable with vertical incident times between 150 and 250 msec.

## Appendix B: VSP Data and Interpretations

1. Velocity model. The first break traveltime is picked up to generate interval velocity and average velocity models in these three wells. Precaution should be made in interpretation of these velocity models. Errors in picking the first break traveltime are transferred into the velocity models, especially the interval velocity model. The relative errors in the interval velocity models could be as high as ±20% of the true value. The errors in the average velocity models are normally less than ±5% of the true average velocities, which are much less than those in the interval velocity models.

Velocity models from depth 0 m to 10 m (VSP 1), to 18 m (VSP 2), and to 12 m (VSP 3) are also derived from downhole geophone data. The overlaps between velocity models derived from hydrophone data and downhole geophone data (from depth 8 m to 10 m of VSP 1, 4 m to 18 m of VSP 2, and 8 m to 12 m of VSP 3) could be used to evaluate the accuracy of the velocity models. The relative differences in two average velocities are less than 5% for VSP 1 and VSP 2 and less than 10% for VSP 3.

2. Reflection events. In processed data of VSP 1, although it is relatively difficult to identify shallow reflection events compared with VSP 2 and VSP 3, we can still pick reflection events at depths of 18 m in 9 m source-well-offset gathers and at depths of 33 m in 15 m source-well-offset gathers. These two events are correlated to the gamma ray well log (STRAT-VSP1). Another strong reflection event at a depth of 73 m can be easily determined in 18 m to 30 m source-well-offset gathers.

In processed data of VSP 2, two strong shallow reflection events can be identified at depths of 17 m and 37 m in 10 m source-well-offset gathers. These two events are correlated to the gamma ray well log (STRAT-VSP2). The 17 m event could also be seen in 6 to 18 m source-to-well-offset gathers. Several strong reflection events at depth below 70 m can be easily determined in 15 to 45 m source-well-offset gathers.

In processed data of VSP 3, two shallow reflection events can be identified at depths of 17 m and 33 m in 10 m source-well-offset gathers and others. These two events are correlated to the gamma ray well log (STRAT-VSP3). Several strong reflection events at depths below 70 m can be easily determined in 12 to 58 m source-well-offset gathers.

3. Corridor stacking. Several gathers are picked to generate the corridor stacking section: 15 m source-well-offset gather of VSP 1, 10 m source-well-offset gather of VSP 2, and 10 m source-well-offset gather of VSP 3.

**Table B1**
**VSP Processing**

| | |
|---|---|
| 1. AGC scale | 50 msec time window) |
| 2. Bandpass filter | (50/100/300/450 trapezoidal, dominant frequency 190 Hz) |
| 3. F-K filter | (reject direct wave 0.25 ms/trace to 1.5 ms/trace; eject downgoing tube wave 2.3 ms/trace to 4.4 ms/trace; reject upcoming tube wave -4.4 ms/trace to -2.3 ms/trace) |
| 4. Bandpass filter | (50/100/300/450 trapezoidal, remove F-K artifacts) |
| 5. Edit | (first arrival mute to remove wrap around noise of fk filter) |
| 6. Static correction | (datum correction to the well head; i.e., two way travel time) |
| 7. Corridor stacking | (30 to 150 msec trace summing, only reflections will be horizontal) |

**Table B2**

**Depth vs Time**

| Depth (m) | Two-way Time (ms) VSP 1 | VSP 2 | VSP 3 | Depth (m) | Two-way Time (ms) VSP 1 | VSP 2 | VSP 3 |
|---|---|---|---|---|---|---|---|
| 1.5 | 3.8 | 3.9 | 4.2 | 31.9 | 49.3 | 48.6 | 55.0 |
| 3.0 | 7.8 | 7.7 | 8.2 | 33.5 | 50.9 | 50.7 | 56.2 |
| 4.6 | 11.6 | 11.6 | 12.1 | 35.0 | 52.3 | 52.4 | 57.9 |
| 6.1 | 14.9 | 14.7 | 15.7 | 36.5 | 54.1 | 54.2 | 59.2 |
| 7.6 | 18.2 | 17.3 | 20.2 | 38.0 | 55.9 | 55.9 | 61.1 |
| 9.1 | 21.3 | 19.6 | 23.2 | 39.5 | 57.8 | 57.6 | 63.1 |
| 10.6 | 23.4 | 21.6 | 26.0 | 41.1 | 59.3 | 59.4 | 64.8 |
| 12.2 | 25.7 | 23.9 | 28.5 | 42.6 | 61.4 | 61.0 | 66.2 |
| 13.7 | 27.5 | 26.0 | 31.7 | 44.1 | 62.6 | 62.5 | 67.9 |
| 15.2 | 29.6 | 28.2 | 33.7 | 45.6 | 64.2 | 64.0 | 69.8 |
| 16.7 | 31.2 | 30.2 | 35.4 | 47.2 | 66.0 | 65.7 | 71.7 |
| 18.3 | 33.0 | 32.1 | 37.7 | 48.7 | 67.3 | | 72.9 |
| 19.8 | 34.9 | 34.0 | 9.9 | 50.2 | | | 74.0 |
| 21.3 | 37.0 | 35.7 | 42.0 | 51.7 | | | 76.1 |
| 22.8 | 38.8 | 37.6 | 43.7 | 53.2 | | | 77.6 |
| 24.3 | 40.3 | 39.5 | 45.7 | 54.8 | | | 78.9 |
| 25.9 | 42.1 | 41.0 | 47.6 | 56.3 | | | 81.0 |
| 27.4 | 43.9 | 42.7 | 49.6 | 57.8 | | | 82.5 |
| 28.9 | 45.3 | 44.3 | 51.2 | 59.3 | | | 84.2 |
| 30.4 | 47.4 | 46.4 | 53.0 | 60.8 | | | 86.1 |

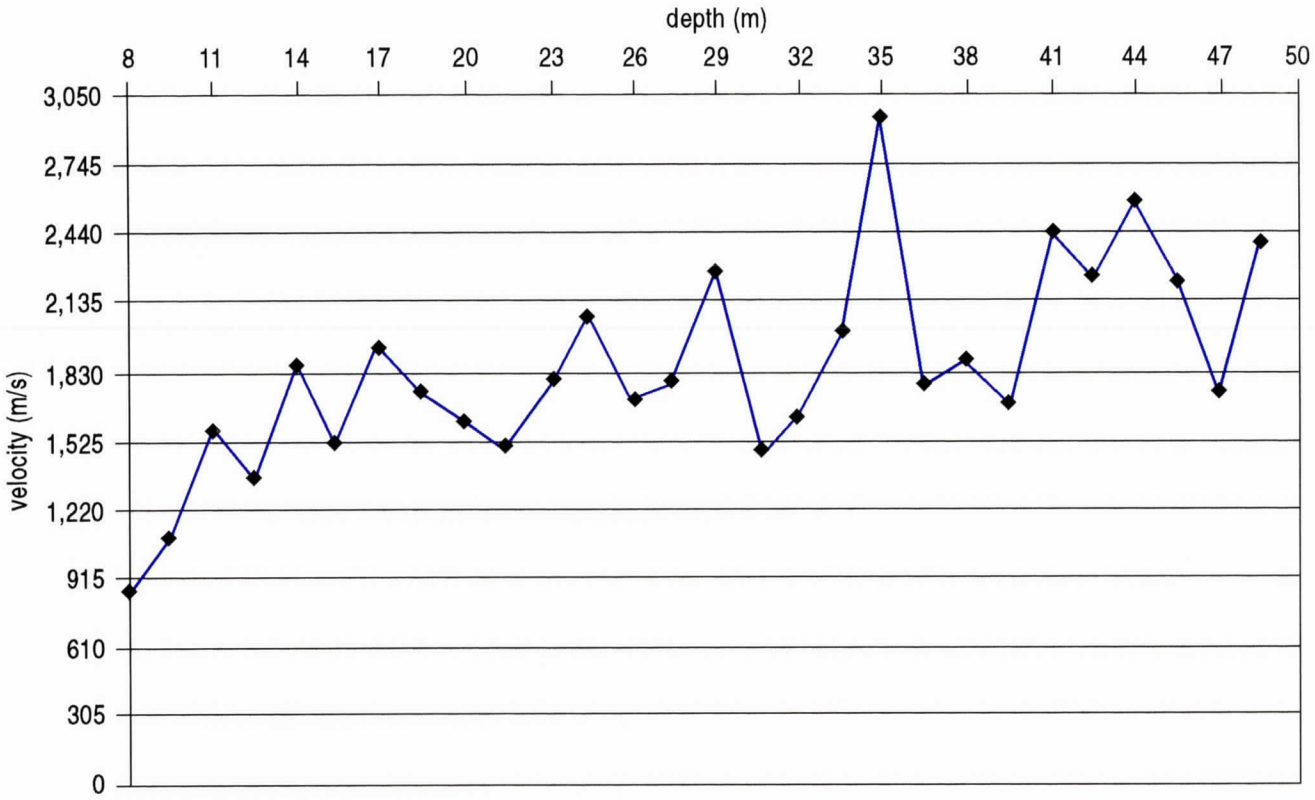


Figure B1. Interval velocity plot of VSP #1 using the hydrophone receiver.

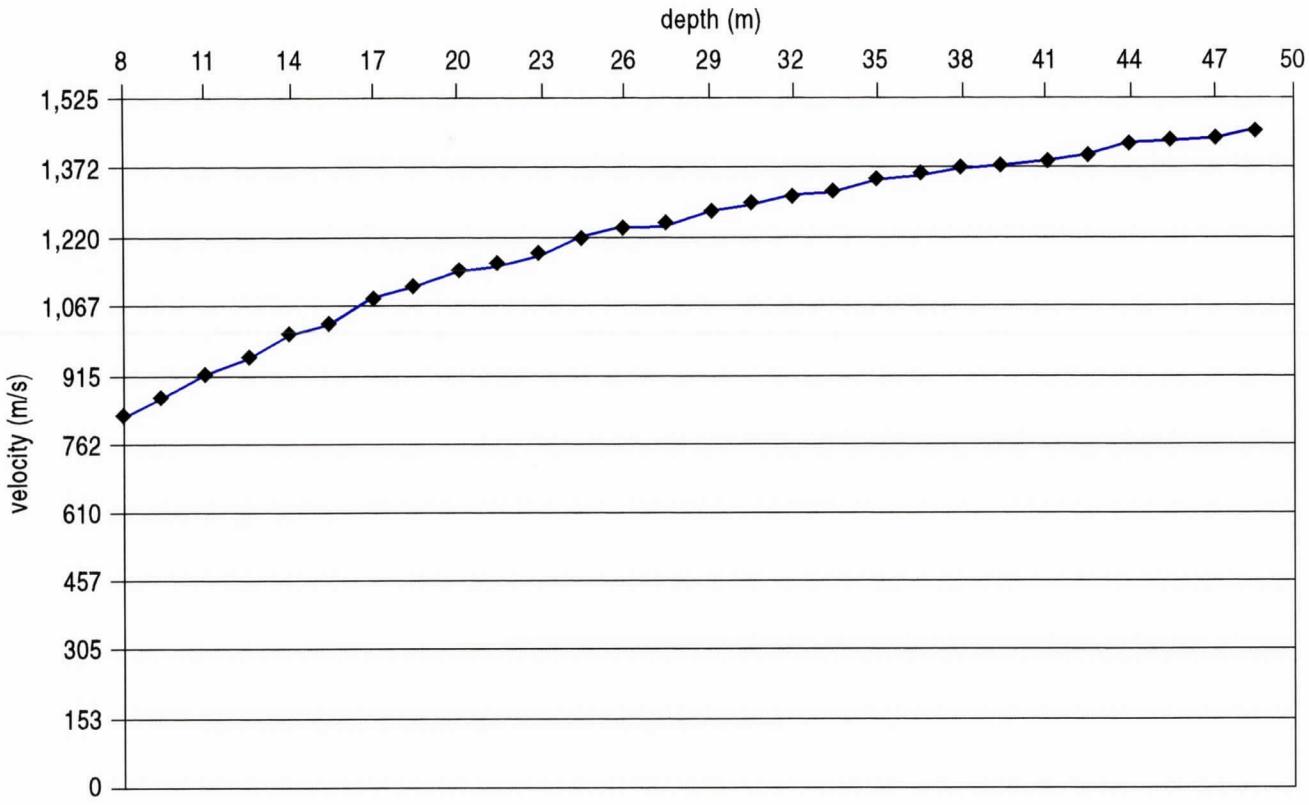


Figure B2. Average velocity plot of VSP #1 using the hydrophone receiver.

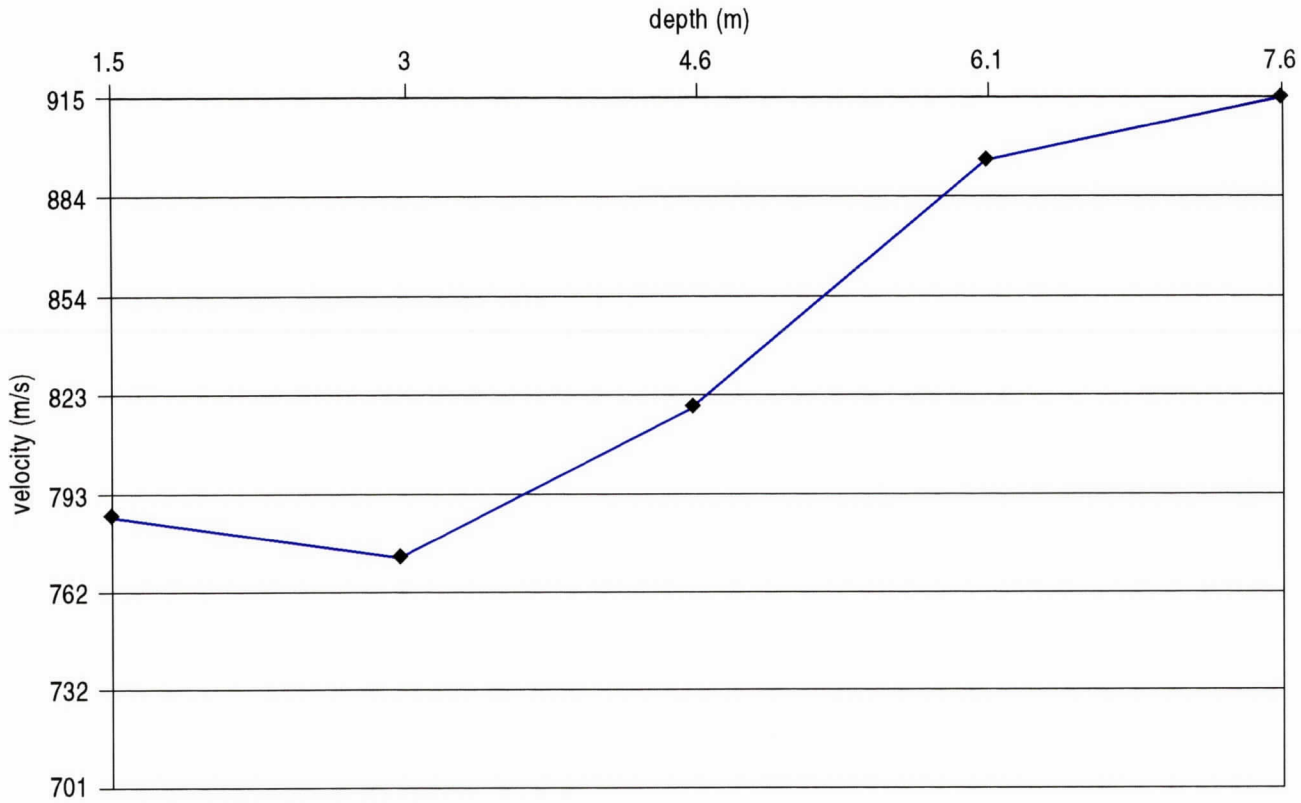


Figure B3. Interval velocity plot of VSP #1 using the hole-lock geophone.

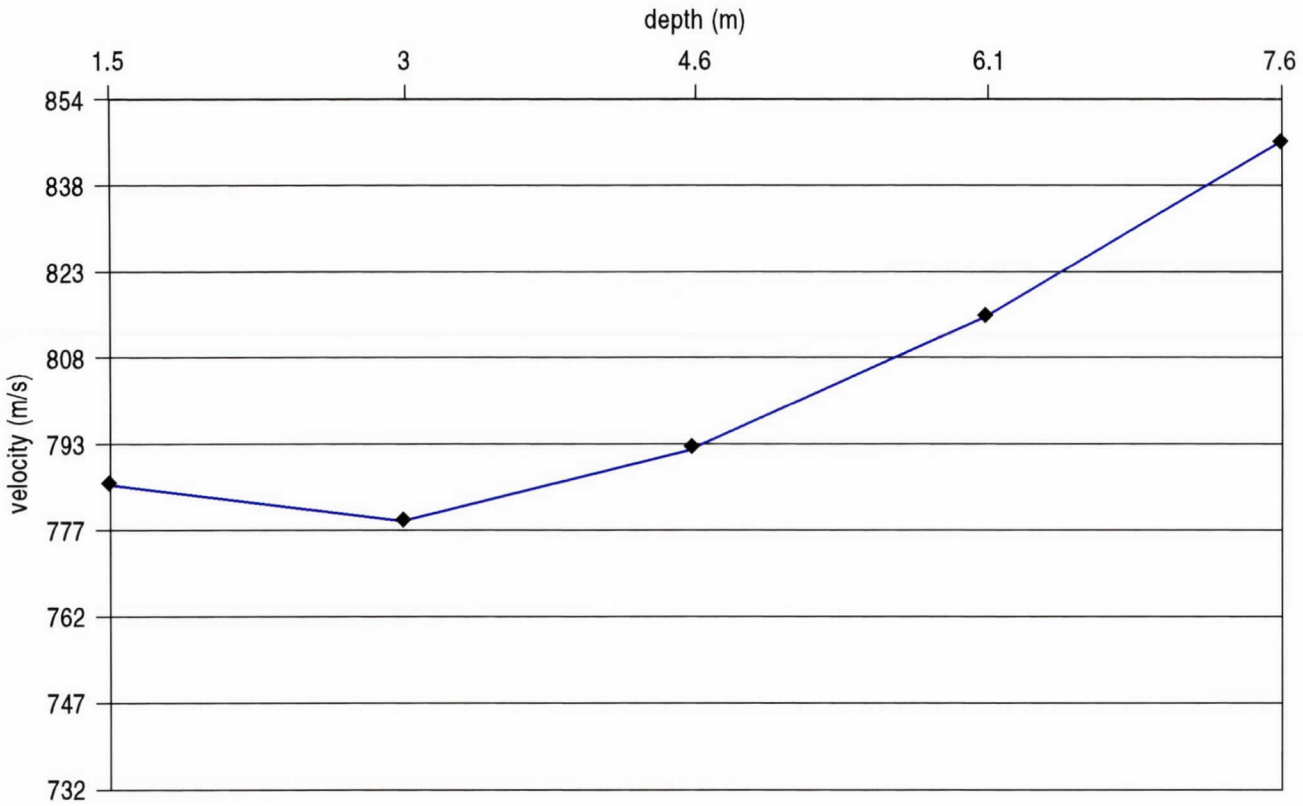


Figure B4. Average velocity plot of VSP #1 using the hole-lock geophone.

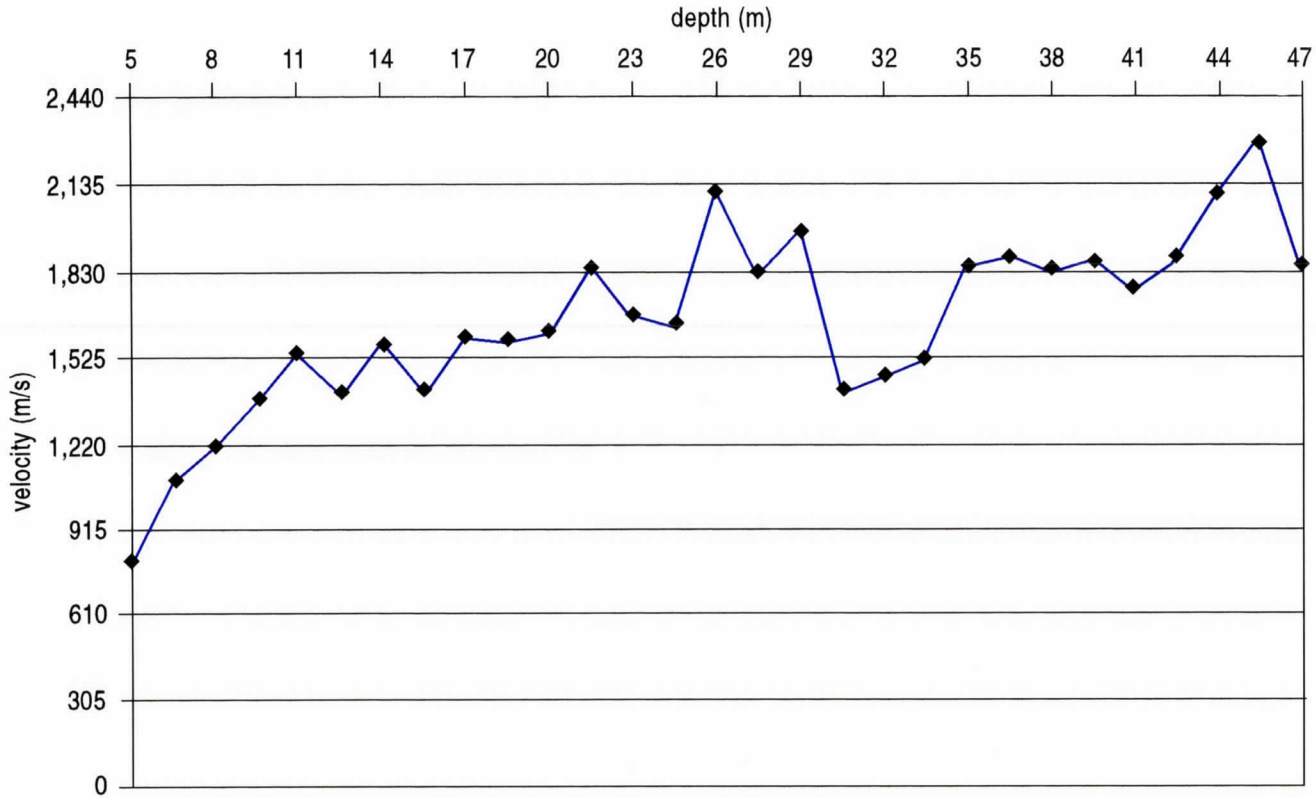


Figure B5. Interval velocity plot of VSP #2 using the hydrophone receiver.

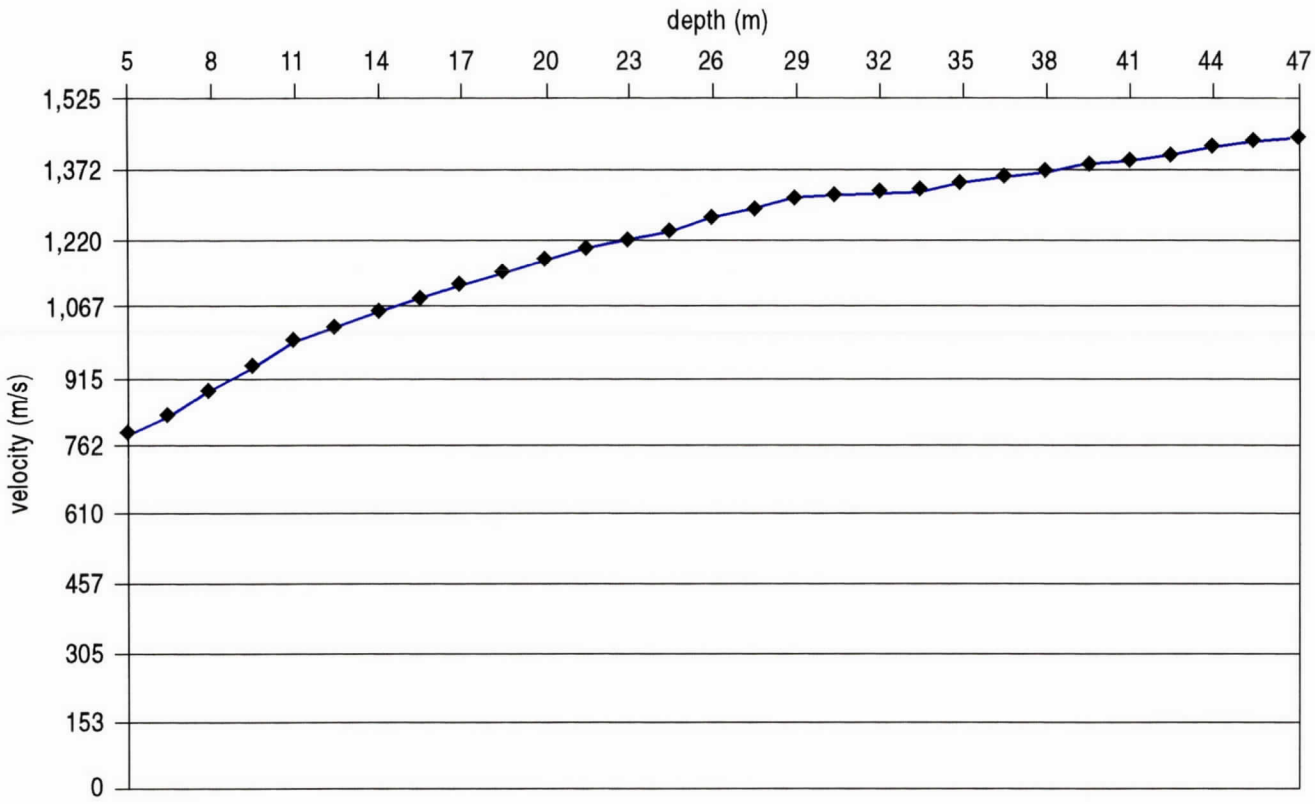


Figure B6. Average velocity plot of VSP #2 using the hydrophone receiver.

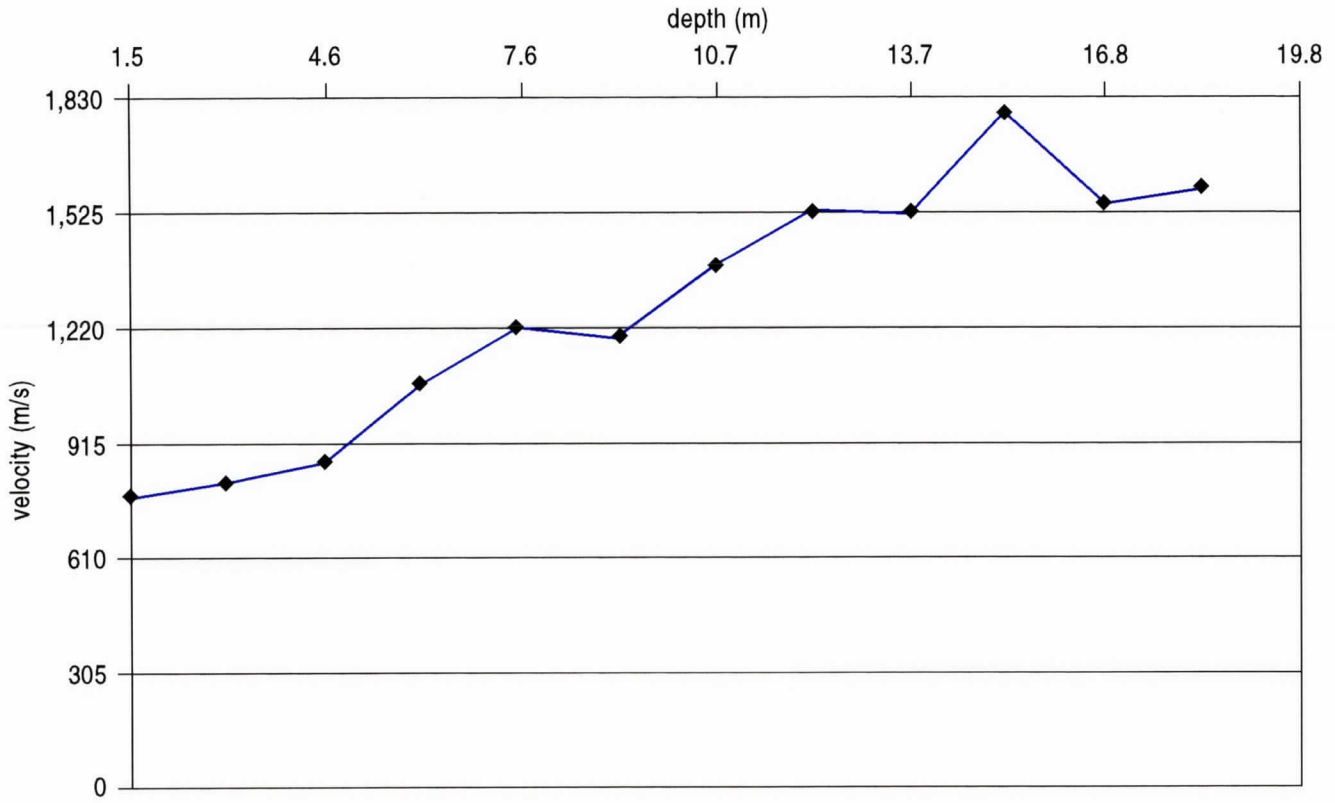


Figure B7. Interval velocity plot of VSP #2 using the hole-lock geophone.

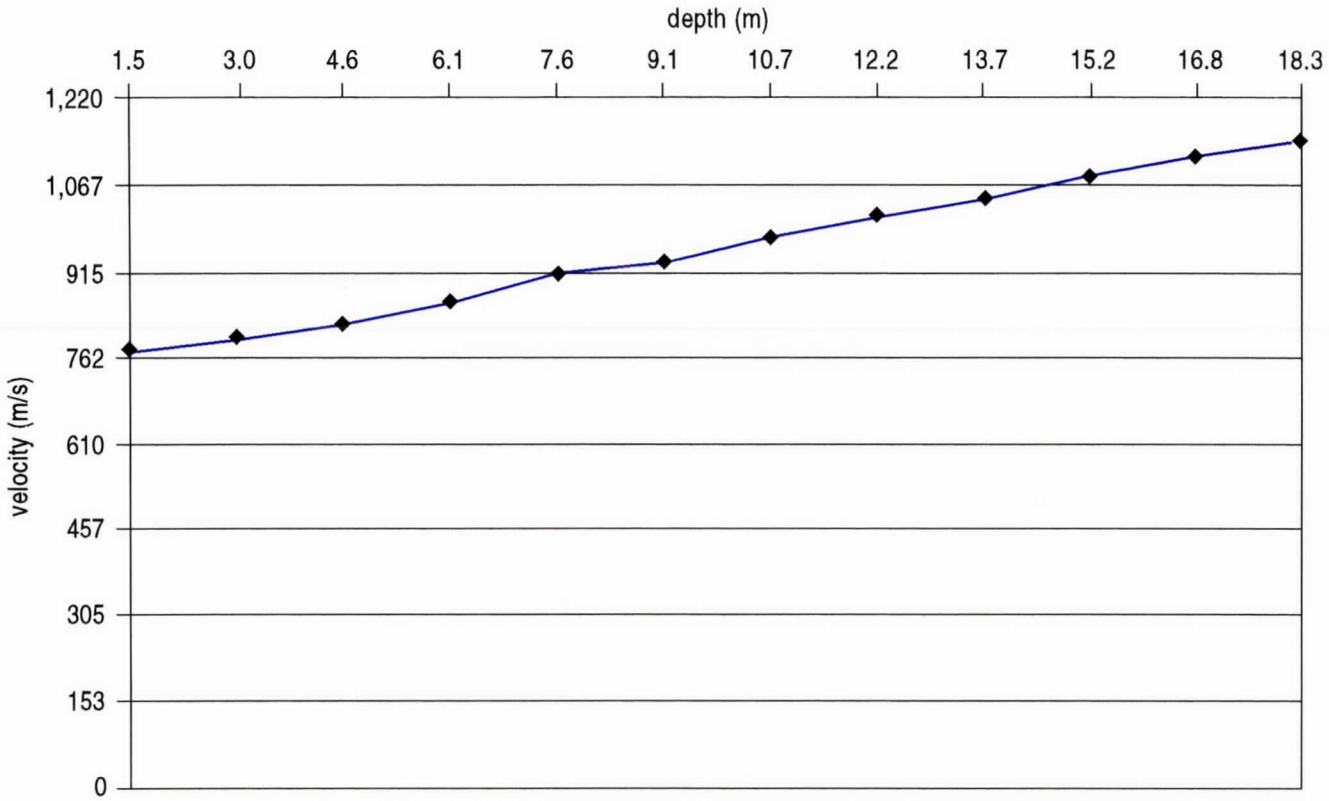


Figure B8. Average velocity plot of VSP #2 using the hole-lock geophone.

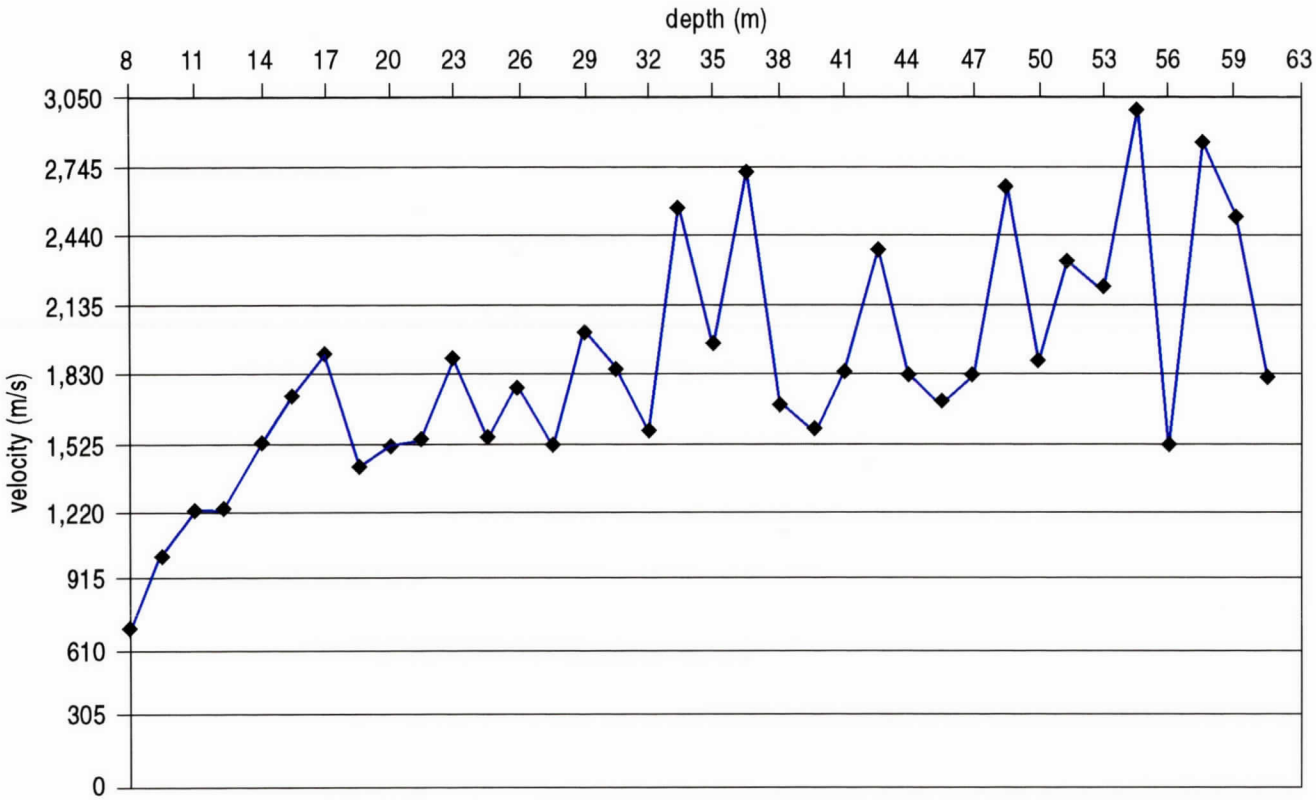


Figure B9. Interval velocity plot of VSP #3 using the hydrophone receiver.

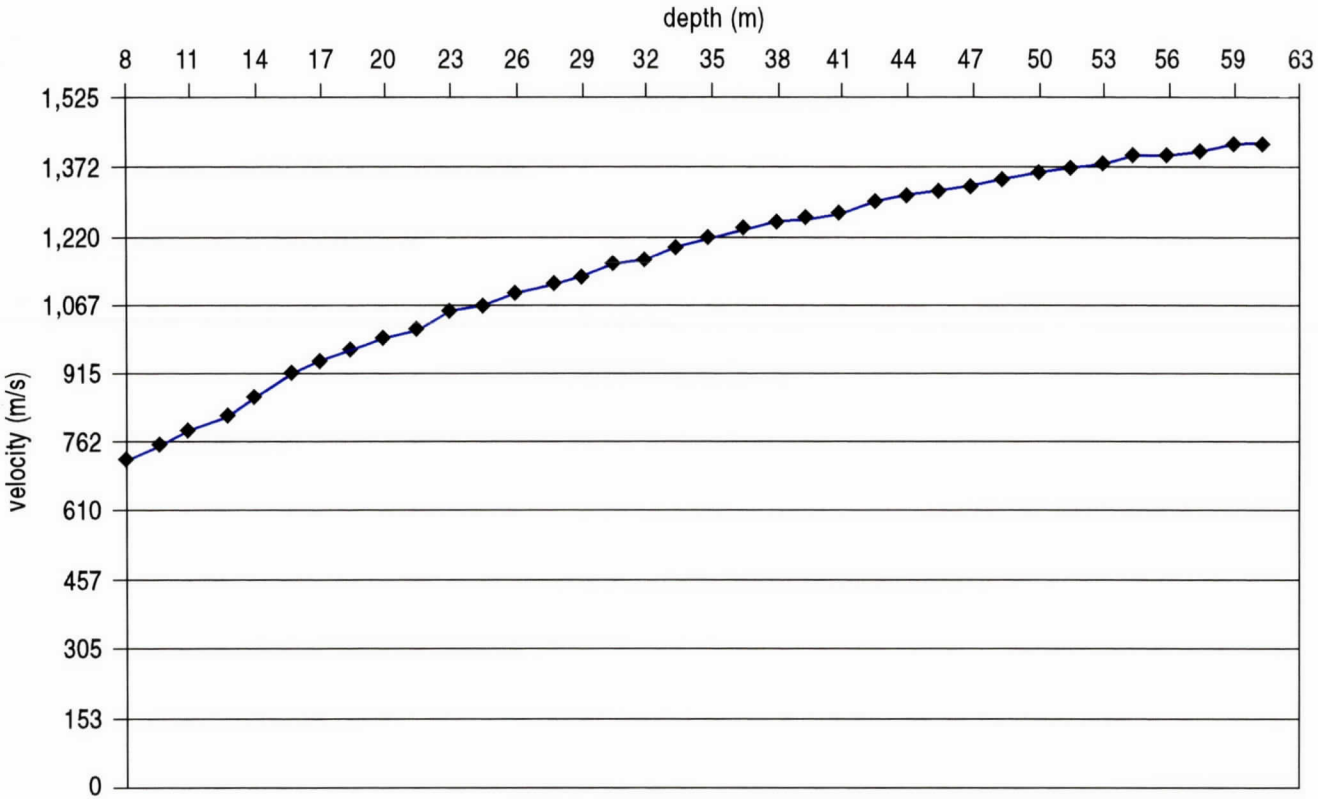


Figure B10. Average velocity plot of VSP #3 using the hydrophone receiver.

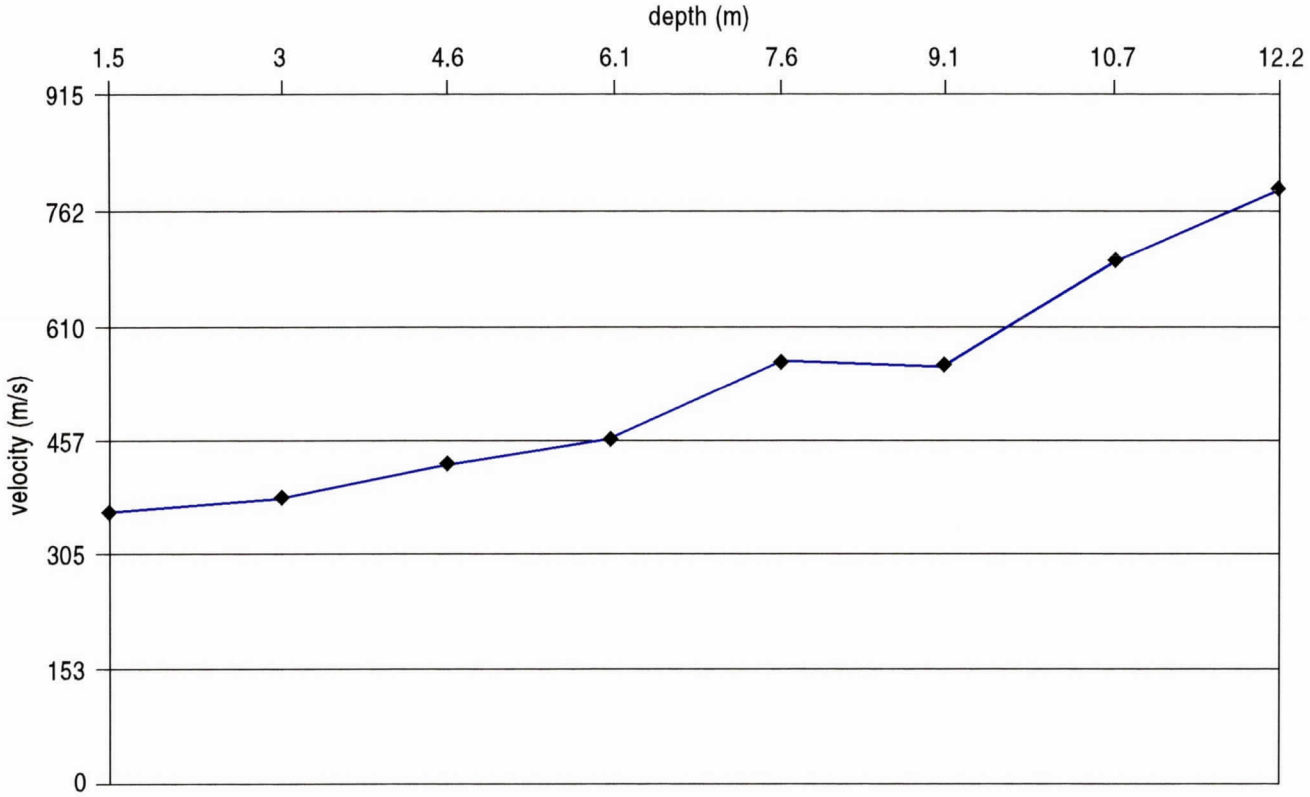


Figure B11. Interval velocity plot of VSP #3 using the hole-lock geophone.

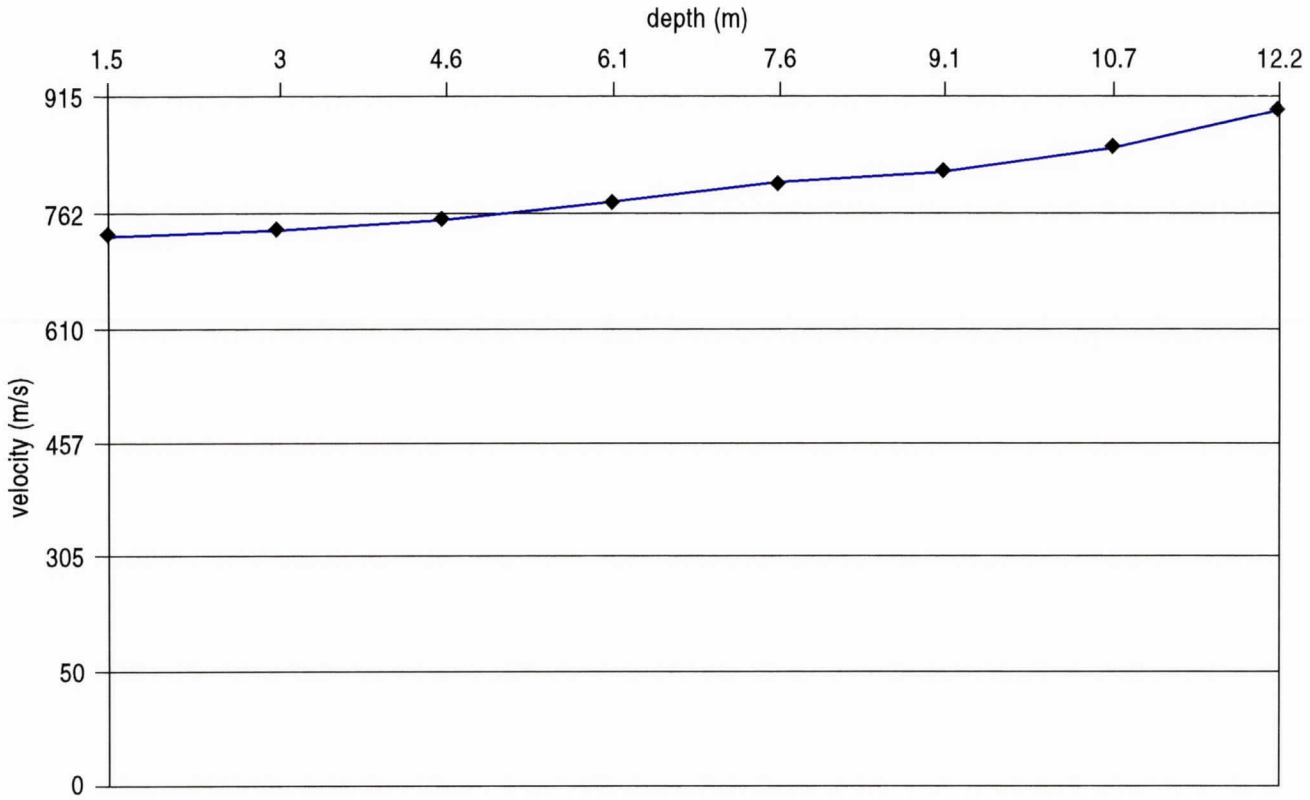


Figure B12. Average velocity plot of VSP #3 using the hole-lock geophone.

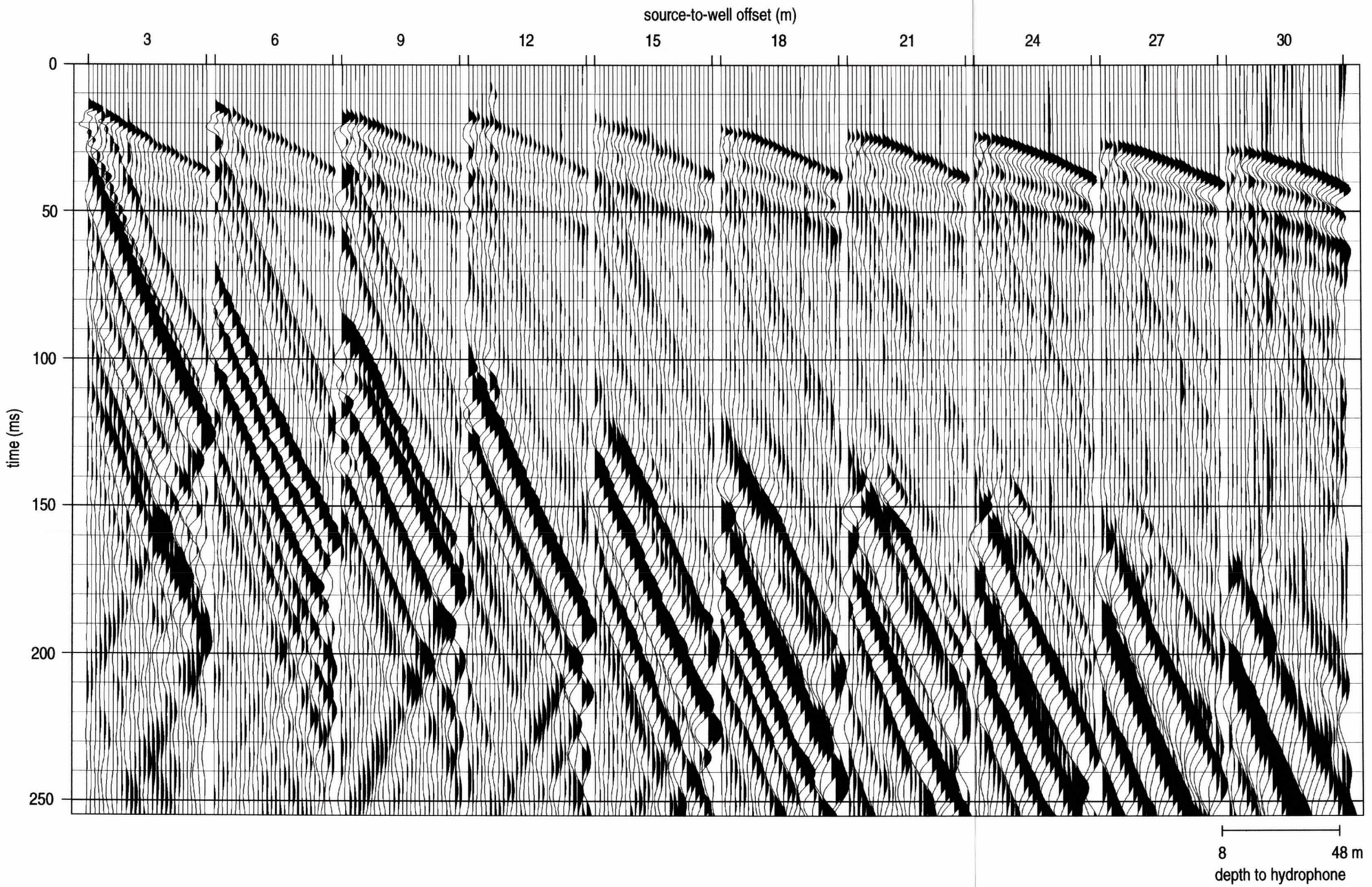


Figure B13. VSP #1 raw hydrophone data. There are a total of 28 traces in each source offset gather with depths from 8 m to 48 m.

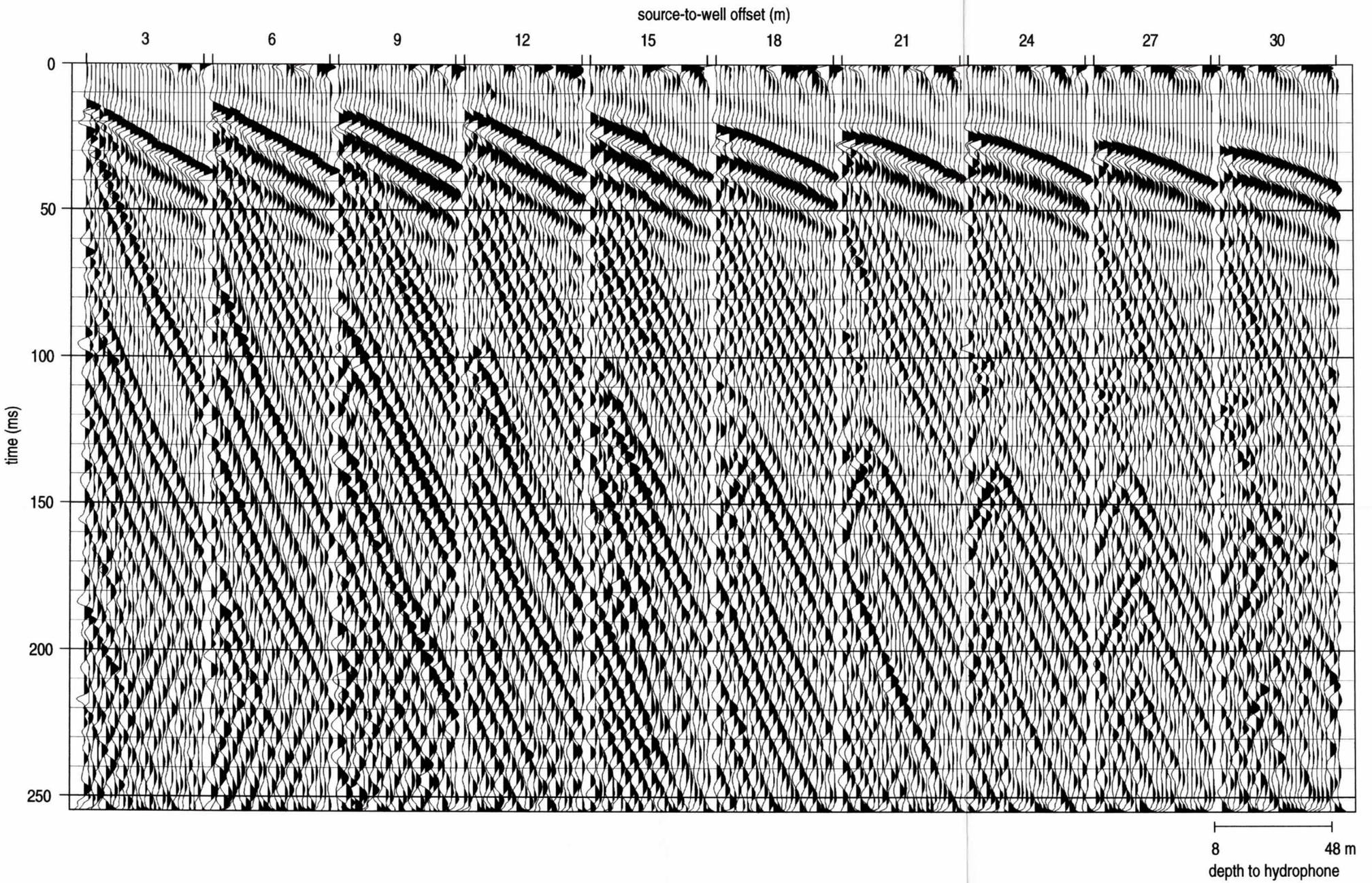


Figure B14. VSP #1 hydrophone data (Figure B13) band-pass filtered (50 100 300 450) and AGC (50 ms) scaled.

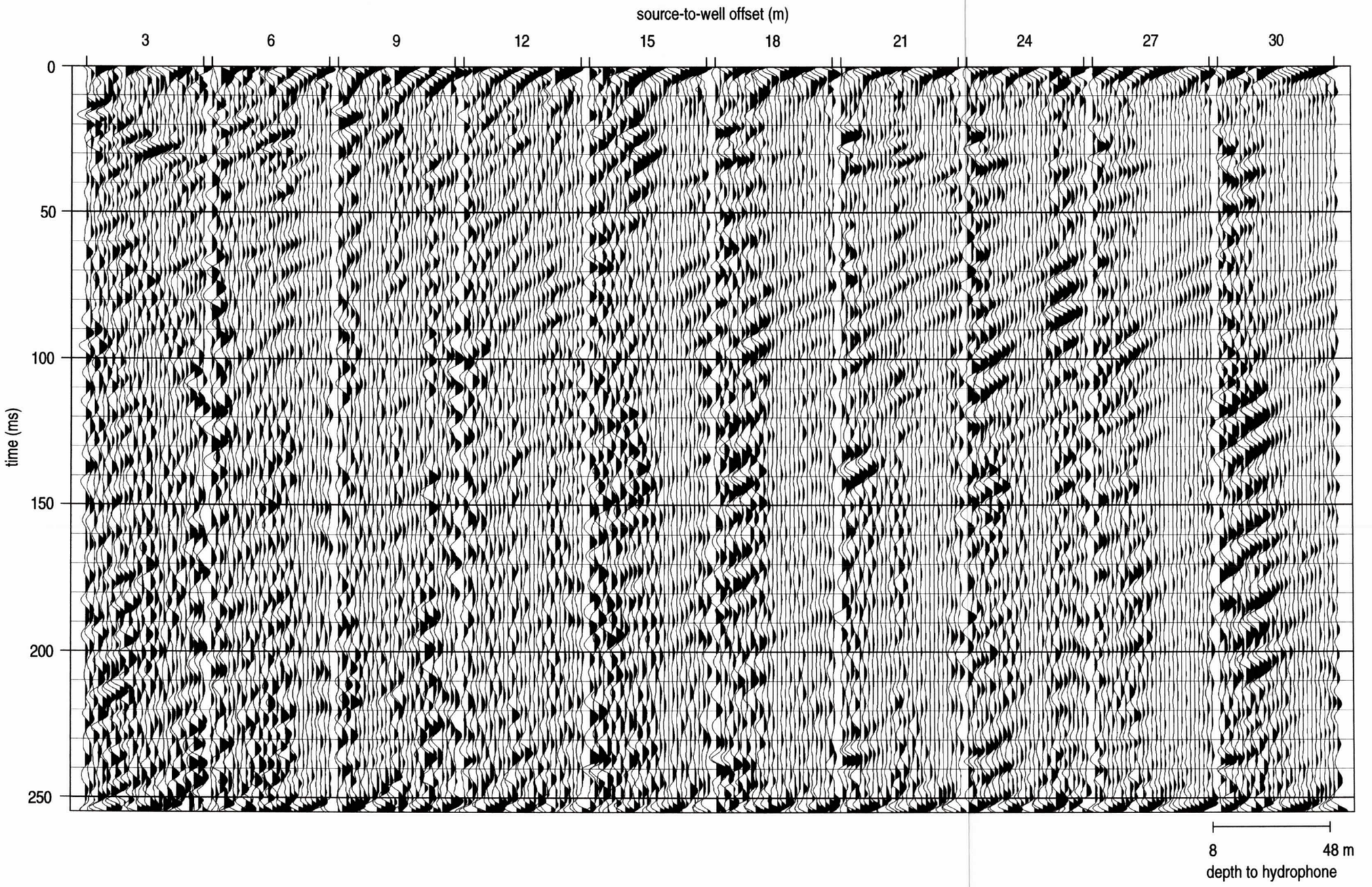


Figure B15. VSP #1 up-coming waves. Two positive fan reject fk filters (0 – 1.5 ms/tr. and 2.0 – 4.0 ms/tr.) applied to filtered and scaled data (Figure B14) to eliminate down-going waves and one negative fan reject fk filter (-2.0 – -4.0 ms/tr.) is also applied to the filtered data to take out strong up-coming tube waves.

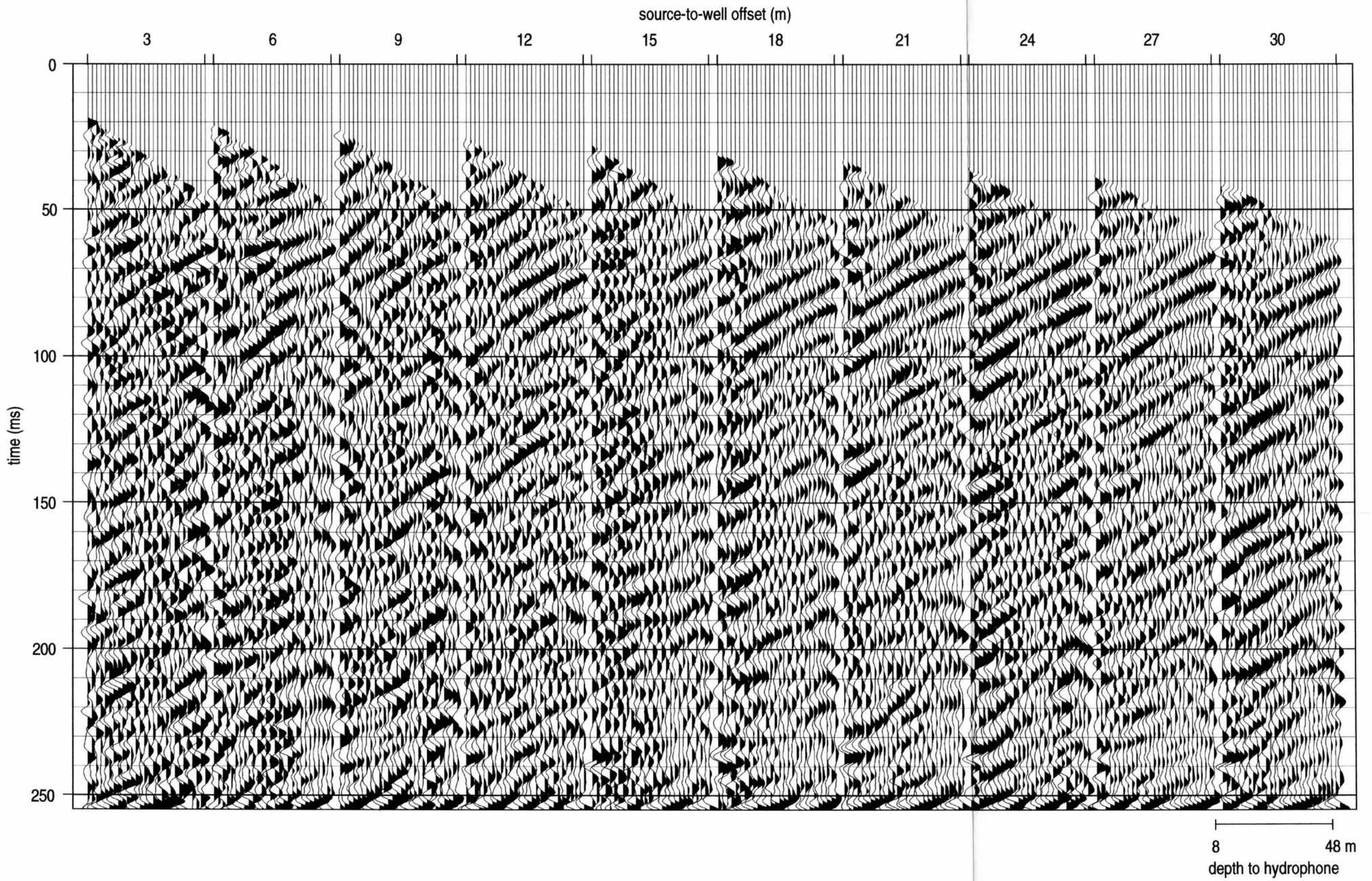


Figure B16. VSP #1 hydrophone data first arrival muted. The first arrival mute is applied to fk filtered data (Figure B15).

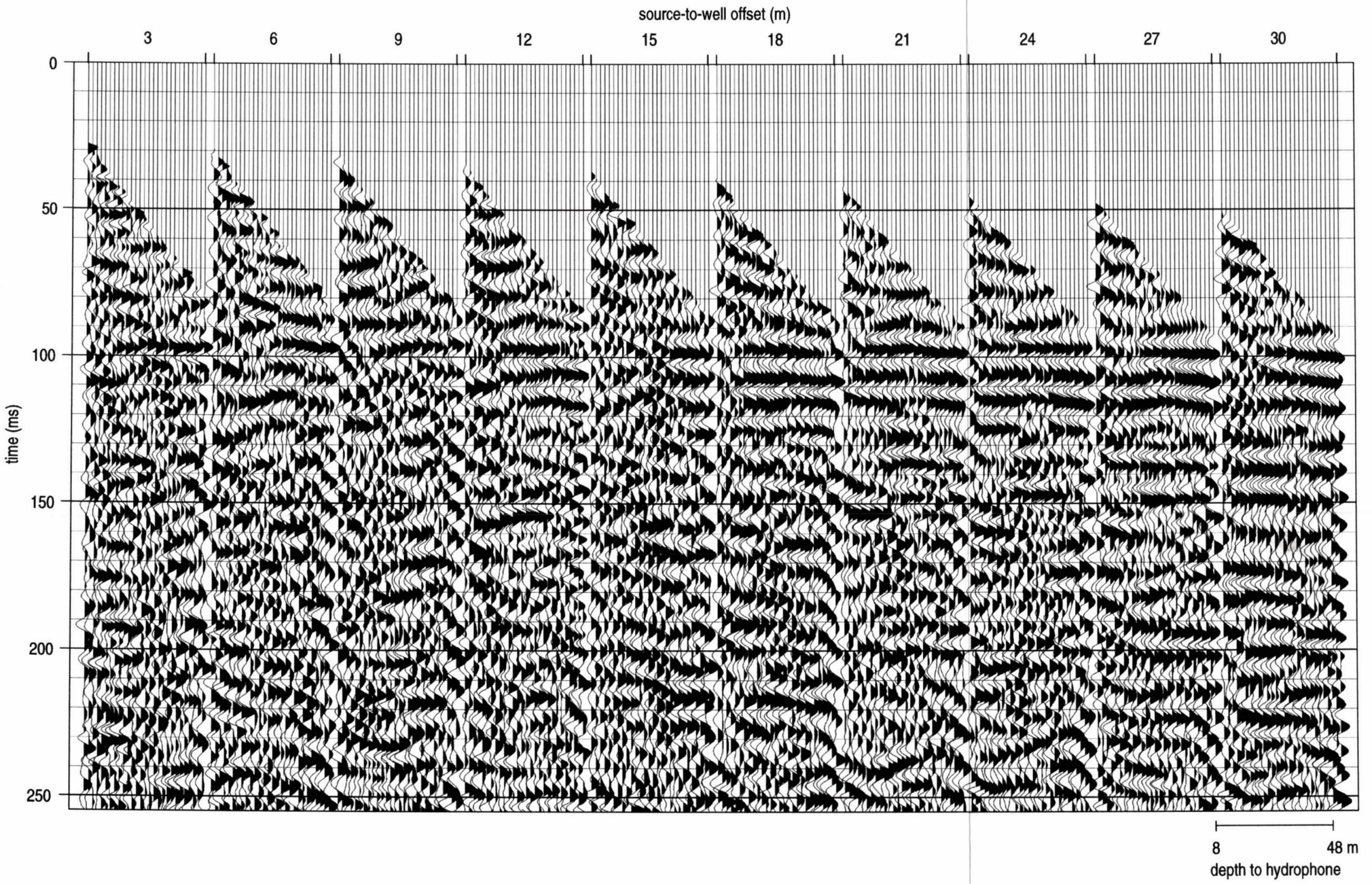


Figure B17. VSP #1 hydrophone data static corrected to vertical incidence. The static correction is applied to first arrival data, datum correcting all hydrophones to the well head.

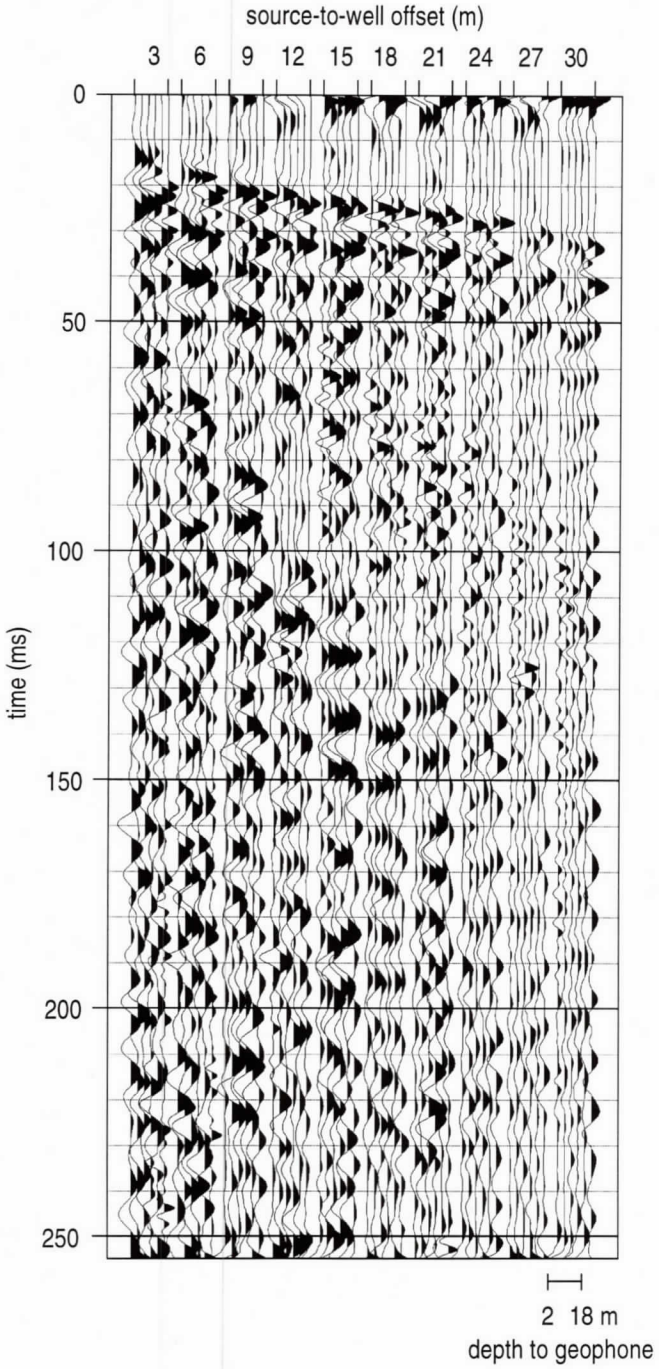


Figure B18. VSP #1 geophone data band-pass filtered (50 100 300 450) and AGC (50 ms) scaled. There are a total of 6 traces in each gather with depths from 2 m to 18 m.

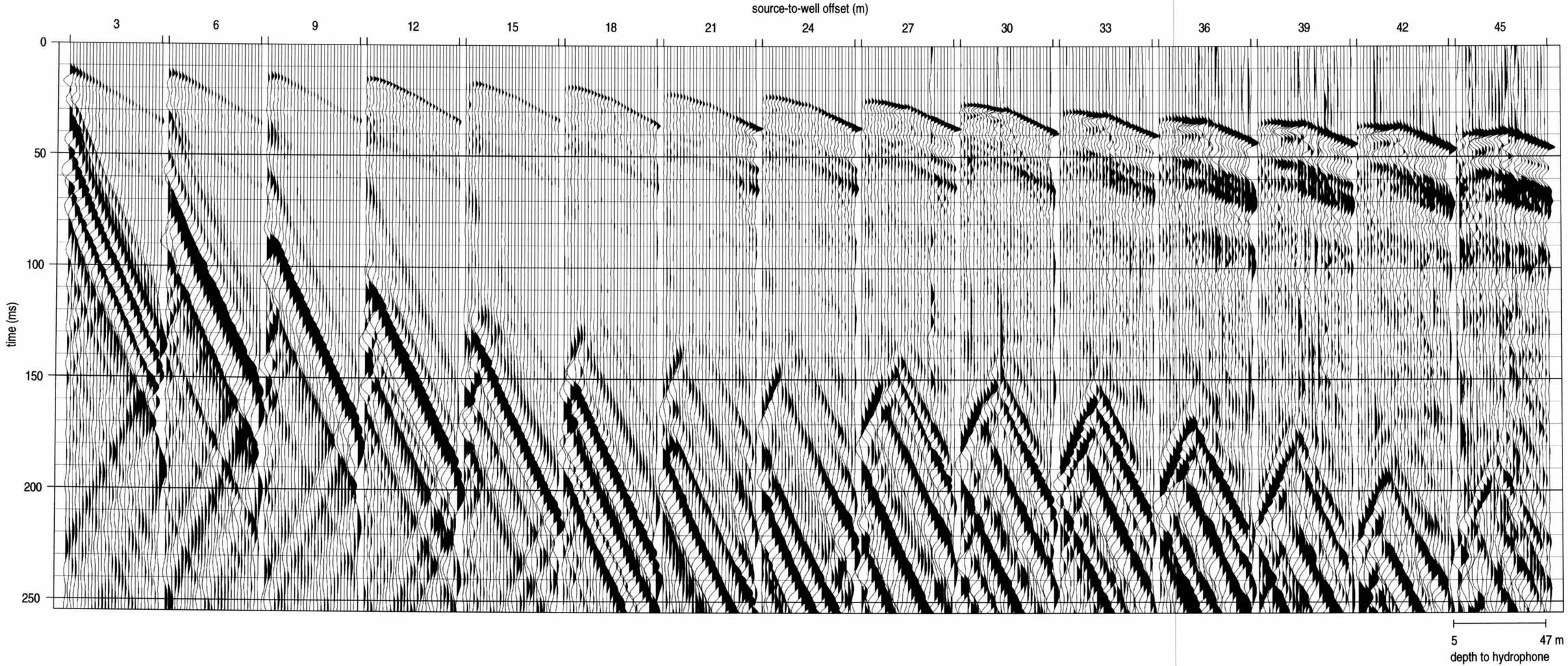


Figure B19. VSP #2 raw hydrophone data. There are a total of 29 traces in each source offset gather with depths from 5 m to 47 m.

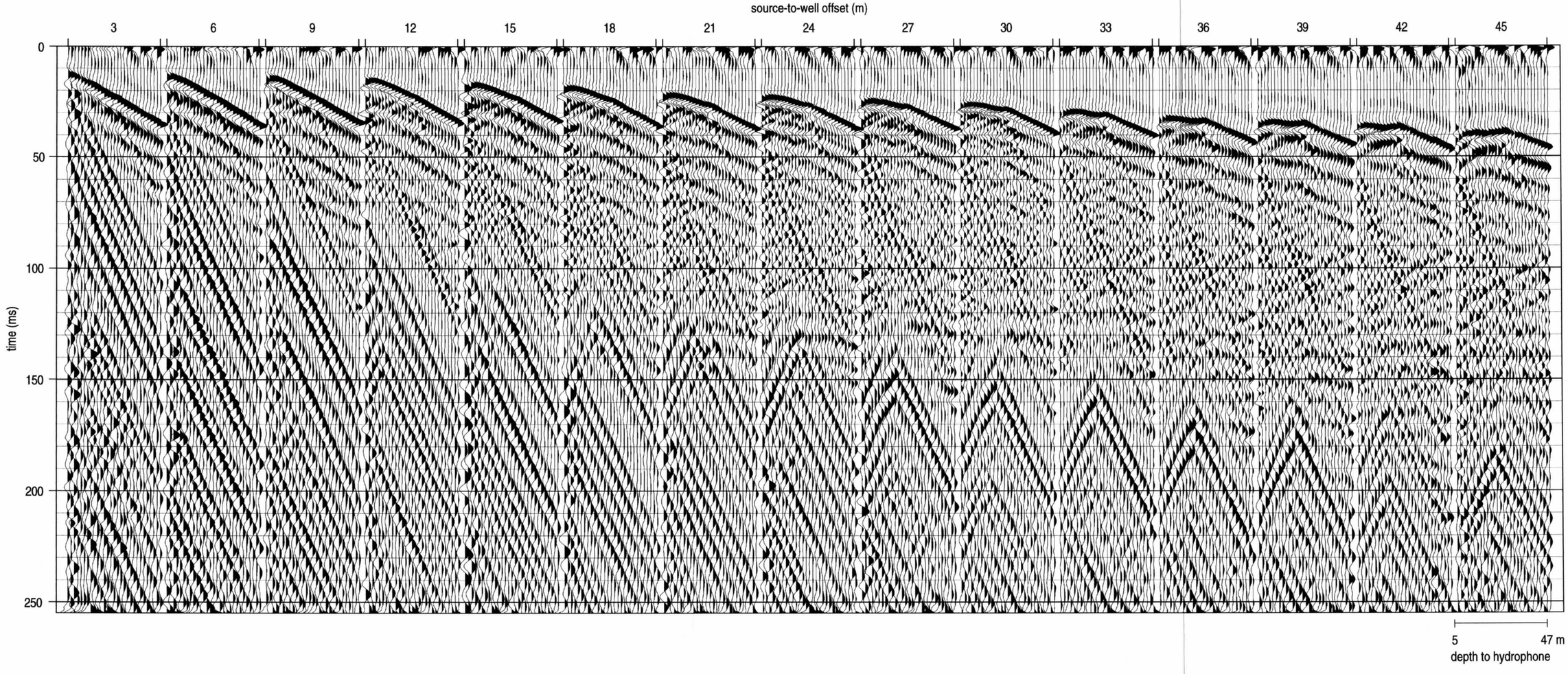


Figure B20. VSP #2 hydrophone data (Figure B19) band-pass filtered (50 100 300 450) and AGC (50 ms) scaled.

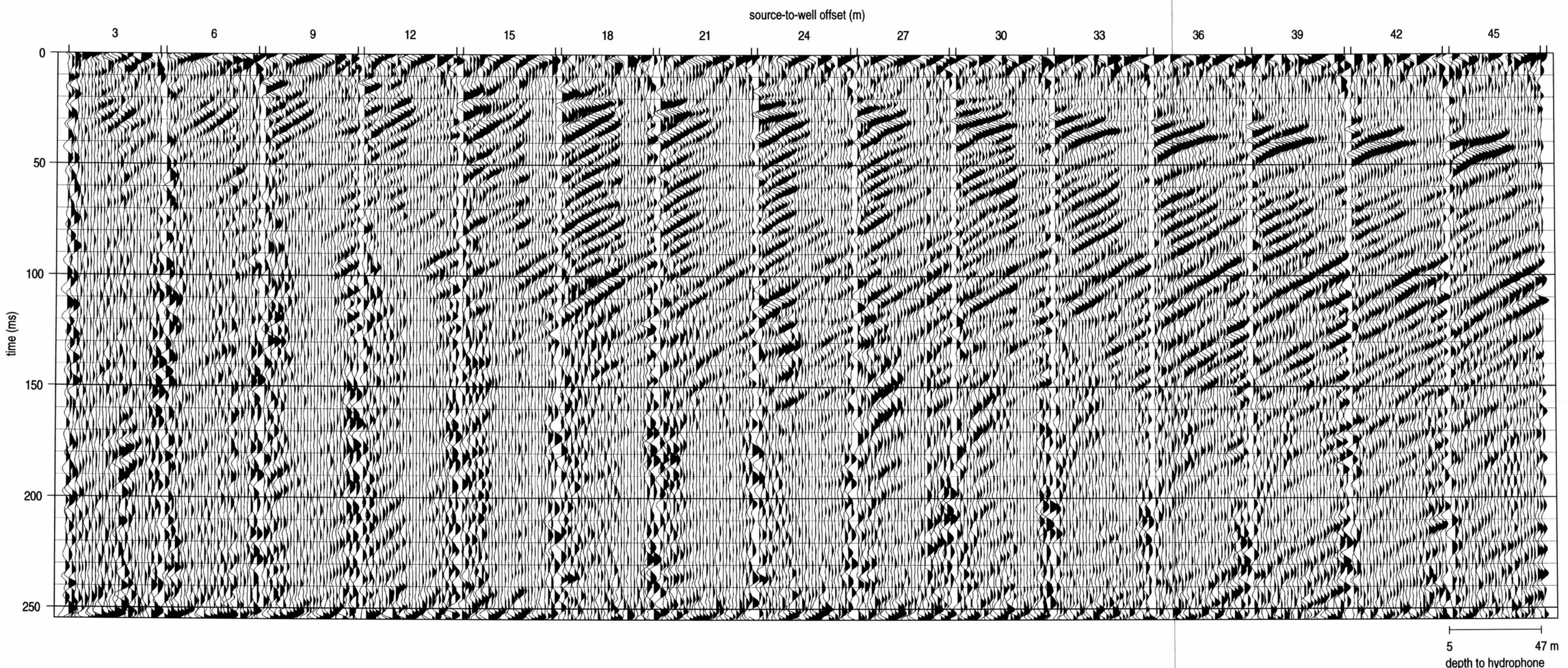


Figure B21. VSP #2 up-coming waves. Two positive fan reject fk filters (0 – 1.5 ms/tr. and 2.0 – 4.0 ms/tr.) have been applied to filtered and scaled data (Figure B20) to eliminate down-going waves and one negative fan reject fk filter (-2.0 – -4.0 ms/tr.) has also been applied to the filtered data to take out strong up-coming tube waves.

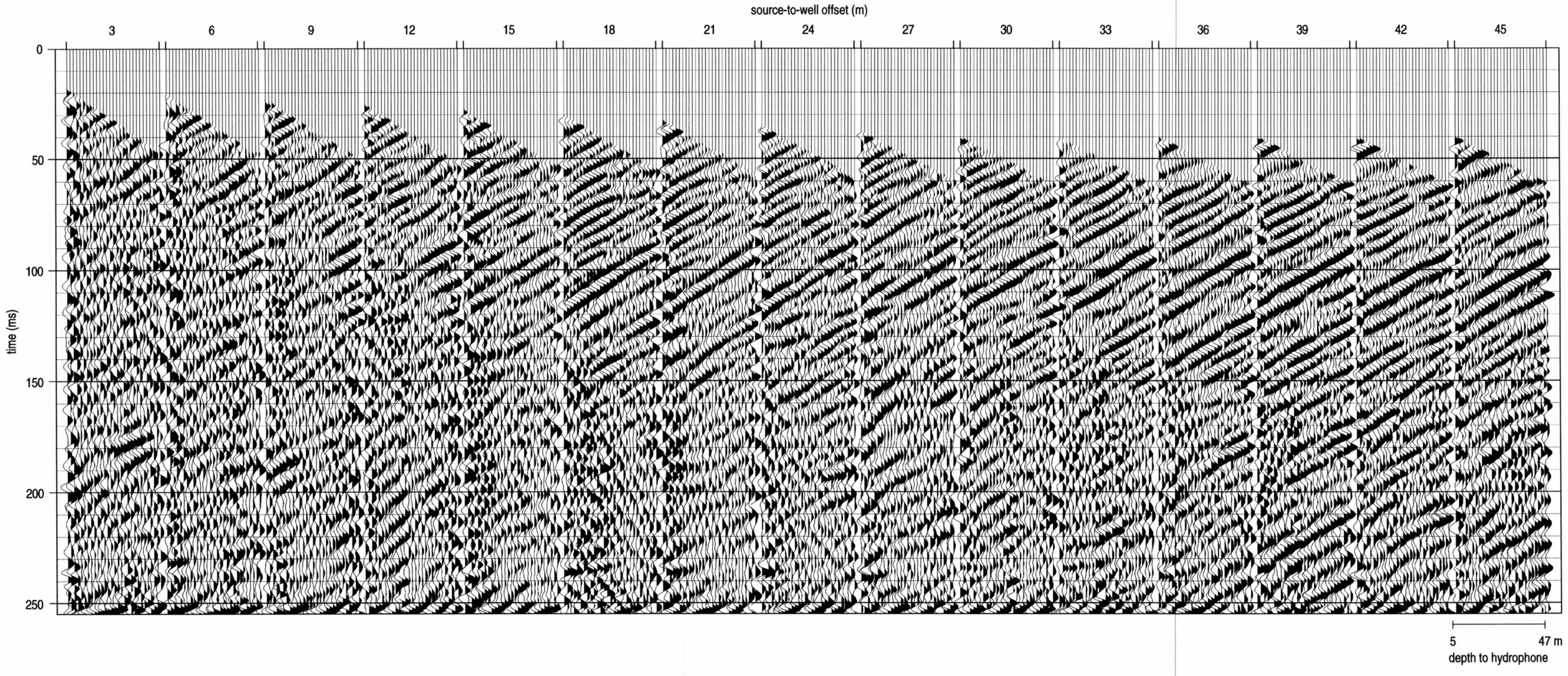


Figure B22. VSP #2 hydrophone data first arrival muted. The first arrival mute is applied to fk filtered data (Figure B21).

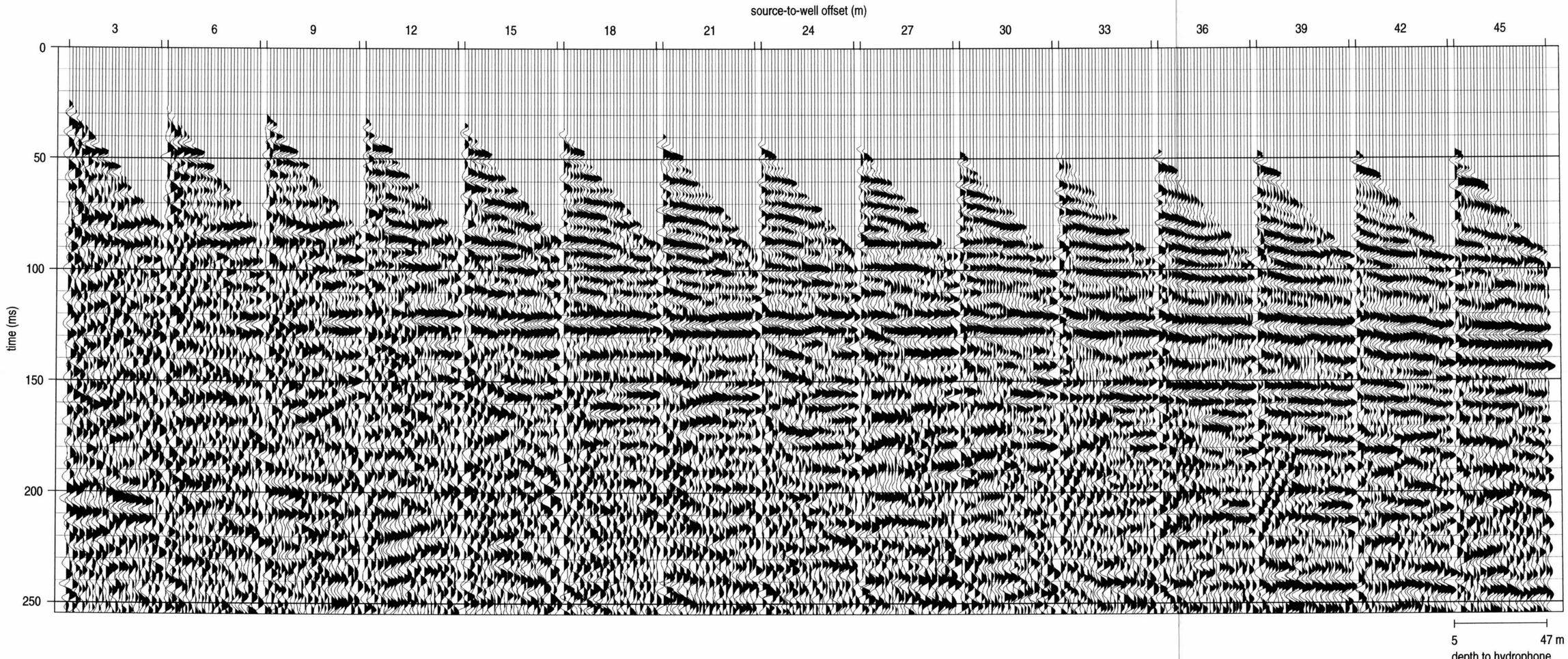


Figure B23. VSP #2 hydrophone data static corrected to vertical incidence. The static correction is applied to first arrival data, datum correcting all hydrophones to the well head.

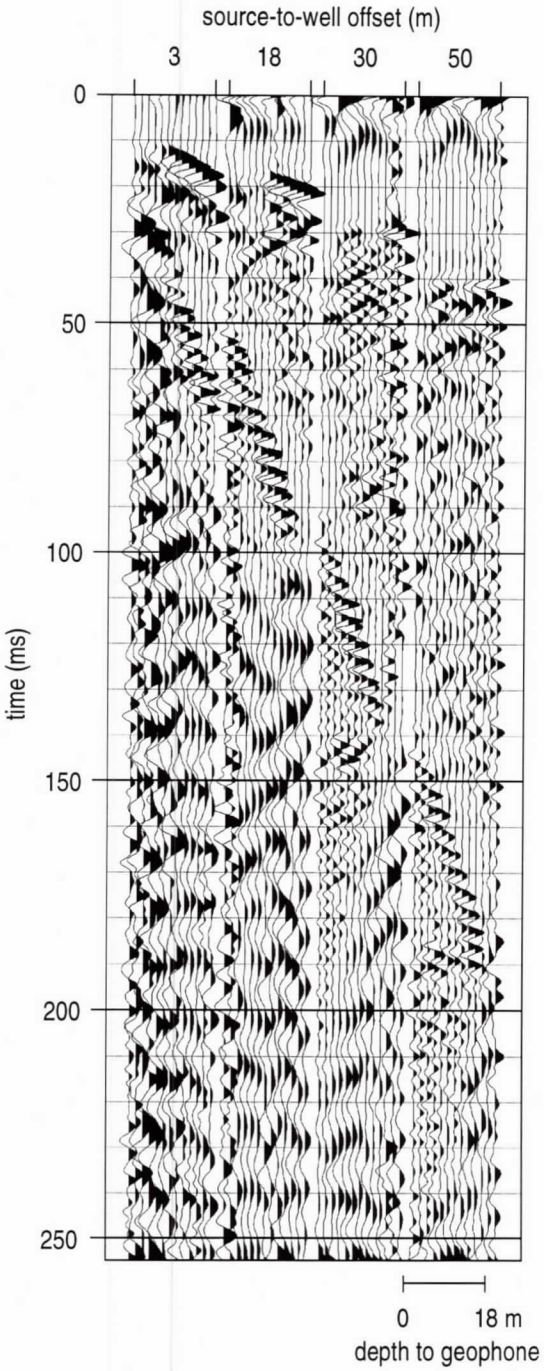


Figure B24. VSP #2 geophone data band-pass filtered (50 100 300 450) and AGC (50 ms) scaled. There are a total of 13 traces in each gather with depths from 0 m to 18 m.

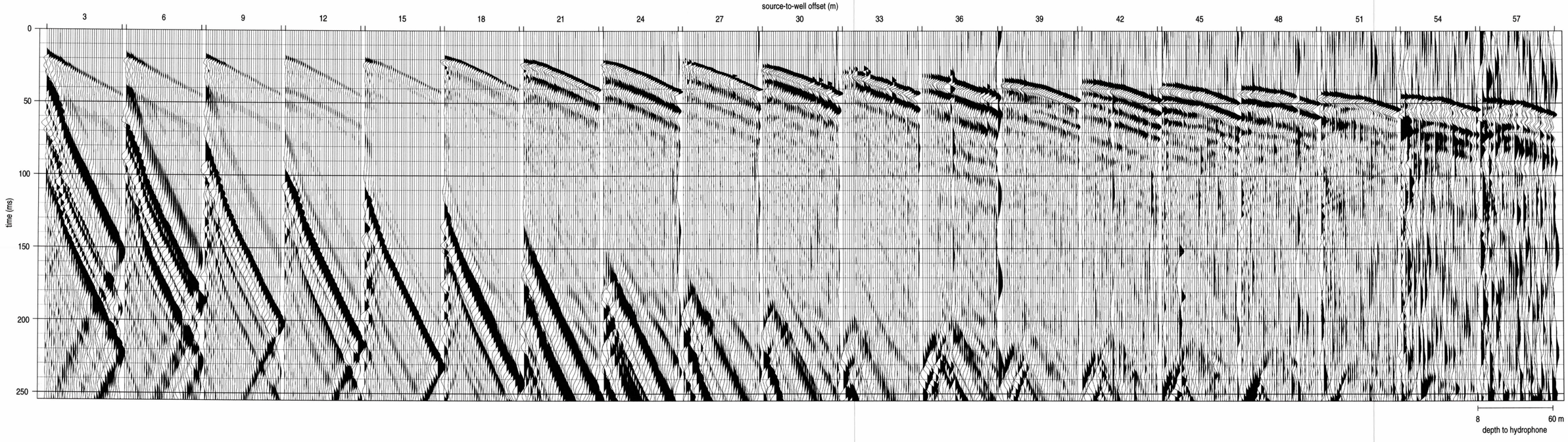


Figure B25. VSP #3 raw hydrophone data. There are a total of 36 traces in each source offset gather with depths from 8 m to 60 m.

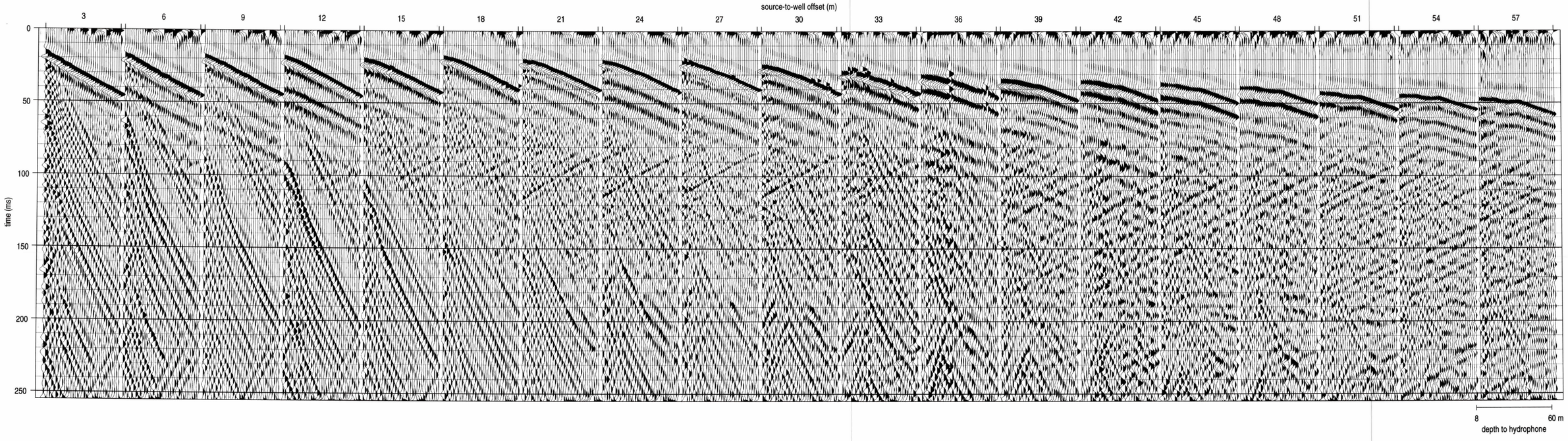


Figure B26. VSP #3 raw hydrophone data. There are a total of 28 traces in each source offset gather with depths from 8 m to 60 m.

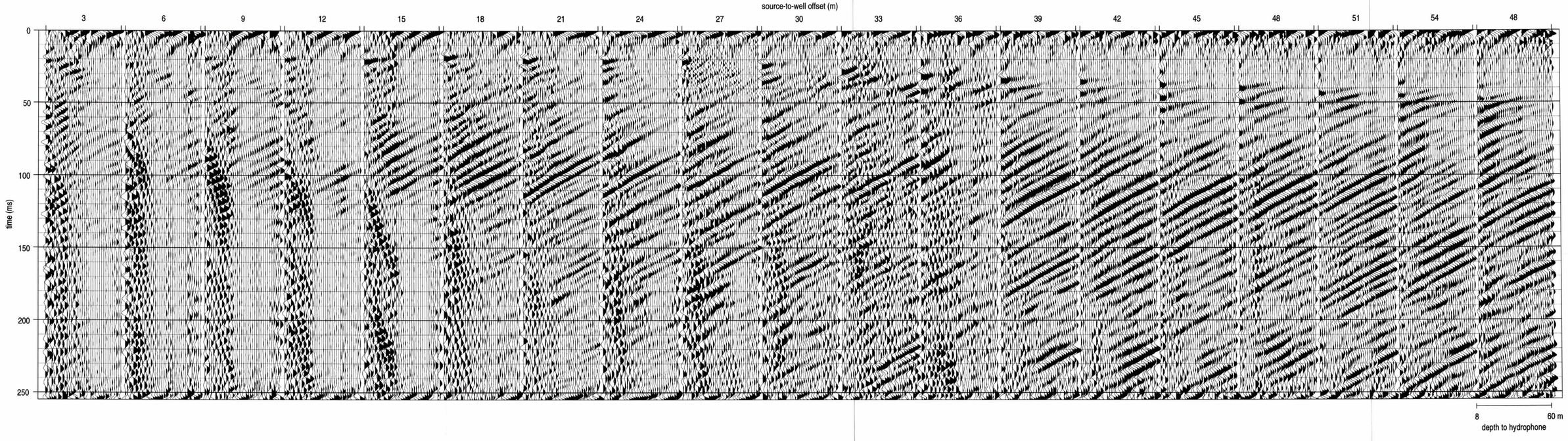


Figure B27. VSP #3 hydrophone data (Figure B26) band-pass filtered (50 100 300 450) and AGC (50 ms) scaled.

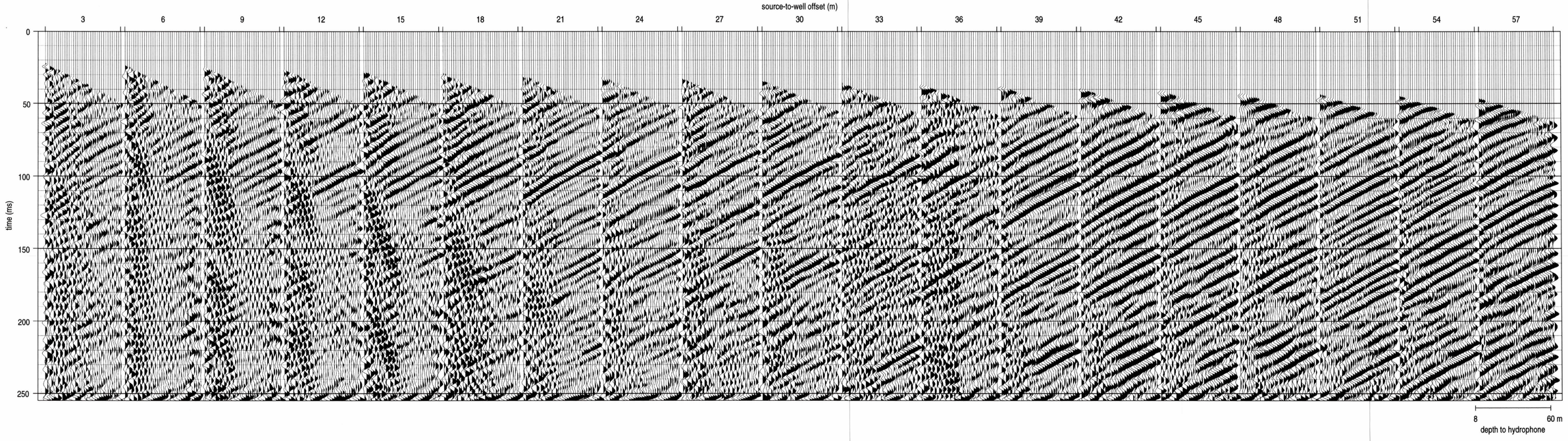


Figure B28. VSP #3 up-coming waves. Two positive fan reject fk filters (0 – 1.5 ms/tr. and 2.0 – 4.0 ms/tr.) have been applied to filtered and scaled data (Figure B27) to eliminate down-going waves and one negative fan reject fk filter (-2.0 – -4.0 ms/tr.) has also been applied to the filtered data to take out strong up-coming tube waves.

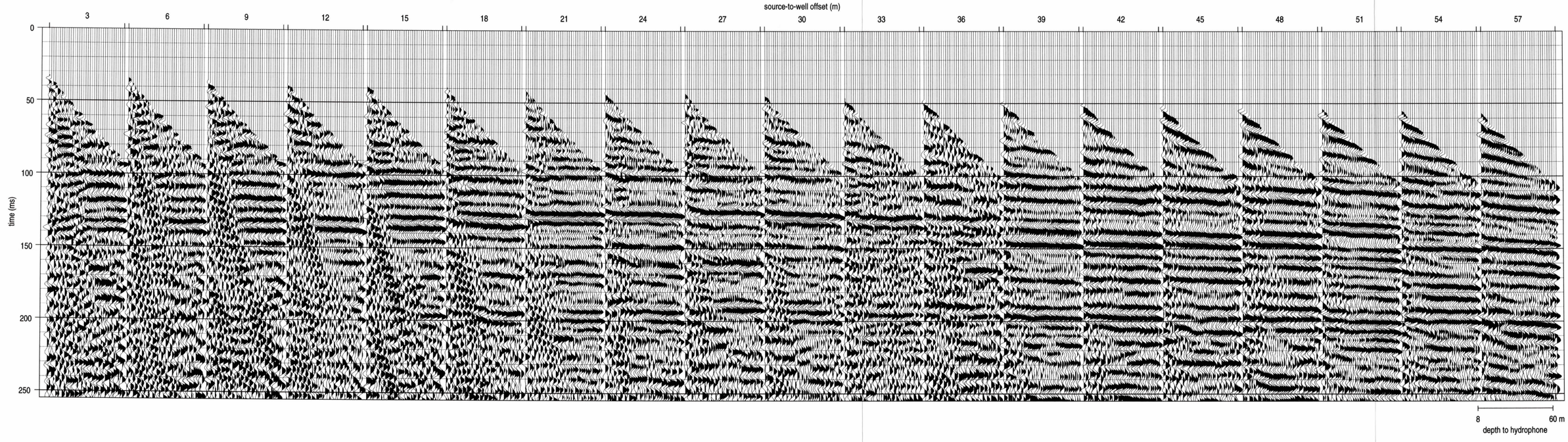


Figure B29. VSP #3 hydrophone data first arrival muted. The first arrival mute is applied to fk filtered data (Figure B28).

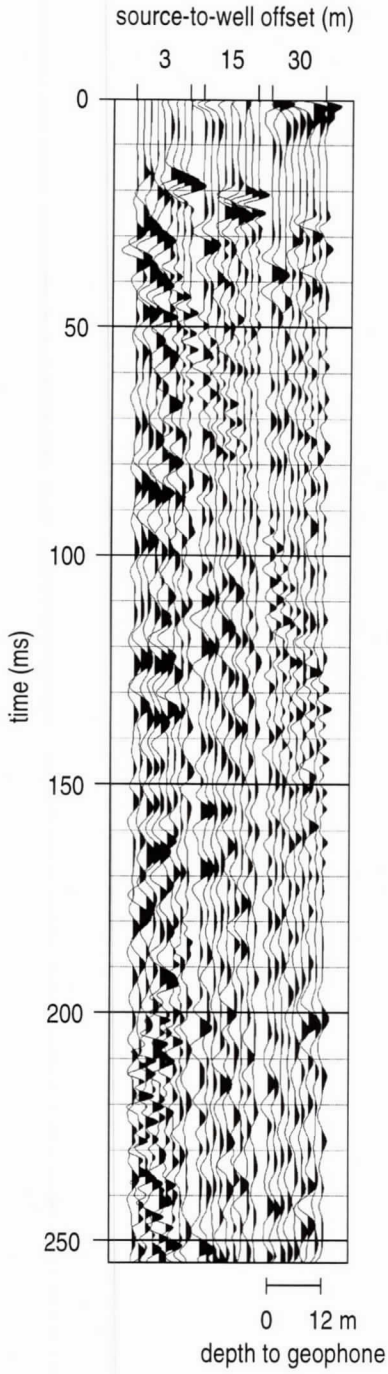


Figure B30. VSP #3 geophone data band-pass filtered (50 100 300 450) and AGC (50 ms) scaled. There are a total of 9 traces in each gather with depths from 0 m to 12 m.